2. Particle analysis

Particle analysis in gravel-bed rivers includes the analysis of particle size, particle shape, particle density and bulk density. These four topics are presented and discussed below.

2.1 Size analysis

Particle-size analysis comprises the measurement and analysis of the three particle axes that define the three-dimensional shape of a particle. For many applications, it is much more convenient to characterize particle size by only one variable, such as the length of the intermediate particle axes or the size of the sieve on which a particle was retained. Once the sizes of particles are determined, they are statistically analyzed, so that particle-size distributions and statistical parameters characterizing them can be compared between streams or over time. The mean particle size on a streambed, a particular particle-size percentile, a characteristic large particle size, as well as the entire spectrum of particle sizes all affect the hydraulics of flow as well as bedload transport rates. Studies concerned with the mechanics of particle entrainment, particle transport and deposition need to include the description and comparison of particle shapes.

2.1.1 Particle axes

The analyses of particle sizes and particle shape parameters are based on the length of three mutually perpendicular particle axes: the *longest* (*a*-axis), the *intermediate* (*b*-axis), and the *shortest* (*c*-axis) axis. The demand for the *a*, *b*, and *c*-axes being truly the longest, the intermediate, and the shortest axes agrees with the demand for perpendicularity of the three particle axes only if the particle shape is ellipsoidal (e.g., like a lightly-worn bar of soap). Particles with a rhombic shape cannot fulfill both demands, and this might leave the user confused on whether to base particle identification on the absolute lengths of particle axes or on perpendicularity. The identification of the *a*- and the *b*-axes is affected most by this discrepancy, whereas the position and length of the *c*-axis is usually clear.

The crucial point is whether the analysis starts with the definition of the *a*-axis as the longest axis, with the *b*-axis following as the longest intermediate axis perpendicular to the *a*-axis as done in the Canadian guidelines (Yuzyk and Winkler 1991) (Fig. 2.1), or whether the analysis starts with identifying the *b*-axis as the "shortest axis of the maximum projection plane (the plane with the largest area) perpendicular to the *c*-axis" (Gordon et al. 1992. 198-199). If the *a*-axis is subsequently defined as perpendicular to the *b*-axis, then the *a*-axis is not necessarily the longest distance between two points on a given particle. The *b*- and *a*-axes are along the heavy black arrows ***a*** and ***b*** in Fig. 2.1 according to the definition by Gordon et al. (1992).

14

Differences in the definition of the *a*- and *b*-axis are most pronounced in particles of rhombic shape (Fig. 2.2, left). *a*- and *b*-axes follow the gray stippled lines *a* and *b* when defined according to Yuzyk and Winkler (1991), and along the black solid lines **a** and **b** according to the definition by Gordon et al. (1992). Both lines **a** and **b** are longer than *a* and *b*.
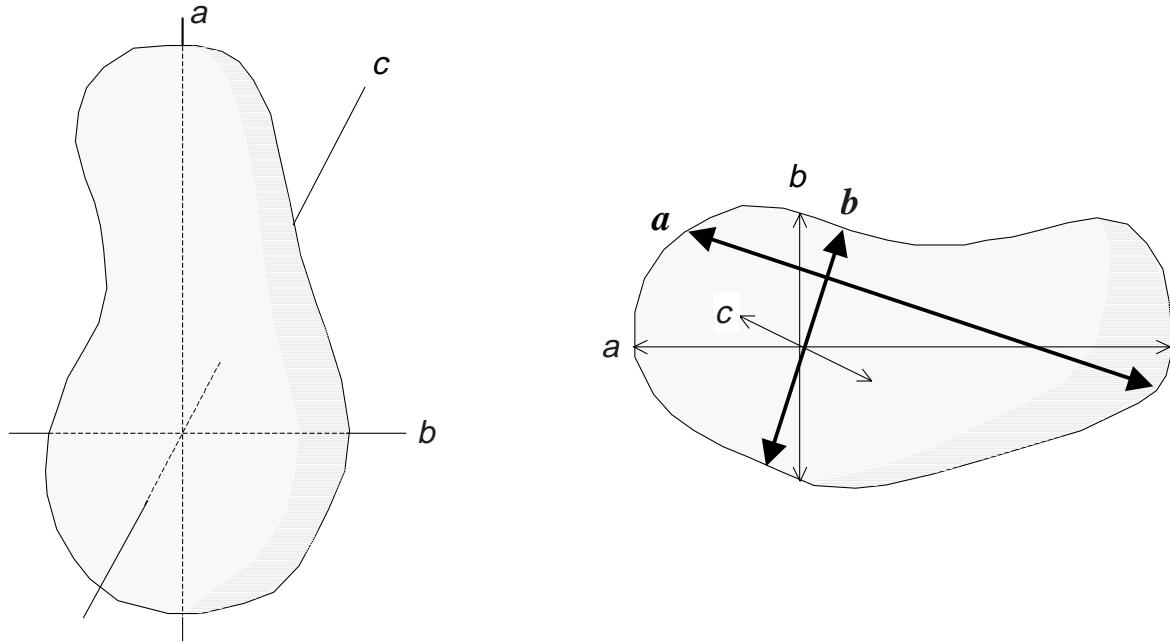
Fig. 2.1: Definition of particle axes (Redrawn after Yuzyk 1986, and Yuzyk and Winkler 1991).
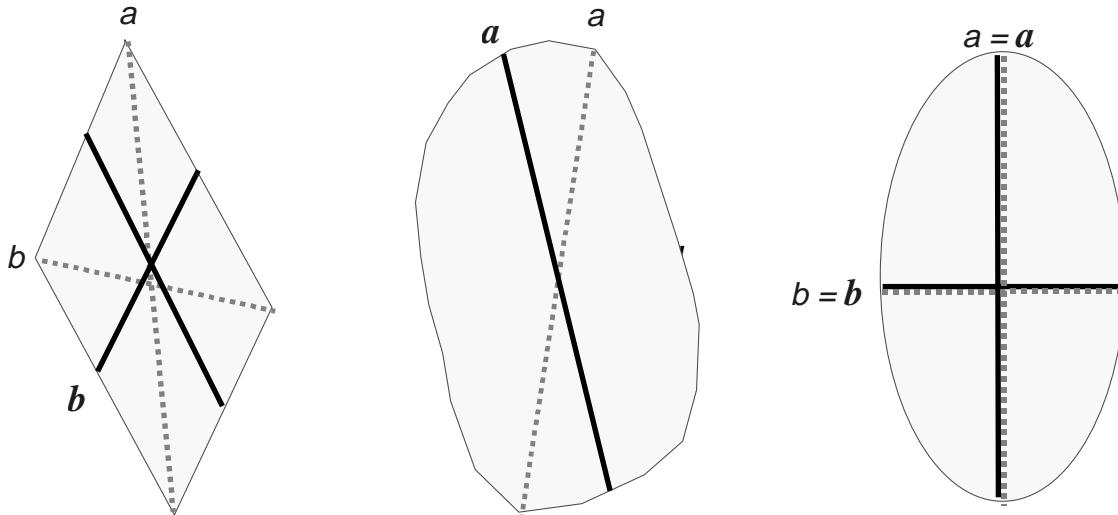
Fig. 2.2: Discrepancy in *b*- and *a*-axes definitions for rhombic, irregular ellipsoidal, and ellipsoidal particle shapes.

The differences in the two axis definitions become irrelevant for smooth ellipsoidal shapes (Fig. 2.2). Consequently, the definition of particle *b*-axes should be unproblematic for well rounded and ellipsoidal particles in alluvial streams in which all particles experienced a long fluvial transport. However, particle-axes measurements can be difficult in mountain streams with a non-fluvial sediment supply, or in headwaters where fluvial transport is short and the particles can be angular and rhomboidal.

Ultimately, the study aim needs to decide how particle axes are measured. If hand-measured *b*-axis lengths are to be compared with sieve sizes, *b*-axis measurement should stimulate the way a particle drops through a sieve opening. Measurements of *a*- and *c*-axis then follow the rules of perpendicularity. Measurements of *b*-axis lengths automatically follow this procedure if templates are used. The *b*-axis measurements performed with rulers, calipers, and the pebble box on rhomboid particles (Section 2.1.3) are prone to orient the *b*-axis perpendicular to the longest (*a*-axis), which is least problematic to identify. Such *b*-axis measurements tend to produce longer *b*-axis lengths than template measurements.

2.1.2 Particle sizes and size classes

The size of a particle can be determined in three different categories: the actual *b*-axis length, the nominal diameter, and the particle-sieve diameter. The three approaches are used for different purposes.

Actual b-axis length
Measuring the actual lengths of particle *b*-axes in units of mm or cm may be important for studies that are concerned with a small range of particle sizes, a range smaller than distinguished by two consecutive sieves in a standard sieve set. An example for such a study is the determination of the dominant particle size. This is computed as the arithmetic mean of particle *b*-axes measured on about 30 large, but not the very largest, particles found within a deposit.

Nominal diameter
If the mass or volume of a particle is of more importance for a study than the particle *b*-axis length or the sieve diameter, the nominal diameter is used. The nominal diameter is a three-dimensional approach and describes particle size by its smallest characteristic diameter. The *nominal diameter* denotes the diameter a particle would assume if its volume was expressed as a sphere and is computed from:

$$D_n = (a \cdot \ b \cdot \ c)^{1/3} \tag{2.1}$$

D_n is directly related to particle volume $V_D = \dfrac{\pi}{6}(a \cdot \ b \cdot \ c)^3$.

16

Particle sieve-diameter

Particles contained in a sediment deposit are commonly analyzed by grouping particles of various sizes into particle size-classes that correspond to the size of sieve openings. The particle sieve-size can be defined as the smallest sieve size through which a particle can pass (D_{pass}) or as the largest sieve size through which the particle did not pass, the retaining sieve size (D_{ret}). For a given particle, passing or retaining sieve size differs by one size class, thus, it is important to indicate whether reference is made to the passing or retaining sieve size. Particle sieve-diameter also depends on whether sieves with square or round-holes were used; whereas for particles of equal weight, sieve diameter varies with particle shape (Sections 2.1.3.1, 2.1.3.4, and 2.1.3.5).

Sieve diameter and nominal diameter are identical for spheres and ellipsoidal particles with certain axes ratios such as *a* = 3/2 *b*, and *c*=2/3 *b,* but deviate for other particle shapes. Compared to a sphere with an identical *b*-axis, a disc has a smaller D_n due to its small *c*-axis, whereas the D_n of a rod-shaped particle exceeds that of a sphere because of its long *a*-axis. Acknowledgment of this discrepancy can become important because sedimentation, i.e., erosion, transport, and deposition of particles, is tied to particle weight and shape (particularly the area projected towards the direction of flow). The analysis of particle shape is discussed in Section 2.2.

2.1.2.1 The Wentworth scale of particle sizes

If particle size-classes progress in a linear scale, e.g., 10, 20, 30 mm, the frequency of particles per size class in fluvial gravel tends to be approximately logarithmically distributed. Logarithmic distributions are statistically more difficult to work with than normal distributions. In order to obtain an approximately normal distribution of particle sizes, particle-size classes were made to increase by a factor of 2 (Wentworth scale). Thus, particle sizes in units of mm double in consecutively larger size classes (2 - 4 mm, 4 - 8 mm, 8 - 16 mm, 16 - 32 mm, etc.). These size classes are grouped into six major particle-size categories - boulders, cobbles, gravel, sand, silt and clay (Table 2.1). Silt and clay content are rarely analyzed in studies of gravel-bed rivers, thus, these size categories are included only in an abbreviated form in Table 2.1.

The mass of a spherical particle increases by a factor of 8, when the particle diameter doubles. This 8-fold range of particle mass per size class is quite large, and many studies therefore carry out particle-size analyses in size classes half as large as the Wentworth classes (see sieve sizes in Section 2.1.3).

2.1.2.2 Particle size in ϕ-units

The frequency distribution of the weight or number of particles per size class tends to follow approximately a lognormal distribution (Section 2.1.4.3) when particle sizes are expressed metrically in mm. Consequently, the arithmetic mean particle size and the arithmetic median particle size are not the same (mean is usually larger than median). If a

Table 2.1: Size gradation for sediment in the range of sand to boulders (Wentworth scale)

Description of particle size			$\phi = -\log_2$	mm	$\psi = \log_2$
	———		- 12.0 ——	4096 ——	12.0
	very large		- 11.5	2896	11.5
	———		- 11.0 ——	2048 ——	11.0
	large		- 10.5	1448	10.5
Boulder	———		- 10.0 ——	1024 ——	10.0
	Medium		- 9.5	724	9.5
	———		- 9.0 ——	512 ——	9.0
	small		- 8.5	362	8.5
			- 8.0 ——	**256** ——	**8.0**
	large		- 7.5	181	7.5
Cobble	———		- 7.0 ——	128 ——	7.0
	Small		- 6.5	90.5	6.5
			- 6.0 ——	**64** ——	**6.0**
	very coarse		- 5.5	45.3	5.5
	———		- 5.0 ——	32 ——	5.0
	coarse		- 4.5	22.6	4.5
	———	**Pebble**	- 4.0 ——	16 ——	4.0
Gravel	medium		- 3.5	11.3	3.5
	———		- 3.0 ——	8 ——	3.0
	fine		- 2.5	5.66	2.5
	———		- 2.0 ——	4 ——	2.0
	very fine	**Granule**	- 1.5	2.83	1.5
			- 1.0 ——	**2** ——	**1.0**
	very coarse		- 0.5	1.41	0.5
	———		0 ——	1 ——	0
	coarse		+ 0.5	0.707	- 0.5
	———		+ 1.0 ——	0.500 —	- 1.0
Sand	medium		+ 1.5	0.354	- 1.5
	———		+ 2.0 ——	0.250 —	- 2.0
	fine		+ 2.5	0.177	- 1.5
	———		+ 3.0 ——	0.125 –	- 3.0
	very fine		+ 3.5	0.088	- 3.5
			+ 4.0 ——	**0.063** –	**- 4.0**
Silt					
			+ 8.0 ——	**0.0039** -	**- 8.0**
Clay					
			+ 12.0 ——	**0.00024** -	**- 12.0**

particle-size distribution was truly logarithmic, log transformation of particle-size units would produce a normal distribution. It is desirable to work with normal distributions, because standard statistical procedures can be used to analyze them.

Any kind of logarithmic transformation, e.g., the simple log of the particle size *D*, i.e., log (*D*), applied to the original data will produce a normal distribution. However, in order to obtain convenient, integer values after a log transformation, sedimentologists and geomorphologists (Krumbein 1934) expressed particle size *D* as the negative logarithm to

the base of 2 and called the result the ϕ-scale. ϕ, spelled out as phi, is the Greek letter for *f*. Particle sizes in ϕ-units are computed from particle sizes *D* in units of mm by

$$\phi_i = -\log_2(D_i) \tag{2.2}$$

Since the negative logarithm to the base of 2 is not routinely programmed in scientific calculators it needs to be computed from

$$\phi = -\frac{\log(D_i)}{\log(2)} \tag{2.3}$$

Since $\log(2) = 0.3010$, this expression can be simplified to

$$\phi_i = \frac{-\log(D_i)}{0.301} = -3.3219 \log(D_i) \tag{2.4}$$

For example, $-3.3219 \log(64) = -3.3219 \cdot 1.8062 = 6.0$. Conversely, particle sizes *D* in units of mm are obtained from particle sizes in ϕ-units by

$$D_i = 2^{-\phi i} \tag{2.5}$$

This expression can easily be solved by scientific calculators or spreadsheet programs. An alternative expression dating from the time of logarithmic and exponential tables is

$$D_i = e^{-\phi i \ln(2)} = 10^{-\phi i \log(2)} = 10^{-0.301\,\phi i} \tag{2.6}$$

Table 2.1 presents particle sizes in units of mm and ϕ.

2.1.2.3 Particle size in ψ-units

The ϕ-transformation produces positive values for particle sizes smaller than 1 mm and negative values for particle sizes larger than 1 mm. This feature is convenient for studies that focus on sand and smaller sediment. However, this feature is inconvenient for studies in gravel-bed rivers, because having smaller, negative numbers for larger particle sizes is

counterintuitive. Consequently, the ψ-scale was developed (Greek letter y spelled out as *psi*) which produces increasingly larger values as particle sizes increase from sand to boulders. ψ-units are the negative values obtained in ϕ-units ($\psi = -\phi$, or $\phi = -\psi$). ψ-units are computed from particle size D in units of mm by

$$\psi_i = \log_2 (D_i) \tag{2.7}$$

By analogy to Eq. 2.2, this expression is solved by

$$\psi_i = \frac{\log(D_i)}{\log (2)} \tag{2.8}$$

which can be simplified to $\psi_i = 3.3219 \log (D_i)$. For example, $3.3219 \log(64) = 3.3219 \cdot 1.8062 = 6.0$. Particle sizes in ψ-units are provided in Table 2.1. Particle size D in mm-units is obtained from particle sizes in ψ-units by

$$D_i = 2^\psi = e^{\psi \ln (2)} = 10^{\psi \log (2)} \tag{2.9}$$

2.1.3 Sieving and manual measurements of particle size

The size of gravel particles can be measured manually or by sieving. The different equipment used in both approaches can affect the results. This makes it necessary to compare different methods of particle-size measurements and to determine conversion factors.

Sieving usually employs square-hole sieves, although some labs still have round-hole sieves. Square- and round-hole sieves produce different size gradation curves, especially for flat particles. Manual particle-size measurements traditionally use rulers and calipers. These devices are prone to operator error that can be avoided by using templates (Section 2.1.3.6). Notwithstanding operator error, ruler and template measurements differ to the same degree as do size gradations based on round-hole and square-hole sieves. Pebble boxes are a handy device if all three particle axes are to be measured (Section 2.1.3.8) because they help to reduce operator error and speed up the measurements.

2.1.3.1 Square-hole sieves

Square-hole mesh wire sieves are the standard laboratory sieves for sand and gravel. They have size gradations between 0.063 and 64 mm. Sieve sizes, i.e., the side length of the mesh width D_s, typically advance as a logarithmic series based on 2, i.e.,

20

$$D_s = 2^x \qquad\qquad\qquad\qquad\qquad\qquad\qquad\qquad\qquad\qquad (2.10)$$

where x usually assumes values in increments of 0.5, so that D_s advances in 0.5 units of ϕ or ψ (Table 2.1). For sediment from gravel-bed rivers, a stack of sieves in 0.5 ϕ units usually has 64 mm as the coarsest sieve, and consecutive smaller sieves have mesh widths of 45.3, 32, 22.6, 16, 11.3, 8, 5.66, 4, 2.83, and 2 mm. If the sand fraction is of concern, sieve sizes continue with 1.4, 1.0, 0.71, 0.5, 0.35, 0.25, 0.18, 0.125, 0.088, and 0.063 mm. Sieves typically used in the United States produced by the American Society for Testing and Materials (ASTM E-11) follow the 0.5 ϕ or ψ-gradation only approximately for particle sizes in the gravel range. This deviation stems from expressing particle-size classes as fractions of an inch. Sieves that retain particles larger than 22.6 and 11.3 mm are commonly labeled 22.4 and 11.2 mm, suggesting an arithmetic mean between -4.5 ϕ (=22.6 mm) and 7/8 inch (= 22.2 mm). Likewise, the 11.2 mm sieve size is the mean between -3.5 ϕ (=11.3 mm) and 7/16 inch = 11.1 mm. Sometimes, ASTM E-11 sieves indicate three different mm sizes for the same sieve size. The "45 mm" (1¾ inch) sieve, for example, sometimes indicates 44.45 mm, the mm equivalent of 1¾ inch, sometimes 45.3 mm, the exact mm equivalent of -5.5 ϕ, and sometimes 45 mm, which is an intermediate value between the two. This discrepancy is problematic if size classes are first expressed in mm, and then mathematically converted to ϕ or ψ- units for further particle-size analysis.

Sieving in 0.5 ϕ-units is recommended for many sampling projects in gravel-bed rivers. However, some study objectives may require sieving in 0.25 ϕ-increments, while for others units of 1.0 ϕ may be sufficient.

2.1.3.2 Relation between *b*-axis size and square-hole sieve sizes

Particles found within one 0.5 ϕ sieve class can have *b*-axes lengths that range over a factor of almost 2. The smallest *b*-axis length of a particle retained on a -4.5 ϕ = 22.6 mm sieve is 22.7 mm, the largest *b*-axis length is 45.2 mm. For a given particle shape, the range of *b*-axes lengths is $\sqrt{2} \cong 1.41$. Perfect spheres have the smallest *b*-axes. The smallest sphere retained on the 22.6-mm sieve has a *b*-axis of 22.7 mm, whereas the largest sphere to fit through the -5 ϕ = 32-mm sieve has a *b*-axis of 31.9 mm. Extremely flat particles have the largest *b*-axes, ranging from 31.9 to 45.2. Thus, the flatter the particle, the larger the *b*-axis that fits through a square sieve opening (Fig. 2.3). Particle flatness can be expressed by the ratio of shortest to intermediate axis c/b. The relation between the ratio of a square-hole sieve opening D_s to *b*-axis size and particle flatness (i.e., the ratio of c/b) is given by Eq. 2.11 and shown in Fig. 2.4. Fig. 2.4 can likewise be used to illustrate the ratio

$$\frac{D_s}{b} = \sqrt{\frac{1}{\sqrt{2}} \cdot \ 1 + \left(\frac{c}{b}\right)^2}$$

(2.11)
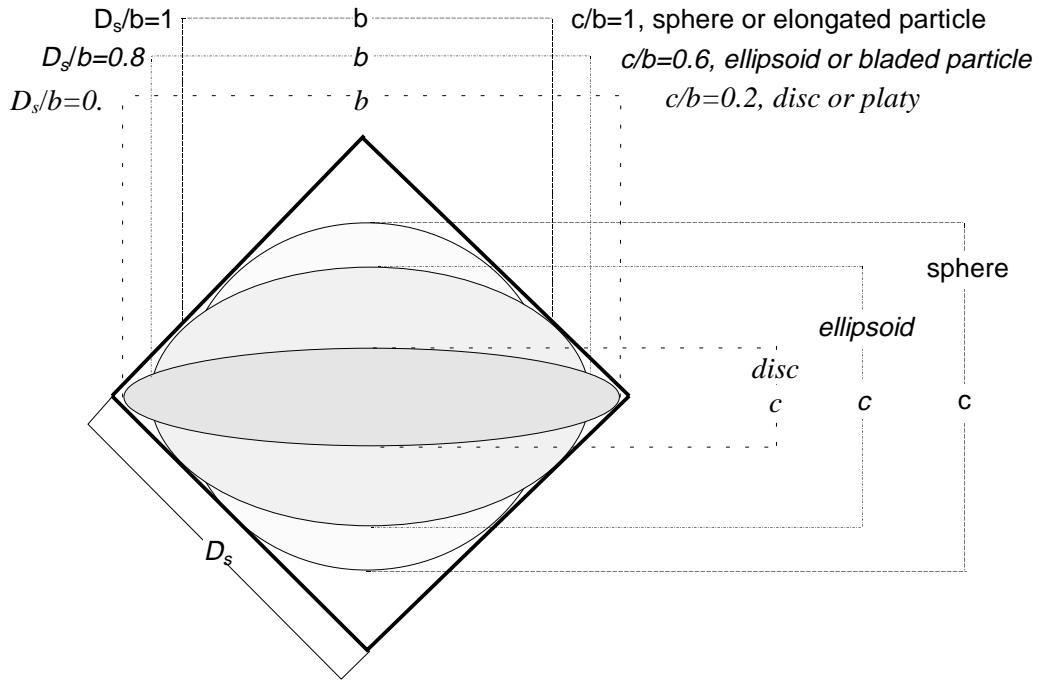
Fig. 2.3: Illustration of effect of particle shape on largest *b*-axis size to fit through a square-hole sieve (Redrawn from Church et al. 1987; by permission of John Wiley and Sons, Ltd.).
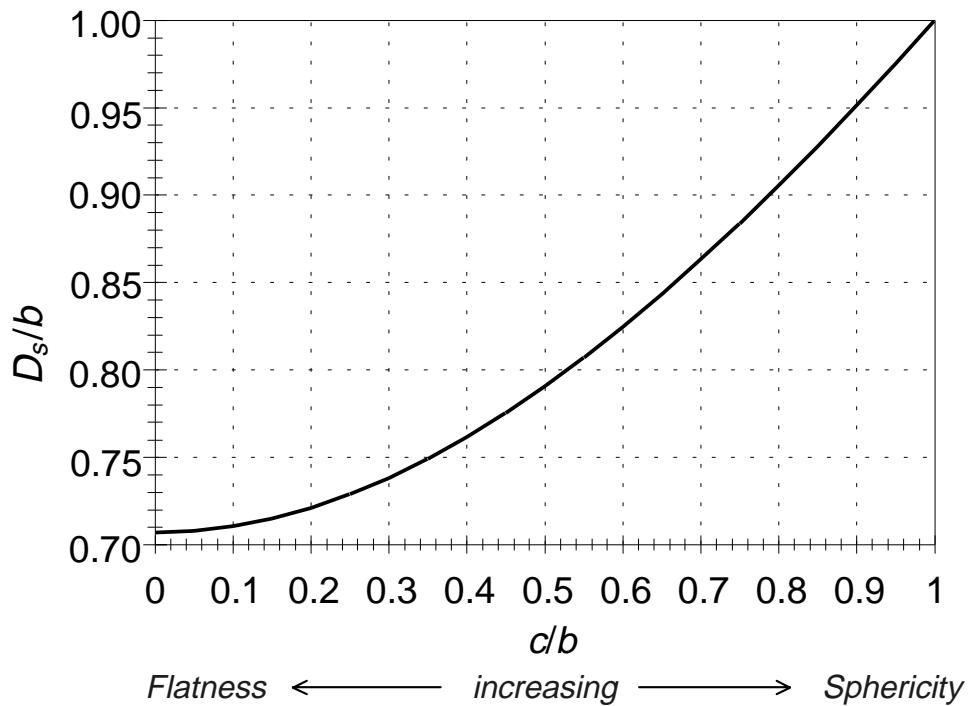
Fig. 2.4: Ratio of square-hole sieve opening D_s to measured *b*-axis size as a function of particle flatness, i.e., the ratio of *c/b* (Redrawn from Church et al. 1987; by permission of John Wiley and Sons, Ltd.).

of square-hole sieve size to round-hole sieve size for various degrees of particle flatness (Section 2.1.3.5).

2.1.3.3 Round-hole sieves

Some sieves consist of metal plates with round borings of the diameter D_s. Since square-hole sieves and round-hole sieves have openings of different shapes, both sieves produce different sieve results, except for particles with perfect spherical shapes. A sphere with a diameter of 3.99 mm fits through both a round-hole and a square-hole sieve of 4 mm, and a ball 46 mm in diameter is likewise retained on both the square and the round-hole sieve of 45 mm. However, sieving ellipsoidal or flat particles with both sieve types produces different gradation curves (i.e., cumulative frequencies). Differences in mean particle b-axes length and conversion factors between round and square-hole sieve results are discussed in Sections 2.1.3.4 and 2.1.3.5.

2.1.3.4 Center of class and mean particle b-axes length per size class

Sometimes, computations require that an entire particle-size class is represented by a single particle-size value. Commonly, this value is taken as the "center of class", D_c, which is the hypothetical *sieve* size between the retaining and the passing sieve size. D_c is therefore determined from the logarithmic mean between the retaining sieve size D_{ret} and the next larger, passing sieve size D_{pass} which is equal to the diagonal of the retaining sieve size.

$$D_c = 10\char`^\left(\frac{\log (D_{ret}) + \log (D_{pass})}{2}\right)$$
(2.12)

For example, center of class for the 16 mm sieve is $D_c = 10^{(\log 16 + \log 22.6)/2} = 19.02$ mm. In terms of ϕ-units, the center of class is the arithmetic mean between the retaining and the passing sieve size. Thus, ϕ_c for the -4 to -4.5 ϕ size class is (-4 +-4.5)/2 = 4.25 ϕ = 19.03 mm. Eq. 2.12 can likewise be expressed by the best-fit regression between D_c and D_{ret}, which yields the linear function

$$D_c = \text{-}0.00284 + 0.841\ D_{ret}$$
(2.13)

The center of class D_c (the central sieve size between the retaining and the passing sieve) is only equal to the particle size of the weight midpoint D_{mc} of the sediment between the retaining and the passing sieves if a sufficiently fine gradation of sieve sizes is chosen (Folk 1966). In order to avoid an imbalance between D_c and D_{mc}, fluvial gravel ranging from sand to cobbles should rather be sieved in increments of 0.5 ϕ than in increments of 1.0 ϕ.

Mean particle b-axes length per size class
The center of class D_c is not generally equal to the (geometric) mean particle b-axis length b_m within that size class and thus can usually not be used as a substitute for b_m. D_c and b_m are only identical for perfect spheres. D_c for the size class 16 to 22.6 mm is 19.02 mm. The range of spheres retained on the 16-mm sieve extends from 16.1 to 22.5 mm with a geometric mean of 19.03 mm.

The b-axes sizes of very flat particles retained on a given sieve are a factor of up to $\sqrt{2} \cong$ 1.4 larger than the b-axes of spheres, extending from 31.9 to 22.5 mm, with a geometric mean of 26.8 mm. Thus, for a sediment mixture of spheres and very flat particles, the geometric mean b-axis length of particles retained on the 16-mm sieve would be somewhere within the range of 19 and 26 mm.

Uneven distribution of particle sizes per sieve class
Fluvial gravel particles are usually not of equal particle shape, particularly not in mountainous areas where bed material comprises a variety of particle shapes due to highly variable transport distances of particles within a reach. This variety of shapes produces an uneven, and approximately normal, distribution of particle b-axes lengths within one sieve class. Small particles are scarce on a sieve because small particles are only retained if they are spherical, while flat particles of the same b-axis length are not retained. Large particles are scarce on a sieve because only those large particles that are flat are passed through the next larger sieve, while round particles of the same b-axis size are retained on that larger sieve. The mid-size range of particles per sieve class comprises all particle shapes, thus mid-sized particles make up the majority of particles per sieve class. Using round-hole sieves, the passing sieve retains all particles with a b-axis larger than the passing sieve size (instead of letting the flat ones through). Thus, the majority of particles retained on a round-hole sieve are close to the passing sieve size when sieving sediment of mixed particle shapes.

2.1.3.5 Comparison of sieve results using round-hole and square-hole sieves

Sieving a given particle mixture with a set of square-hole sieves produces a finer size distribution than would be obtained from sieving the same particle mixture with round-hole sieves. This is because a round-hole sieve may retain particles that are not retained on a square-hole sieve of the same size. For example, an ellipsoidal particle with a b-axis of 50 mm and a c-axis of 30 mm will not pass through a 45-mm round-hole sieve, but will pass through a 45-mm square-hole sieve. Thus, this 50-mm particle will be tallied as larger than 45 mm when using round-hole sieves, and as smaller than 45 mm when using square-hole sieves.

If all particles of the sample are of the same and known shape, results from round-hole and square-hole sieving are convertible. Conversion factors between round-hole and square-hole sieves range from 0.71 for extremely flat particles to 1.0 for spheres (Church et al. 1987) and Fig. 2.4 can be used for conversion between round and square-hole sieve

results. Fluvially transported particles in wadable gravel-bed streams are most likely to be approximately ellipsoidal in shape and therefore are likely to have a conversion factor between 0.8 and 0.9. Note that particle shapes may vary between different size classes or different lithologies. Thus, different conversion factors may have to be applied within one sample to account for this fact.

2.1.3.6 Templates

During field studies, gravel particle sizes are best determined with templates because template measurements provide higher accuracy than measurements with rulers and using templates reduces variability between different operators. A template, also called a gravelometer, is a thin aluminum or plastic plate with several sieve-sized square-holes. The holes usually correspond to the sizes of standard 0.5 ϕ-increment sieve sets, starting at 2 mm, and reaching to 128 or 180 mm, depending on the size of the template. Templates can also be designed with holes in 1, or 0.25 ϕ-increments (Fig. 2.5). A gravelometer made of plastic, about 25 by 30 cm in size, and 0.5 cm thick, can be purchased from Hydro Scientific in Great Britain (Fig. 2.6). U.S. Government agencies can purchase templates from the Federal Interagency Sedimentation Project (FISP) in Vicksburg, Mississippi[1]. The FISP gravelometer US SAH-97 is made of aluminum, is 0.32 cm thick, and has 14 square-holes in 0.5 ϕ-units ranging from -1 to -7.5 ϕ (2 to 180 mm). The overall dimensions are 28 by 34 cm (Fig. 2.7).

Templates are especially useful for pebble counts (Section 4.1.1. and 4.1.2). The operator picks up a particle and pushes the particle through various holes. The aim is to determine a particle's sieve diameter either in terms of "*not passing or larger than*" the hole of a given size, or in terms of "*passing or smaller than*" the hole of a given size. The "larger than" approach records the largest hole size (i.e., sieve size D_s) that is smaller than the particle diameter (equivalent to the sieve size on which the particle was retained). Particle size is tallied as "larger than D_s" where D_s is the next smaller hole size. The "smaller than" approach records the smallest hole size through which the particle could be passed (equivalent to sieve size through which the particle could pass), and tallies the particle as "smaller than D_s", where D_s is the next larger hole size. For example, a rock with a 60 mm *b*-axis would be tallied in the larger than 45 mm class using the "larger than" approach, or as smaller than 64 mm in the "smaller than" approach. It does not matter which approach is followed, as long as one approach is followed consistently. The "larger than" approach seems to be more intuitively connected to note taking when sieving, equivalent to recording the weight of particles "retained on the sieve" with the sieve size D_s. The "smaller than" approach, equivalent to recording the weight of particles "passing a sieve" eliminates one step in the computation of cumulative frequency distribution, which is customarily computed as "percent of particles finer than" or "percent passing", but seems to be less intuitive.

---

[1] *For further information contact FISP at (601) 634-2721.*
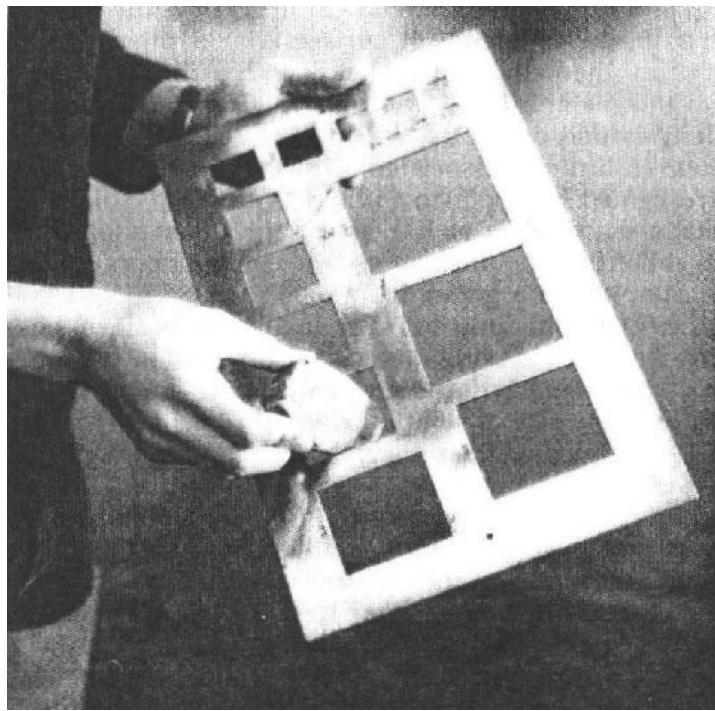
Fig. 2.5: Template in 0.25 ϕ-units used by Hey and Thorne (1983); Reproduced by permission of the American Society of Civil Engineers.
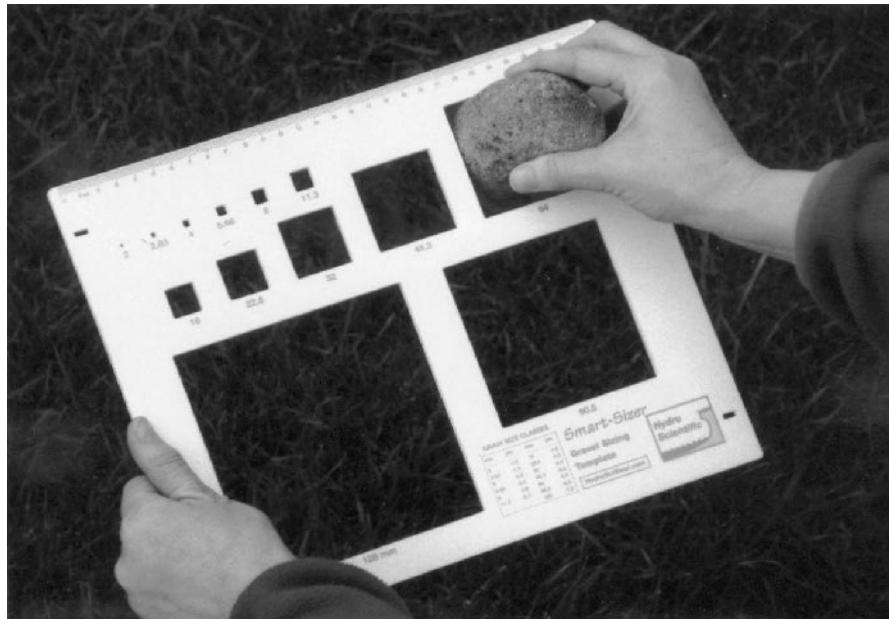
Fig. 2.6: Template available from Hydro Scientific Limited, Stratford-on-Avon, Warwickshire CV37 8EN, UK, Fax/phone:+44-1789-750965, email: HydroSci@aol.com; website: http://members.aol.com/HydroSci. Photo courtesy of Hydro Scientific.
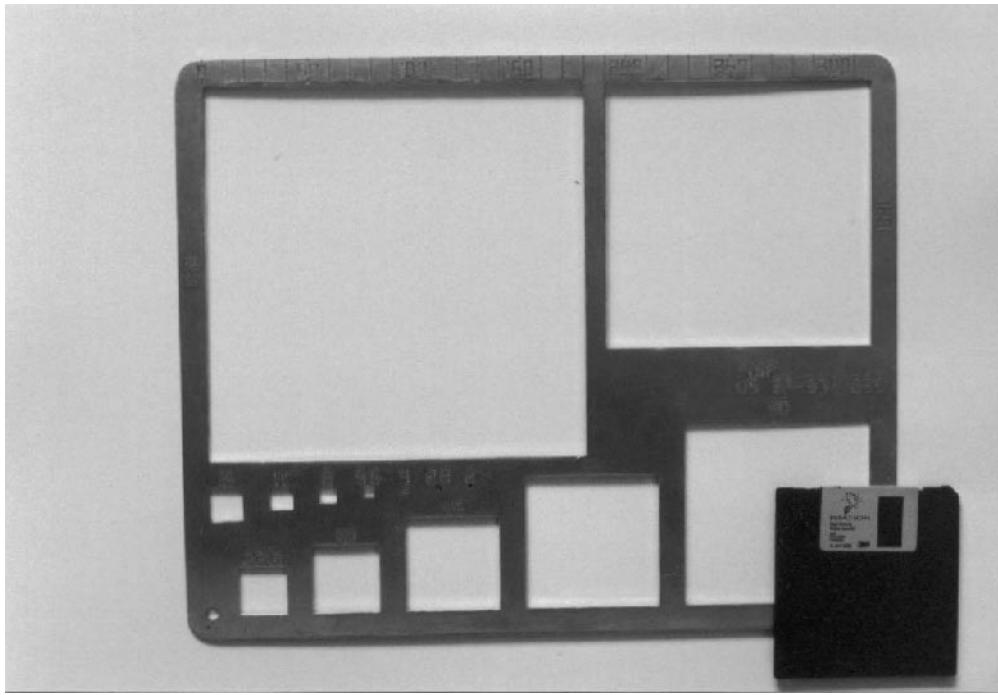
Fig. 2.7: Template US SAH-97, produced by the Federal Interagency Sedimentation Project, website: http://fisp.wes.army.mil/.

Measuring particle sizes with templates is expedient because the appropriate "larger than" or "smaller than" hole size can usually be determined on the first or second try. Templates are also useful for field sieving individual bulk samples. Template measurements are preferable to ruler and caliper measurements for particle-size analyses because potential errors arising from improperly defining the b-axis (Section 2.1.1), or from misreading the ruler can be avoided (Hey and Thorne 1983; Stream Notes, April 1996). The magnitude of errors avoided by template measurements becomes apparent if replicate b-axes measurements with rulers are performed on re-measured rocks. The same operator can usually reproduce particle b-axis measurements correctly. However, when multiple operators re-measure pre-measured particles using a ruler, individual operators produce different results (Wohl et al. 1996). Differences between operators' results are more pronounced when angular particles shapes, and particle structures due to layering or metamorphic processes make the correct identification of the b-axis difficult (Marcus et al. 1995). The use of templates largely eliminates these measurement errors.

2.1.3.7 Rulers and calipers

Some field studies measure the particle b-axis size with a ruler. This procedure is only recommended if the study focuses on measuring particle sizes within a fairly narrow range. An example is the determination of the dominant large particle size from among perhaps 30 large, but not the largest, particles within a given sampling area.

Measuring the particle b-axes size with a ruler or caliper is not recommended in studies that tally b-axes measurements in ϕ units. First, ruler measurements are prone to error because the operator has to accurately determine the orientation of the b-axis (Marcus et al. 1995). Secondly, ruler measurements do not correspond to measurements made with templates, or square-hole sieves. Ruler measurements correspond to measurements with round-hole sieves. Thus, when comparing or merging ruler with template measurements, the same procedures as discussed in Section 2.1.3.5 apply, and particle sizes need to be converted, using for example Fig. 2.4. Finally, no additional information on particle size is gained from measuring b-axes to the nearest mm with a ruler or calipers, if these measurements are then tallied in 0.5-ϕ size classes.

Tallying particle sizes in ϕ units assumes that particle sizes are normally distributed in terms of ϕ units. This assumption does often not hold in a strict statistical sense for particle-size distributions from gravel beds. Nevertheless, a normal distribution is often assumed for convenience, so that standard statistical procedures can be used (Section 2.1.4.3). However, if the assumption of a normal distribution cannot be accepted, measuring particle b-axes lengths to the nearest mm or cm allows for more options in the statistical analysis.

Rulers, or better, calipers, are appropriate for analyses of particle shape in the lab when particle axes are measured by a person aware of the difficulties involved in proper identification of the three particle axes. If large quantities of pebbles need to be measured, a pebble-box (Section 2.1.3.8) may be needed.

2.1.3.8 Pebble-box

The pebble-box was developed by Ibbeken and Denzer (1988) who conducted several large studies of gravel particle shapes. The pebble-box is a convenient device for easy measurements of the three particle axes because it does not require repositioning the particles between measurements, as ruler measurements do, and ensures all three measured particle axes are at right angles. A pebble-box can be constructed of two 3-sided corner pieces each formed by joining the edges of 3 square pieces of plywood. The dimension of the box depends of the particle sizes to be measured. A box 15 - 20 cm along the sides, made of plywood 0.5 - 1 cm thick is suitable for pebbles and small cobbles. A diagonal handle made from a broomstick or a dowel stick is attached to one of the corner pieces (Fig. 2.8). Thin clear plastic rulers in cm and mm gradations are glued to the two top edges and the front edge of the corner piece with no handle. The "zero" marks of all rulers need to be in the corner, so that the distance from the corner can be read.

To measure the three axes a pebble is pushed into the corner of the first pebble-box. The second pebble-box (the one with the handle) is alternately placed along the top, side, and front of the pebble in the box. The length of each particle axis can then be read on the tape measures. The pebble-box is particularly useful when measuring the three axes of a
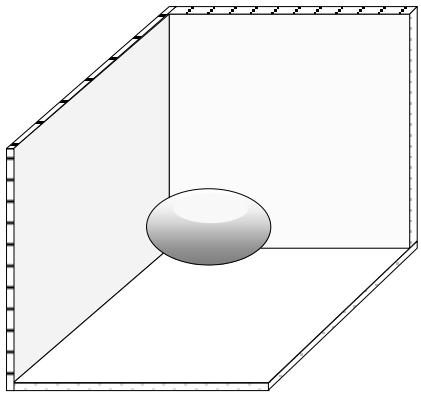
(1) A particle in the stationary corner piece
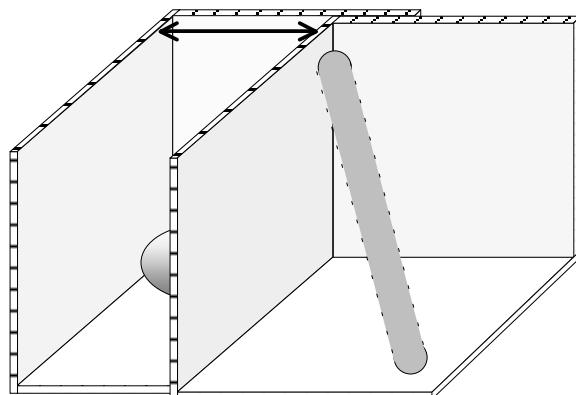
(2) Measuring the longest axis
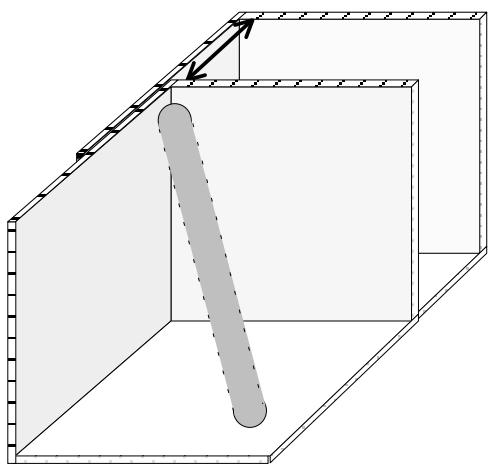
(3) Measuring the intermediate axis
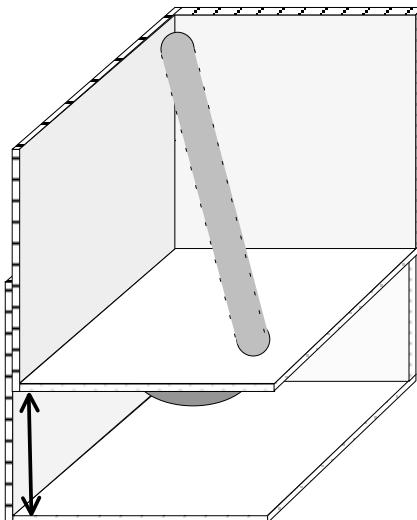
(4) Measuring the shortest axis

Fig. 2.8: Measuring the three particle axes with the pebble-box.

large number of particles. It takes about 20 minutes to measure 100 particles if a second operator records the measurements.

Particle *b*-axes measurements with the pebble-box are similar to measurements with a ruler, or caliper. Thus, particle sizes need to be converted if they are to be compared to particle sizes determined with square-hole sieves (Fig. 2.3 and Section 2.1.3.5). Compared to sieve or template measurements, pebble-box measurements may slightly overpredict the *b*-axes of rhombic or diamond-shaped particles. Particles of this shape

tend to align in the box in such a way that *b*-axes are measured across the largest width, rather than parallel to the sides of the particle (i.e., along the stippled line *b* instead of the solid line *b* in Fig. 2.2).

2.1.3.9 Lab sieving

Sediment from gravel-bed rivers is usually dried before sieving[2]. Wet sediment can be dried on metal pans (e.g., disposable 10-inch pie plates). Two or three days of exposure to air at room temperature is usually sufficient to dry gravel, but the drying process can be accelerated by placing the sediment in an oven at 90ºC (194ºF) overnight. Particles should be allowed to cool to room temperature before sieving and weighing, not only to avoid burning oneself, but also to avoid measuring an increase in particle weight as the particle absorbs air moisture during the cooling phase.

For sieving, the gravel from one or more pie plates is poured into the sieve stack that has a sieve pan at the bottom. The amount of sediment that can be sieved at a time depends on the number of sieves used and on the particle sizes. It is important not to overfill the sieves. As a rule of thumb, particles should not cover the sieves in a layer more than one or two particles thick. Filled in this way, the sieving process takes about 10 minutes when sieves are mounted on a shaker (ROTAP), a sieving apparatus that automatically shakes and taps the sieve stack. If an automatic shaker is not available, the shaking and tapping motion can be imitated by placing the sieve stack onto the floor. The operator sits on a stool in front of the stack, rotating, and tilting the stack forward and backward. A piece of wood placed under the sieve stack protects the floor and the sieves from damaging each other, and provides a hard enough surface when sieving in the field. Gravel particles larger than 8 mm may not require a full 10 minutes of shaking, but particles might still be sieved out of fine gravel and sand after 10 minutes. Some particles will get stuck in the sieves and should be removed and added to the sample before sieving the next subsample. Scrubbing the backside of the sieve and tapping the mesh and the sides of the sieve with a long handled fine wire brush helps clean the fine gravel sieves. Gentle prying with a screw-driver removes particles stuck in larger and more sturdy sieves. Care must be taken not to damage the sieve.

The weighing process depends on the weight range of the scale available in the lab. Sieved size fractions are weighed individually for each sieved subsample for small range scales, but individual size fractions from all subsamples should be combined for large range scales.

It is recommended to prepare data sheets with one column for retaining (or passing) sieve sizes, and one or several other columns for the weight retained on each sieve, depending on the number of subsamples into which the entire sample had to be divided for the sieving process. The example data sheet shown in Fig. 2.9 is for gravel and further differentiation of the sand into size fractions was not needed for that study. Particle weight is usually

---

[2] *Wetsieving as a measure of particle dispersion is not necessary for gravel and sand.*

recorded in grams or in kg. If the scale has only English units, those should be recorded on the data sheets. Unit conversions and all subsequent computations such as adding subsample mass, calculating frequencies and cumulative frequencies should be performed at a later stage after all data have been entered into a spreadsheet program.

Stream:	Date/Time:			
Person sieving:				
Standard sieve set: yes / no ROTAP: yes / no				
Sieving duration: (min)				
Notes:				
Particle size (mm or *f*)	Mass (g) of subsample			
	1	2	3	n
Total				
64				
45.3				
32				
22.6				
16				
11.3				
8				
5.6				
4				
2.8				
2				
<2				

Fig. 2.9: Example data sheet for sieve analysis.

The range of the scale permitting, each subsample should be weighed as a total before sieving. Close correspondence between the total weight and the summed weight of all size fractions makes sure that all recordings are accurate. If this control is not available, it is important to double-check the proper recording of each value. All samples should be retained and put back into their sample bags until after the particle-size analysis, so that samples can be re-measured if results suggest errors.

Sample splitting
The fine part of a large sediment sample from a gravel bed consists of fine gravel and sand, and might weigh 10 – 20 kg. This is considerably more sediment than is needed for a representative particle-size analysis of this size range (see, e.g., Fig. 5.14 for required sample mass for a given D_{max} particle size). It might therefore be useful to split the sample before sieving. A sample is best split using a sample splitter. A riffle splitter consists of a hopper under which a series of up to about 10 equally sized compartments is located. The

bottom outlets of the compartments are alternately directed to the left or the right side of the splitter (see riffle splitter in Fig. 2.10).

Sediment is poured evenly along the entire length of the hopper, making several passes from side to side. The compartments funnel the sediment alternately to the left or the right side of the splitter where the sediment is caught in containers. This process splits the sample in half. Usually, the compartmentalization does not induce sediment sorting, so that an approximately equal amount of sediment of near-equal size distribution is contained in each of the two containers. However, the sediment to be split in a splitter must be dry. Otherwise, fine particles may cling to the compartment walls and produce subsamples with less fines than the original sample.

One passage through the sample splitter divides the sample in half. If one only needs $1/8^{th}$ of the total sample mass, the sample is run through the splitter 3 times, one portion is discarded each time, the remaining portion is split again. If the splitting aim is to obtain a subsample with about $1/5^{th}$ of the total sample mass, the sample is first split into 8 subsamples, two of which are discarded. Three of the $1/8^{th}$ splits are combined and split again to yield a subsample that has $3/16^{th}$ of the total sample volume.

Only one of the subsamples is sieved, unless the operator chooses to sieve several subsamples in order to compute the accuracy of the sieving result (see two-stage sampling, Section 5.4.2.1).

2.1.3.10 Field sieving, weighing, volume determination, and counting

Field sieving, templates and sieve sets
The sample mass required for a good statistical analysis of particle sizes is often approximated by 20 - 100 times the mass of the D_{max} particle size. This amounts to 160 - 800 kg in a gravel bed with a D_{max} of 180 mm (Section 5.4.1.1). Unless vehicle access of the field site and to the lab is excellent, such large samples can best be accommodated by sieving the coarse portion of the sample down to 16 or 11.3 mm in the field.

Field sieving requires a relatively large open and dry work space, and dry weather so that particles can air dry. The surfaces of pebbles air-dry within a day even under overcast skies, provided particles are well spread out on tarps. The weight difference between air-dried and oven-dried particles is usually negligible for pebbles and cobbles, but can make a difference for sand, or for highly porous particles that retain a measurable amount of water. The drying process in the field can be accelerated by using black plastic perforated landscaping cloth instead of tarps, because the fine perforation prevents water puddles on the cloth, and the black color heats up quickly in the sun. Landscaping cloth is light-weight, especially when precut into long strips, but not very durable, and some of the fine sand may pass through the perforation.

After particles are air-dried, any dry sand sticking to larger rocks is brushed off before sieving. Cobbles and boulders larger than the largest sieve size or template hole are

measured with calipers or a ruler. All three axes are measured, and the corresponding sieve diameter of those particles is estimated from the particle *b*- and *c*-axis dimensions.

The equipment used to sieve cobbles and pebbles in the field depends on the scale of the sampling event. A few tarps, one or two templates, a few sturdy plastic shopping bags, and a hanging scale are sufficient for small sample volumes of only a few buckets. Such a field sieving kit is also recommended when working at a remote, hike-in, field site. Starting with the largest particles on the tarp, each particle is picked up and its size class is measured with a template. This task is actually less daunting than it might appear at first. For example, a sample of 135 kg from a gravel-bed stream might only contain 26 particles larger than 64 mm, but these account for 35% of the total weight of the sample (Table 2.2). Continuing with field sieving down to the 22.6 or 16 mm size class, which requires handling roughly 600-1000 particles, analyzes 2/3 to 3/4 of the total sample weight already. Particles of a given size class are collected in plastic bags, or in piles on an extra tarp. The particles of each size class are then weighed using the hanging scale. Alternatively, the number of particles per size class may be counted, and that number can be converted into mass per size class at a later stage.

If the site has vehicle access or is a short distance away from the vehicle, it is advisable to take a lab sieve set to the field when sieving larger volumes of gravel. Less bulky than a stack of lab sieves is a (home-made) sieve box consisting of a frame (approximately 0.2 by 0.3 m, 0.1 m high, into which screens of different mesh width can be inserted (Tom Lisle, pers. comm, 1998)[3]. Particles sieved into different size classes are collected on tarps, pails, plastic tubs, or in strong ziploc bags, depending on the extent of the sampling project. After sieving, particles of a size class can either be weighed, or counted.

There is no rule regarding the lowest sieve size for field sieving, although fine gravel and sand can probably be sieved more conveniently in the lab. If the unsieved portion of the sample is large, it can be split in the field so that sufficient sediment for the remaining largest particle-size class is taken to the laboratory for a standard sieve analysis. A subsample mass of 6 kg is quite sufficient if particles larger than 16 mm have been removed in the field (Eq. 5.40 and Fig. 5.14 provides a relation between required sample mass for a given D_{max} particle size). One method of splitting a sample in the field is to distribute scoops of sediment from the sample alternately into a series of empty buckets. The number of buckets used depends on the desired sediment mass for the subsample. The first scoop goes into bucket 1, the second into bucket 2, etc, until all sediment from the sample is evenly distributed. The volume and the mass in each bucket should be equal. A sturdy ladle works well for scooping sandy and fine gravelly sediment. The number of all subsamples is recorded, but only one of the subsamples is then taken to the lab.

Well thought out field sieving equipment is essential when undertaking an extensive field-sampling program. The minimum field equipment consists of a large rockable sieve-box (ca. 0.5 by 0.5 m, and 0.15 m high) with exchangeable pieces of meshwire corresponding sieving and splitting apparatus to the field site. The device (Fig. 2.10) consists of a frame,

---

[3] *Research Hydrologist, Pacific Southwest Forest and Range Experiment Station, Arcata, CA.*

to sieve sizes. When sieving tons[4] of sediment, Ibbeken (1974) recommends bringing a
approximately 0.5 by 0.5 m, and 0.7 m high, into which a sieve and a sample splitter can
be inserted. The bottom of the frame is connected to a springy and rockable stand (old lab
stool). Two operators can sieve 0.5 - 1 tons of gravelly sediment per day with this
apparatus. The large masses of sediment to be handled require a large number of tarps and
tubs, and a robust field scale for weighing.

Particle weighing
Particles collected per sieve class can be weighed in the field using an accurate hanging
scale that is best hung from a strong tree branch, or from a tripod. The particles to be
weighted are placed into a plastic shopping bag. Such bags have negligible weight, but do
not withstand much use, so a supply is necessary.

Two scales with different ranges are useful if the sample contains large cobbles and small
boulders. Particle weight per size class in a unimodal sample of about 150 kg from a
gravel-bed ranges between 1 and 20 kg (Table 2.2). Thus, a scale with a 0.1 - 10 kg is
suitable. Within the 100 g gradation, readings can be visually interpolated to the nearest
10 or 20 g. If the weight per sieve class exceeds 10 kg, particles are weighed in two
batches. Large cobbles and small boulders are weighed individually. If their individual
weight exceeds 10 kg, a scale with a larger range is needed, or the particle weight is
computed by measuring particle volume and multiplying by an assumed particle density.

Determination of particle volume
It may be useful to determine particle volume in the field. If all particles are of known
density, weight can be computed from particle volume. If particles are of distinctly
different densities, such as volcanic rocks that range from massive basalt to vesicular
pumice that floats on water, it is useful to determine both particle volume and weight to
compute particle density. A tall, straight-walled, bucket with a known diameter and a
holding capacity of about 3 to 5 gallons can be used for measuring particle volume. The
bucket is filled with water to about half its capacity and the water level is read before and
after the cobble is completely submerged. The bucket should stand on a level surface
when reading the water level. If a level surface is not available, the bucket can be
shimmed until level, using a builder's level to verify that the bucket is horizontal. If that is
not possible, the water level needs to be read at several locations and averaged.

---

[4] *Ton (English units) = 907.185 kg = 2000 lb; Metric ton = 1,000 kg = 2,204.63 lb.*
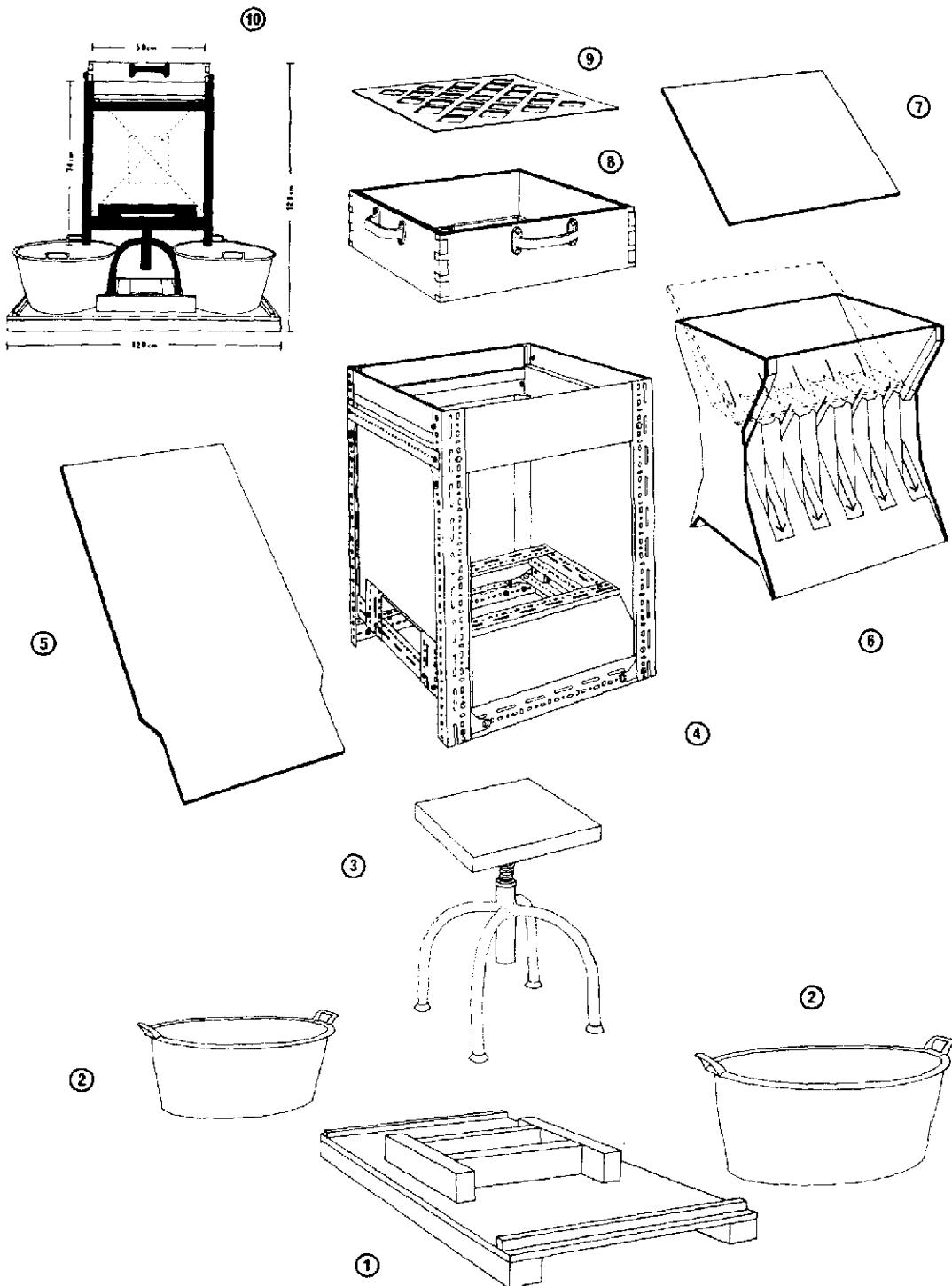
Fig. 2.10: A sieving and splitting device: (1) basal plate, (2) catch bins, (3) rockable, springy stand, (4) central frame, (5) deflecting board, (6) riffle splitter, (7) splitter board, (8) screen frame, (9) screen, (10) assembled device with general measurements (Reprinted from Ibbeken (1974), by permission of the Society of Sedimentary Geology).

Table 2.2: Example of the number of particles and weight per size class in a volumetric bed-material sample. Particles finer than 8 mm were not counted.

Size Class (mm)	No. of Particles	Weight (kg)	% Finer by Weight
256	0	0	100
180	1	16	88
128	1	6	84
90	5	10	76
64	19	14	65
45	66	18	52
32	169	16	40
22.6	326	11	32
16	716	9	25
11.3	1519	7	20
8		6	16
5.6		5	13
4		4	10
2.8		4	7
2		2	5
<2		7	4
		$\Sigma = 135$	

Water levels can be read more easily if a clear plastic tube is mounted along the outside of the bucket. The tube is connected to the inside of the bucket through a hole at the top and the bottom of the bucket. Thus, the water level in the bucket is equal to the water level in the tube outside of the bucket. A ruler mounted next to clear plastic tubing and a drop of dye in the tubing makes the reading even easier. Again, it is essential that the bucket is level.

Particle counting
Counting the number of particles per sieve class is an option if conditions are unfavorable for field weighing. Since the laboratory sieve analysis of sand and pebble particle sizes is mass based, the number of particles counted per sieve class needs to be converted to mass as well. A generalizable relationship can be obtained from the following study.

A relation between mean weight of particles m_{mi} (g) and the retaining sieve size $D_{ret(sq)i}$ (in mm) was established for six bedload- and bed-material samples from mountain gravel-bed rivers with mainly granitic or andesite petrology. Particle shapes within a sample varied, ranging from compact to elongated. A power function in the form of $m_{mi} = a\, D_{ret(sq)i}{}^{b}$ was fitted through the data and yielded a coefficient of determination $r^2 = 0.999$ (Fig. 2.11). Particle density and shape, as well as measurement errors cause slight variability between samples, but for six sediment samples from various gravel-bed streams examined in a study

by the authors, coefficients ranged between 0.0024 and 0.0036, while exponents ranged between 2.92 and 3.04. The mid point of all coefficients and exponents obtained for mean particle weight per square-hole sieve size yielded the equation

$$m_{mi} = 0.00307 \, (D_{ret(sq)i})^{2.98} \tag{2.14}$$

where m_{mi} is the mean weight of particles (g) and $D_{ret(sq)i}$ is the retaining sieve size (in mm) Eq. 2.14 is applicable to mountain gravel-bed streams where bed material comprises a variety of different particle shapes and where a particle density of approximately 2.65 g/cm^3 can be assumed.
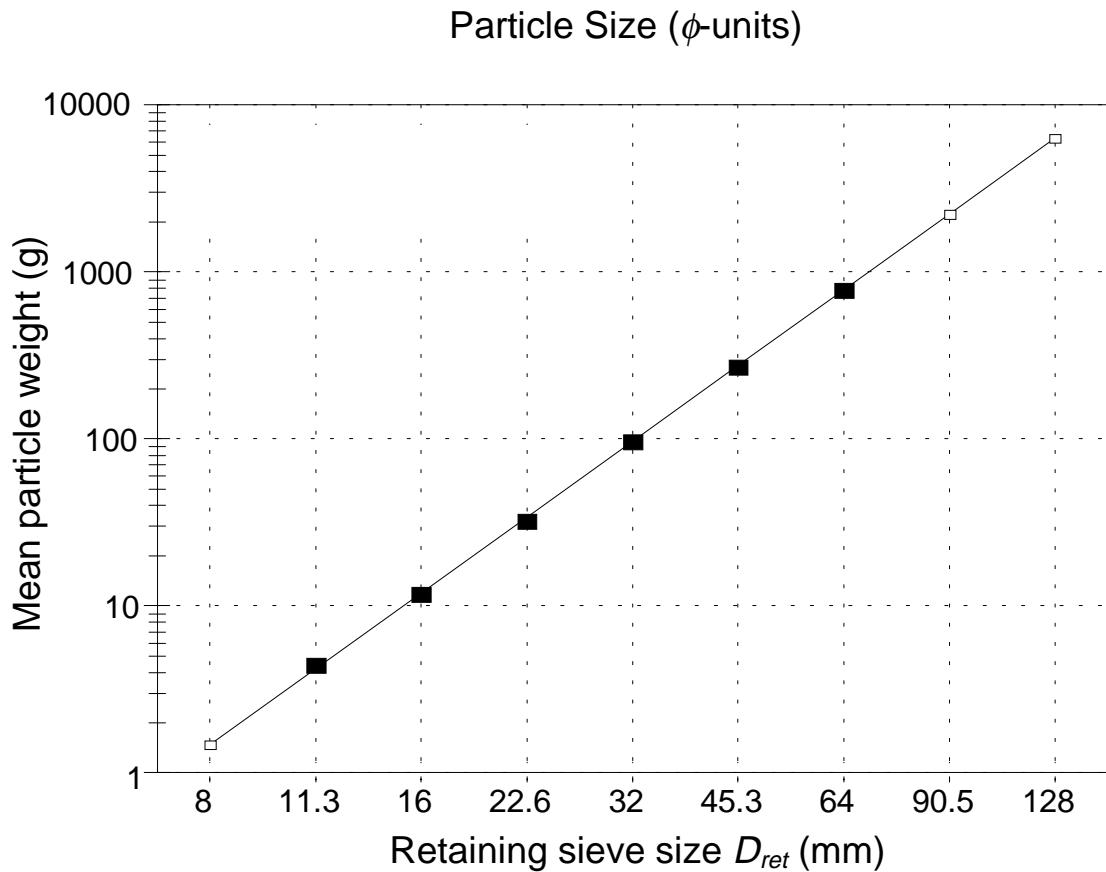
Fig. 2.11: Measured mean particle weight for sieve sizes in 0.5 ϕ-increments for square-hole sieves (■) and the regression function (□). Sediment from Squaw Creek, MT.

2.1.4 Computation of the particle-size distribution

The statistical analysis of a bed-material sample starts with computing a particle-size frequency and percentage frequency-distribution from which a cumulative frequency distribution is computed in the third step. Percentiles are determined from the cumulative distribution curve, and used by themselves, for example when comparing D_{50} sizes, or to derive particle-distribution parameters such as mean, sorting (i.e., standard deviation) and skewness that characterize the distribution as a whole. Particle-distribution parameters can also be computed directly from a frequency distribution (moment methods).

2.1.4.1 Particle-size frequency and cumulative frequency distribution

The result of a laboratory or field particle size-analysis is a record of particle weight (or particle numbers) retained on each sieve size (see data sheet in Section 2.1.3.9). The weight per size class is then entered into a spreadsheet table (see column 1 and 2 in Table 2.3) for all subsequent computations. The first step of analysis is to compute the percentage weight or number frequency for each size class. The weight or number of particles in each size class is divided by the total sample weight or particle number and multiplied by 100 (column 3). The result can be plotted as a percentage frequency distribution (histogram) using a bar graph (Fig. 2.12). Next, the percentage of particle weight or numbers retained on each sieve is converted into the percentage of particle weight or number passing the next larger sieve size (column 4).

For example, a record showing 9.1% of particle weight retained on sieve size 32 mm becomes 9.1% of particle weight passing the sieve size of 45 mm. The percentage particle weight or particle number per size class is then summed starting with the finest size class. This leads to a cumulative weight distribution (column 5) in terms of percent *finer than* or *percent finer* the indicated size class. The cumulative distribution curve could theoretically also be computed in terms of percent coarser or percent retained, but the percent finer or percent passing approach is the commonly used approach for particle-size distributions.

The cumulative particle size-distribution curve (Table 2.3), also called the *sieve curve*, or the *gradation curve*, is plotted with the particle-size classes from column 1 or 2 as the abscissa (x-axis, horizontal), and the percent finer by weight (column 5) on the ordinate (*y*-axis, vertical) (Fig. 2.12). If the analysis is based on frequency-by-number, such as in a pebble-count, the percent finer by number is plotted on the ordinate. If particle sizes are expressed in ϕ-units, the x-axis is kept linear. If particle sizes are expressed in mm, the *x*-axis should be expressed in a logarithmic scale. Alternatively, the mm-sizes of particle size-classes can be plotted in equally spaced increments along the *x*-axis (as in bar or line graphs). Segments of the cumulative distribution curve are connected by straight lines.

Data plotting is often the first step of analysis, especially when dealing with a sample from a new stream site. Visualization of the frequency histogram and the cumulative frequency

Table 2.3: Example of a particle-size analysis for a 103 kg sample of subsurface sediment taken at midstream in a mountain gravel-bed stream (Squaw Creek, MT).

(1a)	(1b)	(2)	(3)	(4)	(5)	(6)		(7)	
x-axis: Size of sieve		y_1-axis: Weight retained on sieve		Weight passing sieve	y_2-axis: Cumulative weight	Percentiles			
(mm)	(ϕ)	(kg)	(%)	(% finer)	(cum. % finer)	(ϕ_p)	(ϕ)	(D_p)	(mm)
<2	<-1	6.7	6.5	-	-				
						ϕ_5	-0.89	D_5	1.8
2	-1.0	2.3	2.3	6.5	6.5				
2.8	-1.5	2.5	2.4	2.3	8.8				
4	-2	2.6	2.5	2.4	11.2				
5.6	-2.5	3.7	3.6	2.5	13.7				
						ϕ_{16}	-2.82	D_{16}	7.1
8	-3.0	5.3	5.1	3.6	17.3				
11.3	-3.5	7.8	7.6	5.1	22.4				
						ϕ_{25}	-3.67	D_{25}	12.7
16	-4.0	9.6	9.4	7.6	30.0				
22.6	-4.5	10.9	10.6	9.4	39.4				
32	-5.0	9.3	9.1	10.6	50.0	ϕ_{50}	-5.00	D_{50}	32.0
45	-5.5	11.4	11.1	9.1	59.1				
64	-6.0	12.2	10.9	11.1	70.1				
						ϕ_{75}	-6.22	D_{75}	74.7
90.5	-6.5	7.4	7.2	10.9	81.1				
						ϕ_{84}	-6.70	D_{84}	104.3
128	-7.0	5.4	5.3	7.2	88.2				
181	-7.5	6.6	6.5	5.3	93.5				
						ϕ_{95}	-7.61	D_{95}	195.8
256	-8.0	0.0	0.0	6.5	100.0				
total:		102.7	100.0						

distribution provides a first impression of the data and is helpful for interpretation. If the graph is used mainly for demonstrative or visualization purposes, the y-axis is usually plotted in a linear scale. If percentile values are to be read off the graph, plotting the y-axis on probability paper increases the accuracy with which the particle size of small and large percentiles can be read.
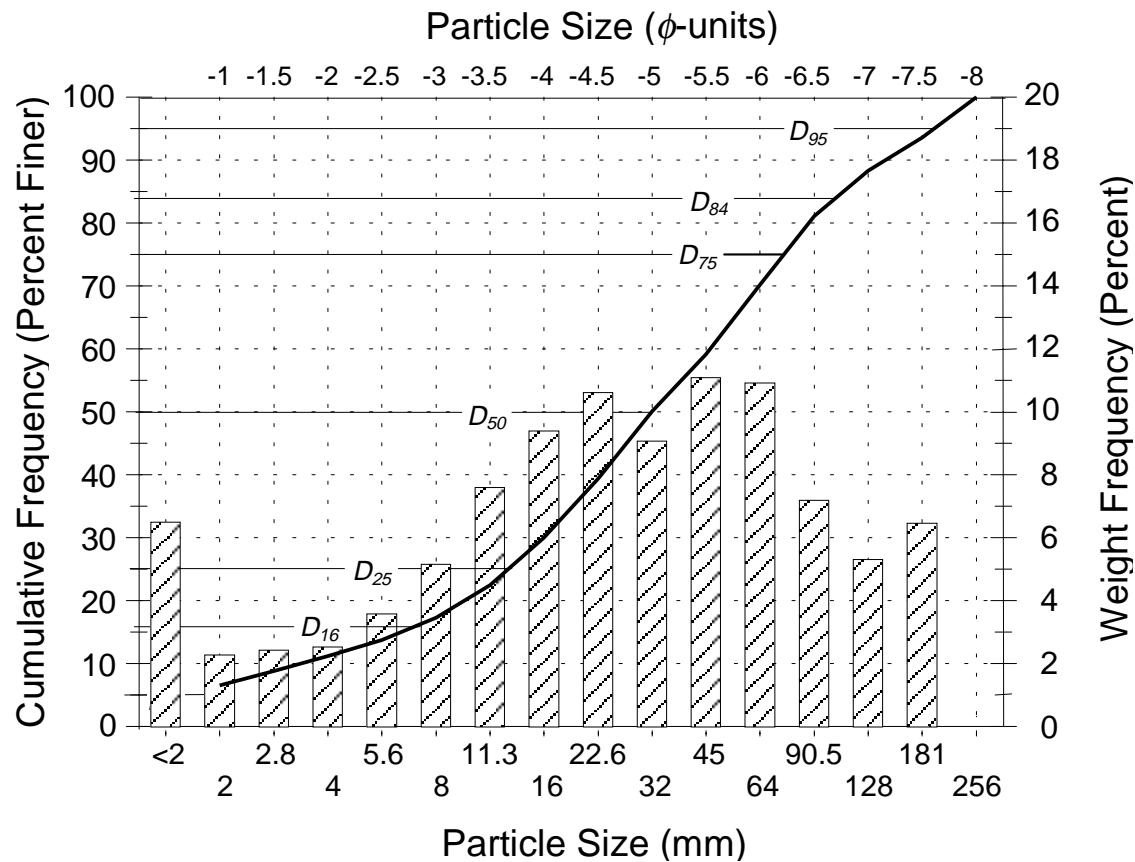
Fig. 2.12: Frequency distribution (histogram with hatched bars) and cumulative frequency distribution curve (thick line) with indicated percentile values for data listed in Table 2.3.

2.1.4.2 Percentiles and their computation

Two sediment mixtures of different particle sizes are usually distinguished by comparing several of the percentile values of the two distributions or the parameters derived from the percentiles. A percentile is a sediment size indicated by the cumulative distribution curve for a particular "percent finer" value. For example, the sediment size for which 80% of the sediment sample is finer is the "80th percentile". The notation is D_{80}, where D represents particle size (in mm) and the subscript "80" denotes 80%. The D_{50} is the median point of the distribution that divides the distribution in two equal parts. The particle size for which 25% of the distribution is finer is the 25th percentile, or the D_{25}. The D_{25} and D_{75} are also called quartiles. Theoretically, any percentile value can be used for comparison, but customarily, the particle sizes of the D_{50}, (i.e., the median), the D_{25} and D_{75} (quartiles), the D_{16} and D_{84}, and the D_5 and D_{95} are used. In a normal distribution, one standard deviation from the median encompasses all data between the D_{16} and the D_{84} and are the points on a distribution curve at which the change of curvature occurs). The D_5 and D_{95} characterize the distribution tails. Data between the D_5 and the D_{95} comprise almost two standard deviations on either side of the D_{50} or median. Those 7 percentiles

may be compared as individual values, or be used to compute distribution parameters such as mean, sorting (i.e., standard deviation), and skewness (Section 2.1.5).

Reading percentiles off a graph plotted on probability paper

Before spreadsheet programs became commonly available, percentiles were often graphically determined from the cumulative particle-size distribution curve plotted on normal probability paper. The y-axis of this graph paper extends from a small value > 0 at the lower end to a value just below 100 at the high end. Probability partitioning spreads the y-axis range at the low and the high end, while compressing the central range around 50. The x-axis is linear for particle sizes in ϕ-units, and lognormal for particle sizes in mm-units. Probability graph paper in linear and logarithmic partitioning is provided in the appendix. The graph of a cumulative particle frequency-distribution approaches a straight line as particle size-distributions approach normality, or lognormality, respectively. A probability plot enables the user to read percentile values in ϕ-units off the graph, but plotting by hand becomes tedious when dealing with large data sets.

Mathematical linear interpolation

An alternative to plotting on probability paper is to compute percentiles mathematically by linear interpolation between two known data pairs of sieve size in ϕ-units and their percentile values in a cumulative distribution. Particle size-classes in mm require a logarithmic interpolation, which means that the mm size classes need to be log-transformed before the interpolation ($\log D$). A particle size ϕ_x of a desired percentile x in ϕ-units can be computed from:

$$\phi_x = (x_2 - x_1) \cdot \left(\frac{y_x - y_1}{y_2 - y_1} \right) + x_1 \tag{2.15}$$

y_2 and y_1 are the two values of the cumulative percent frequency just below and above the desired cumulative frequency y_x (see shaded values in Table 2.3, column 5), and x_2 and x_1 are the particle sizes in ϕ-units associated with the cumulative frequencies y_2 and y_1 (see shaded values in column 1b in Table 2.3). The example below illustrates how the particle size of the percentile ϕ_{16} is computed for the particle-size distribution in Table 2.3 using Eq. 2.15.

$$\phi_{16} = (-3 - -2.5) \cdot \left(\frac{16 - 13.7}{17.3 - 13.7} \right) + -2.5 = -2.82\phi \quad (= 7.1 \text{ mm}) \tag{2.15a}$$

Likewise, the D_{16} is computed from:

$$D_{16} = 10 \wedge \left((\log (8) - \log (5.67)) \cdot \left(\frac{16 - 13.7}{17.3 - 13.7} \right) + \log (5.67) \right) = 7.1 \text{ mm} \qquad (2.15b)$$

Note that the error incurred if the computation is performed with particle sizes in mm without log transformation is relatively small and can maximally reach 1.7 % compared to the result that would have been obtained if log transformed data were used.

2.1.4.3 Testing for various distribution types

Gravel deposits are typically not made up of one particle size only, but comprise a variety of particle sizes that may take up various portions of the sediment volume. One possibility is that particle sizes of each size class (in terms of ϕ-units) may comprise approximately even portions of the total sediment volume (uniform distribution). More typically, medium particle sizes comprise most of the sediment volume with little sediment in the finest and coarsest size classes (normal or log-normal distributions).

Fluvially transported sediment from gravel-bed rivers often tends to roughly approximate lognormal distributions if particle sizes are expressed in mm, or approximate normal (Gaussian) distributions if particles sizes are expressed in ϕ-units which are a logarithmic transformation of particle sizes in mm. Assuming an underlying normal distribution for approximately normal particle-size distributions is convenient because normality is the prerequisite for several statistical applications. Normality is required for (1) binning particle sizes in ϕ-units, for (2) confidence in the results of standard descriptive statistical procedures, as well as for (3) confidence in the results of common sample-size equations.

In a strict statistical sense, particle-size distributions in ϕ-units are often not normally distributed (Church and Kellerhals 1978; Church et al. 1987; Rice and Church 1996b). The tolerable degree of departure from normality varies depending on the planned statistical analysis. Small departures from normality usually do not pose problems when applying statistics that assume normality, but large departures do. If normality is wrongly assumed, results of standard descriptive statistical parameters (e.g., the sample mean, sorting, skewness and kurtosis) may not be accurate and may not serve well to discriminate between samples.

Small departures from normality, however, can greatly affect the sample size required for sampling specified percentiles with a preset precision. For example, in distributions that have a tail of fine sediment, a lower sample size than computed from standard sample-size equations may suffice to predict the D_{95} of the distribution with a preset precision. Contrarily, sample size has to be considerable higher than computed to precisely predict the D_5 (Section 5.2.3.4). Church et al. (1987) and Rice and Church (1996b) therefore recommend that no particular distribution should be assumed for sediment from gravel-bed rivers, not even for large samples for which normality is more intuitively assumed than for small samples. Equations have been developed for estimating sample size when no

particular underlying distribution type is assumed (Section 5.4.1.1). Sample mass predicted from these equations is similar to the sample size predicted by equations based on normal distributions for accurate sampling of high percentiles (Section 5.4.3). But equations based on normal distributions predict that a much lower sample mass would suffice to accurately predict central percentiles.

If a user wants to acknowledge that a particle-size distribution is not strictly normal (in terms of ϕ-units), non-parametric statistics could be applied. Non-parametric statistics are necessary if the data severely deviate from normality. However, non-parametric tests are only beginning to enter mainstream statistical analyses in geomorphology, and results from a relatively unknown test might not be very convincing to a reader. The reader is referred to the statistical literature for non-parametric statistics, none of which are described in this document.

A particle-size distribution can be tested for normality and lognormality in several ways:
- visual evaluation of the plotted graph,
- regression analysis between the cumulative frequency and the respective particle-size classes,
- comparison of frequency distribution with ideal Gaussian or Rosin distributions,
- probability plot of residuals with regression analysis, and
- standard tests for normality and lognormality.

Visual evaluation of the plotted graph
The likelihood of whether a given distribution is normal or lognormal can be estimated by plotting the cumulative size distribution of particle sizes in ϕ units on normal probability paper[5]. Lognormal probability paper is used for plotting if particle sizes are in mm[5]. The straightness of the graph is assessed visually. Ideal normal, or lognormal distributions, respectively, plot as straight lines.

Some computer based statistical packages and some newer spreadsheet programs provide plots on a probability-scaled y-axis for a visual assessment of the degree of normality or lognormality. If such a program is not available, a spreadsheet program can be used to approximate a probability scale. The first step is to compute a cumulative particle-size distribution in which the frequency is expressed in decimals, i.e., as 0.4 instead of 40%. The unsieved remaining particles, i.e., the contents of the "pan" should be excluded from this analysis.

The cumulative frequency distribution can be interpreted as the probability with which to expect a particular particle-size class. A standard normal distribution (or standard normal density function) has a given probability p_i (y-axis) for each value z_{pi} (x-axis of a bell-shaped normal distribution). The values for p and z_p are listed in tables of any general purpose statistics book. For example, probabilities of 0.5, 0.75, 0.975, and 0.99 are

---

[5] *Provided in the appendix of this document.*

obtained by z_p values of 0, 0.675, 1.96, and 2.33. Since the normal distribution is symmetrical, probabilities of 1 - 0.99 = 0.01, and 1 - 0.975 = 0.025 are obtained by z_p values of -2.33, and -1.96, respectively. The relationship between z_p and p can also be approximated from various equations. One of the possibilities provided by Stedinger et al. (1993) is the equation

$$z_p = \frac{p^{0.135} - (1 - p)^{0.135}}{0.1975} \tag{2.16}$$

Using this equation, the z_p value associated with each probability, i.e., each decimal fraction of the cumulative particle size-distribution can be computed in a spreadsheet. In a plot of z_p values versus particle size, the resulting graph is a straight line for normally distributed samples (Fig. 2.13). Deviation from a straight line can be visually assessed by comparison with a best-fit handfitted straight line. For particle-size distributions, a deviation from a straight line is usually most pronounced in the distribution tails, a
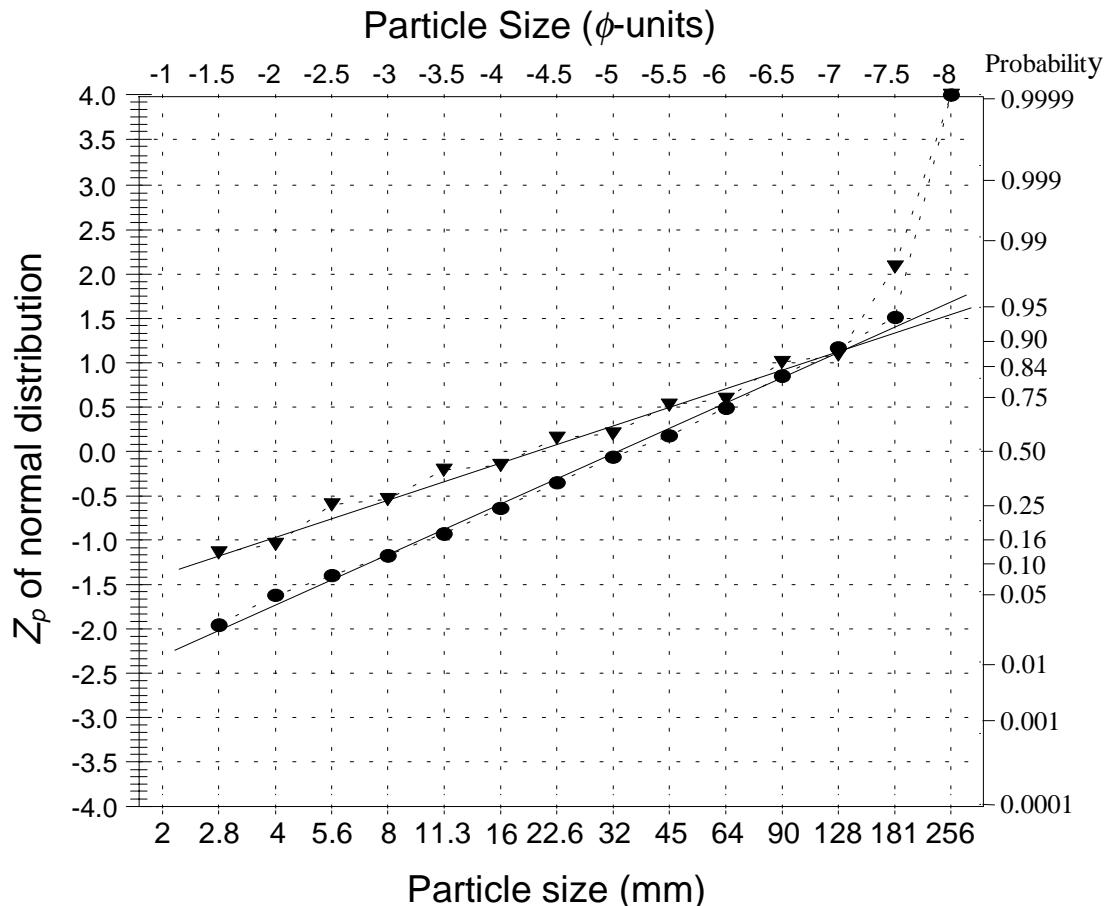
Fig. 2.13: Z_p-values versus particle size for an approximate normal distribution (●) (particle-size distribution shown on Table 2.3 and in Fig. 2.12) and a non-normal block distribution (▼).

44

phenomenon easily checked by the visual assessment. If the deviation of the distribution tails is pronounced, truncating the data set to the range of ϕ_{16} to ϕ_{84}, for example, might straighten the graph.

Caution should be used when interpreting the results of this method. The graph with the black circles in Fig. 2.13 is the particle size-distribution shown in Table 2.3 and Fig. 2.12. The plotted data points seem to resemble a normal distribution well enough to justify the assumption of a normal distribution, and hence to compute distribution parameters or the sampling accuracy for a given sample size. However, non-normal distributions do not necessarily show excessive deviation from a straight line in such plots. Even a definitely non-normally distributed data set that comprises alternate frequencies of 12, 2, 12, 2, etc. for consecutive particle-size classes yields an seemingly reasonable fit to a straight line (graph marked by black triangles in Fig. 2.13). This lack of a standard regarding the tolerable degree of deviation from a straight line is a disadvantage of the visual method.

Evaluation and comparison of regression coefficients
A regression analysis can be performed that regresses ln(y), with y = cumulative frequency, versus x, the particle size in ϕ-units. The coefficient of determination r^2 is computed for the best fit exponential regression y = $a \cdot$ e$^{b \cdot x}$. The closer r^2 approaches the value of 1, the closer the fit with a normal distribution. This approach is useful when comparing the goodness-of-fit to a normal distribution between two samples with a similar range of particle sizes. However, there are no standard values that r^2 needs to obtain in order for the distribution to qualify as normal. This is because the value for r^2 is highly dependent on the particle-size range of the sample.

Comparison with best fit normal and lognormal distributions
Another test for normality of particle-size distributions in ϕ-units is to compute the normal distribution that most closely resembles the measured particle-size distribution and compare the observed and computed distribution. The difference between samples is expressed as a percentage value that then is used to compare the goodness-of-fit between samples. The standard normal distribution in its notation for grouped (i.e., "binned") data is

$$G_{\phi i} = \frac{1}{\sigma \cdot \sqrt{2\,\pi}} \cdot \quad \exp - \left(\frac{(\phi_i - \mu)^2}{2\,\sigma^2} \right) \qquad\qquad (2.17)$$

where $G_{\phi i}$ is the frequency of an equivalent Gaussian distribution for the ith size class in ϕ-units, ϕ_i is the particle size of the ith class in ϕ-units (Schleyer 1987). μ usually denotes the distribution mean, but Schleyer (1987) suggests that the distribution mode (i.e., the size class with the largest frequency) is a more appropriate parameter when analyzing coarse sediment samples in which the finest and the coarsest fractions may not be

representative of the population. Unrepresentative distribution tails affect the distribution mean, but not the mode. If particle frequency-distributions are too irregular in their central parts to benefit from using the distribution mode, the distribution median should be used instead. Various ways of computing a graphic arithmetic mean for particle sizes in ϕ-units are explained in Section 2.1.5.3 (Eqs. 2.31 - 2.34). σ is the distribution standard deviation. In order to minimize the effects of possible truncation on σ, Schleyer (1987) suggests substituting σ by a sorting coefficient s_s which is computed from

$$ s_S = 0.75 \ (\phi_{75} - \phi_{25}) \tag{2.18} $$

and focuses on the more central parts of the distribution[6]. The constant in Eq. 2.19 could be set to 0.5 if normality of the data was not assumed. However, using the constant of 0.75 renders the numerical values of s_S similar to the Inman sorting coefficient s_I (Eq. 2.46, Section 2.1.5.4)

If particle-size data are in mm units, correspondence with a standard lognormal distribution should be tested instead of a normal distribution. The standard lognormal distribution is given by (Gilbert 1987)

$$ L_{Di} = \frac{1}{\sigma \cdot \sqrt{2\,\pi}} \cdot \ \exp - \left(\frac{(\ln D_i - D_m)^2}{2\,\sigma^2} \right) \tag{2.19} $$

where L_{Di} is the frequency of an equivalent lognormal distribution of the ith size class in mm. D_m is the arithmetic mean of the log-transformed data and could be computed as

$$ D_m = \frac{1}{m_{tot}} \ \sum_{i=1}^{n} (D_{ci} \cdot \ m_i) \tag{2.20} $$

where D_{ci} is the center of class in ϕ-units of ith size class, m_i is the weight of particles retained for the ith size class, and m_{tot} is the total weight of particles per sample. Eq. 2.19 can also be applied to number frequencies. In this case, m_i in Eq. 2.20 becomes n_i, the number of particles per size class, and m_{tot} becomes n, the total number of particles per sample.

Other possibilities to compute a distribution mean are shown in Section 2.1.5.3. σ is the distribution standard deviation and computed from

---

[6] σ denotes the standard deviation of a population, s denotes the sample standard deviation. Sorting coefficients denoted by s are an abbreviated computation of standard deviation based on a few percentiles of the distribution.

$$\sigma = \sqrt{\frac{1}{n\text{-}1} \sum_{i=1}^{k} (\ln D_{ci} - D_m)^2}$$ (2.21)

In symmetrical distributions, σ could be approximated by

$$\sigma = 100^{\wedge} \left(\frac{\log D_{84} - \log D_{16}}{2} \right)$$ (2.21a)

which is analogous to the Inman (1952) sorting coefficient s_I (Eq. 2.46). The goodness-of-fit to a Gaussian distribution is computed from the absolute differences between the cumulative percent frequency of the ith size class ($\Sigma m_{\%i}$) of a bed-material sample and the cumulative percent frequency of the ideal Gaussian distribution ($\Sigma G_{\%i}$). These differences are summed over all size classes k and divided by k-1 (Schleyer 1987).

$$\% \text{ Gauss fit} = 100\% - \frac{1}{k\text{-}1} \cdot \sum_{i=1}^{k} |(\Sigma m_{\%i} - \Sigma G_{\%i})|$$ (2.22)

Similarly, the goodness-of-fit to lognormal distributions can be computed from:

$$\% \text{ lognormal fit} = 100\% - \frac{1}{k\text{-}1} \cdot \sum_{i=1}^{k} |(\Sigma m_{\%i} - \Sigma L_{\%i})|$$ (2.23)

The percent goodness-of-fit is affected by whether the percent frequency is allotted to the retaining sieve size D_{ret} or the center of class particle size D_c, and by how the data are summed. If the percent frequency is allotted to D_c and summed such that a 100% cumulative frequency is reached at the D_c of the largest size class, the resulting cumulative frequency is in terms of "as large as or finer than" ($\leq$) the center of class of the largest size class. If the percent frequency is allotted to the retaining sieve size D_{ret}, and summed so that 100% cumulative frequency is reached at the size class above the one with the largest particle, the cumulative frequency is in terms of "smaller than" ($<$), or percent finer than the indicated sieve size. Both procedures were applied to the same particle-size distribution (Table 2.3 and Fig. 2.12) to show the resulting difference (Table 2.4 and Fig. 2.14). A goodness-of-fit of 94.3% was obtained when using the center of class D_c, whereas a goodness-of-fit of 97.2% was obtained when using D_{ret}. Thus, computational consistency is important when comparing the goodness-of-fit between samples. The

Table 2.4: Computation of goodness-of-fit for particle-size distribution in Table 2.3 and Fig. 2.12. $\phi_{25} = 3.99$; $\phi_{75} = 6.3$; $s_S = 1.73$ (Eq. 2.18); $\mu = 5.75 \phi$. Resulting goodness-of-fit (Eq. 2.22) = 97.2%.

No. of size class	Size class		Original distribution			Equivalent Gaussian distribution			Absolute difference
			Mass	Freq.	Cum. freq.	Eq. 2.17 Freq.		Cum. freq.	
class	ϕ_i	D_i	m_i	$m_{\%i}$	$\Sigma m_{\%I}$	$G_{\phi i}$	$G_{\%i}$	$\Sigma G_{\%i}$	$\Sigma m_{\%i}$-$\Sigma G_{\%i}$
	(ϕ)	(mm)	(kg)	(%)	(%)	(-)	(%)	(%)	
(1)	(2)	(3)	(4)	(5)	(6)	(6)	(7)	(8)	(9)
1	1.0	2	2.3	2.4	0.0	0.005	0.3	0.3	0.3
2	1.5	2.8	2.5	2.6	2.4	0.011	0.6	0.9	1.5
3	2.0	4	2.6	2.7	5.0	0.022	1.2	2.1	2.9
4	2.5	5.6	3.7	3.8	7.7	0.039	2.1	4.2	3.5
5	3.0	8	5.3	5.5	11.5	0.065	3.5	7.7	3.8
6	3.5	11.3	7.8	8.1	17.0	0.099	5.4	13.1	3.9
7	4.0	16	9.6	10.0	25.1	0.138	7.5	20.6	4.6
8	4.5	22.6	10.9	11.4	35.2	0.178	9.6	30.2	5.0
9	5.0	32	9.3	9.7	46.5	0.210	11.4	41.5	5.0
10	5.5	45.3	11.4	11.8	56.2	0.228	12.4	53.9	2.4
11	6.0	64	11.2	11.7	68.1	0.228	12.4	66.2	1.9
12	6.5	90.5	7.4	7.7	79.8	0.210	11.4	77.6	2.2
13	7.0	128	5.4	5.7	87.4	0.178	9.6	87.2	0.3
14	7.5	181	6.6	6.9	93.1	0.138	7.5	94.7	1.6
15	8.0	256	0.0	0.0	100.0	0.099	5.4	100.0	0.0
totals:			96.0	100.0		1.85	100.0		38.9

computational difference becomes smaller as the number of particle-size classes increases, which could be achieved if the sample size is large enough to facilitate sieving in size classes of less than 0.5 ϕ.

Comparison with best-fit Rosin distribution
The Rosin exponential distribution was developed for coal milling purposes (Rosin and Rammler 1933, cited after Ibbeken 1983) and applies well to crushed rock. Bed-material frequency distributions that follow Rosin's distribution are skewed towards fine particles and the mode corresponds to the 36.78th percentile (Fig. 2.15) which is approximately the D_{63} if the cumulative frequency is computed as the percent finer or percent passing. The Rosin distribution is typical of jointed rock and unweathered slope sediment, and hence to sediment supplied to the stream from hillslopes (Ibbeken 1983). Thus, testing for a Rosin distribution might be worthwhile, if the bed material has a tail of fine sediment (skewed towards fines) and sediment was supplied from unstable hillslopes.

For particle-size distribution where the center of class is a distinct value representing the total class, the ideal Rosin distribution corresponding to the measured distribution is computed from (Schleyer 1987)

$$R_{Di} = \exp - \left(\frac{D_{pass(i)}}{D_{mode}}\right)^{s_R} - \exp - \left(\frac{D_{ret(i)}}{D_{mode}}\right)^{s_R} \qquad (2.24)$$

where R_{Di} is the frequency of an equivalent Rosin distribution for the ith size class, $D_{pass(i)}$ is the passing sieve size for the ith size class in mm, and $D_{ret(i)}$ is the retaining sieve size for
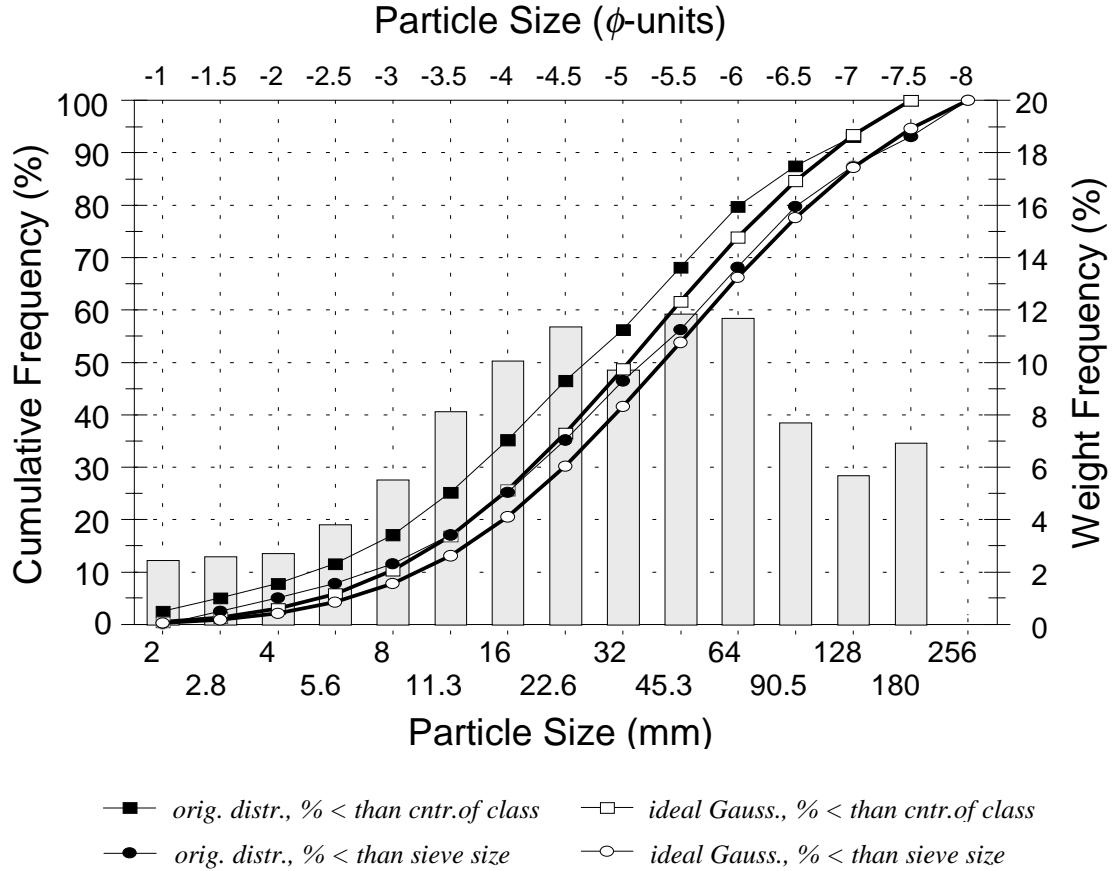
Fig. 2.14: Goodness-of-fit computations based on cumulative frequency in terms of $\leq D_c$, and in terms of $<$ than D_{ret} (% finer or % passing).

the ith size class in mm. D_{mode} is the mode of the distribution, and s_R is the sorting coefficient which for a Rosin distribution is computed from

$$s_R = \frac{2.15}{\phi_{68.4} - \phi_{18.4}} \qquad (2.25)$$
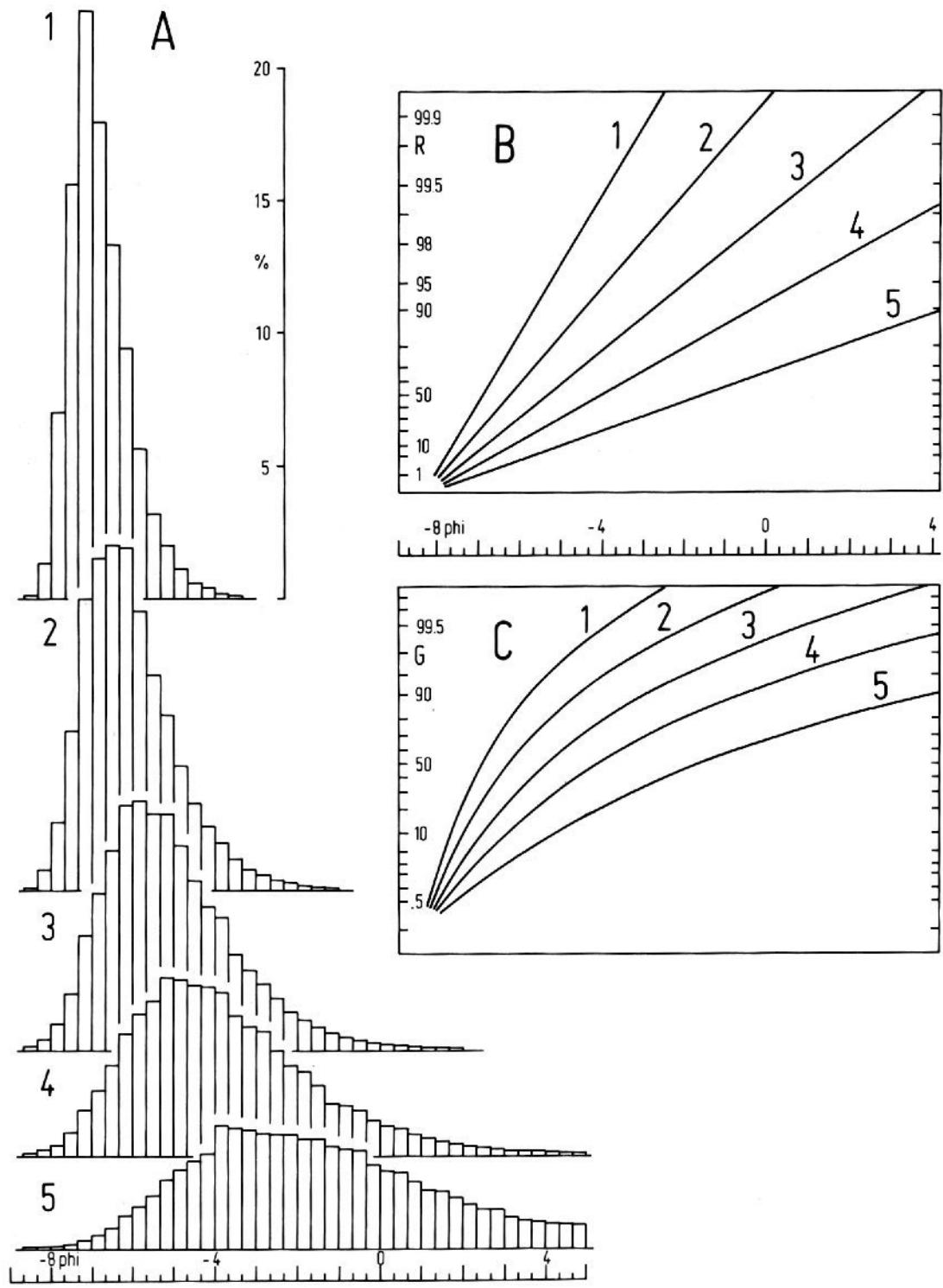
Fig. 2.15: (A) Histograms of ideal Rosin distributions, increasingly poorly sorted from 1 to 5. Cumulative frequency curves of these distributions are plotted on Rosin-coordinate probability paper (B), and on lognormal probability paper (C) (Reprinted from Ibbeken (1983), by permission of the Society of Sedimentary Geologists).

50

The goodness-of-fit to a Rosin distribution can be computed from (Schleyer 1987):

$$\% \text{ Rosin fit} = 100\% - \frac{1}{k-1} \cdot \sum_{i=1}^{k-1} \left| (\Sigma m_{\%i} - \Sigma R_{\%i}) \right| \tag{2.26}$$

where $\Sigma m_{\%i}$ is the cumulative percentage weight frequency of ith sieve class, and $\Sigma R_{\%i}$ is the cumulative percentage frequency of the computed Rosin distribution for the ith sieve class, and k is the number of sieve classes.

Computed this way, the goodness-of-fit to Gaussian and Rosin distributions is *independent* of the range of the particle sizes included in the analysis and the degree of truncation of the size distribution. Hence, bed-material sediment can be partitioned into a gravel and a sand fraction, and goodness-of-fit can be computed for each part individually, a procedure useful for the analysis of bimodal sediment. Goodness-of-fit to Gaussian, or Rosin distributions is also *independent* of the degree of skewness (Section 2.1.5.5) of the bed-material distribution in question. A Gaussian size-distribution that is skewed towards fine particles does not automatically receive a good fit to a Rosin distribution, nor are good Rosin fits reserved for distributions skewed towards fines.

An analysis of the goodness-of-fit to a Gaussian or Rosin distribution can be useful in two ways: First, summary statistics used to describe particle-size distributions may not be meaningful or appropriate, if the fit to a Gaussian distribution is poor. Second, the goodness-of-fit to a Gaussian or a Rosin particle-size distribution can in and of itself serve as a means to analyze fluvial transport distance (Krumbein and Tisdel 1940; Kittleman 1964, both cited in Ibbeken 1983, and Schleyer 1987). A good fit to a normal distribution indicates that the particle-size distribution was derived due to transport controlled factors, whereas a good fit to a Rosin distribution indicates that the particle-size distribution is controlled by supply from the rock source.

Probability plot of residuals and regression analysis
Another procedure to quantitatively evaluate normality is suggested by Neter et al. (1990). The procedure prepares a normal probability plot of residuals and conducts a regression analysis. A residual e_i in a set of x- and y-data is the difference between an observed value y_i and the value Y_i predicted from a regression analysis. For the analysis of normality, the ranked residuals e_i are plotted against the values E_i which the residuals are expected to have under normality. Near linearity of this function indicates that the distribution is near-normal. The degree of linearity, and thus the degree of normality, can be evaluated by the coefficient of correlation r. This value can be compared with table values of r for specified sample sizes and confidence levels to determine whether near-normality can be assumed.

The first step in assessing normality for particle-size frequency distributions is to compute the residuals e_i which are the positive or negative difference between the observed

cumulative percent frequency for a particle size-class D_i and the cumulative percent frequency of an equivalent Gaussian distribution (Eq. 2.17). The next step is to rank the residuals in ascending order from $e_{i=1}$ to $e_{i=k}$, where k is the number of size classes. The expected value E_i of the ranked residuals under normality is computed from

$$E_i = \sqrt{\frac{\sum\limits_{i=1}^{k} e_i^2}{k-2}} \cdot \left[z\left(\frac{i-0.375}{k+0.25}\right) \right] \qquad (2.27)$$

$z(A)$ is the percentile of a standard normal distribution. The table value for $z(A)$ of e.g., 0.841 is 1.00. If A is smaller than 0.5, z is looked up under A-1 and yields a negative value. For example, if $A = 0.159$, $z(0.159 - 1) = z(-0.841) = -1.00$.

Table 2.5 shows the computation of expected values for the residuals E_i using the example particle size-distribution listed in Table 2.3 and shown in Fig. 2.13. The residuals e_i of the observed cumulative percent frequency (column 1 in Table 2.5 and column 6 in Table 2.4) and the cumulative percent frequency of the equivalent Gaussian distribution (column 2 in Table 2.5 and column 9 in Table 2.4) are computed in column 3 of Table 2.5. The residuals e_i are then ranked in ascending order (column 5 of Table 2.5). The summed term in Eq. 2.27 equals 141.02 (sum of column 6) for the example particle size-distribution, and the square-root term is $(141.02/(15-2))^{0.5} = (10.85)^{0.5} = 3.294$.

For the smallest residual e_i with $i = 1$, E_i is computed as:
$$\sqrt{10.85} \cdot z\left(\frac{1-0.375}{15+0.25}\right) = 3.294 \cdot z(0.041) = 3.294 \cdot z(0.959) = 3.294 \cdot -1.739 = -5.728$$

For the second smallest residual e_i with $i = 2$, E_i is computed as:
$$\sqrt{10.85} \cdot z\left(\frac{2-0.375}{15+0.25}\right) = 3.294 \cdot z(0.107) = 3.294 \cdot z(0.893) = 3.294 \cdot -1.243 = -4.094$$

The expected values E_i are symmetrical, so that largest and the second largest values of E_i are 5.728 and 4.094, respectively. Table 2.5 lists all values of E_i in column 10.

For a visual assessment of normality, the ranked residuals e_i are plotted against their expected values E_i (Fig. 2.16). The closer the data points fit to a straight line, the closer is the degree of normality. In addition to a visual assessment, the closeness to a straight line, and thus the degree of normality, can be mathematically quantified. To do so, the ranked residuals e_i are compared to the values expected under normality E_i by computing a linear regression function $E_i = a \cdot e_i + b$. The values E_i predicted from the regression function are listed in column 11 of Table 2.5 and plotted in Fig. 2.16. The coefficient of correlation r is used to indicate the departure from normality. At $r = 1$, the distribution is normal.

52

Table 2.5: Computation of normality for residuals

Orig. distr. Σ% (1)	Gauss. distr. Σ% (2)	residual e_i (1) - (2) (3)	rank (4)	ranked e_i (5)	e_i^2 (6)	$(i-0.375)$ $(k+0.25)$ (7)	(9) - 1 (8)	z (9)	expect. E_i (10)	pred. E_i (11)
0.0	0.3	-0.29	1	-1.56	2.42	0.041	-0.959	-1.739	-5.73	-1.31
2.4	0.9	1.54	2	-0.29	0.08	0.107	-0.893	-1.243	-4.09	-0.27
5.0	2.1	2.94	3	0.00	0.00	0.172	-0.828	-0.948	-3.12	0.35
7.7	4.2	3.50	4	0.25	0.06	0.238	-0.762	-0.713	-2.35	0.85
11.5	7.7	3.80	5	1.54	2.38	0.303	-0.697	-0.516	-1.70	1.26
17.0	13.1	3.95	6	1.87	3.48	0.369	-0.631	-0.335	-1.10	1.64
25.1	20.6	4.58	7	2.18	4.77	0.434	-0.566	-0.168	-0.55	1.99
35.2	30.2	5.02	8	2.37	5.63	0.500		0	0	2.34
46.5	41.5	5.01	9	2.94	8.64	0.566		0.168	0.55	2.70
56.2	53.9	2.37	10	3.50	12.28	0.631		0.335	1.10	3.05
68.1	66.2	1.87	11	3.80	14.41	0.697		0.516	1.70	3.43
79.8	77.6	2.18	12	3.95	15.57	0.762		0.713	2.35	3.84
87.4	87.2	0.25	13	4.58	21.01	0.828		0.948	3.12	4.34
93.1	94.7	-1.56	14	5.01	25.12	0.893		1.243	4.09	4.96
100.0	100.0	0.00	15	5.02	25.17	0.959		1.739	5.73	6.00
		35.17			141.02					
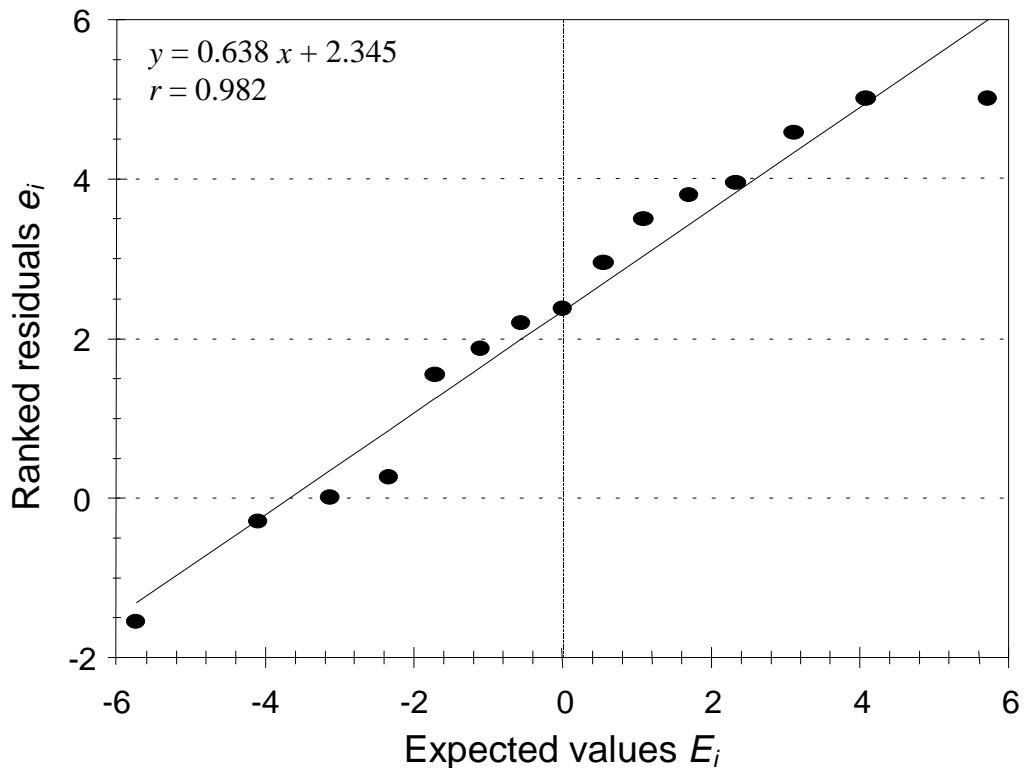
Fig. 2.16: Normal probability plot of ranked residuals versus their expected values under normality. The example particle size-distribution listed in Table 2.3 and shown in Fig. 2.12 is used for the computation.

As *r* becomes < than 1, the distribution departs from normality. Looney and Gulledge (1985) provide table values of *r* that need to be exceeded to assume near-normality for different levels of significance (Table 2.6) and number of data points used for the regression (i.e., the number of size classes *k*). An *r*-value larger than 0.989 for *k* = 15 indicates that the null hypothesis of normality is not rejected in 90 out of 100 cases, and not rejected in 10 out of 100 cases if *r* is larger than 0.951. Neter et al. (1990) suggest that departure from normality is not substantial if *r* exceeds the critical values for $\alpha =$ 0.05. For *k* = 15 this means that even if normality were true, an *r* as small as 0.939 would only occur in 5% of all cases. The example particle size-distribution from Table 2.3 and Fig. 2.12 obtained an *r* = 0.982 in the probability plot (Fig. 2.16). This means that in about 70 out of 100 cases, the null hypothesis of normality is not rejected and near-normality may be correctly assumed for that particle size-distribution.

Table 2.6: Critical values for a coefficient of correlation between ordered residuals e_i and expected residual values under normality E_i when the distribution of error terms is normal (excerpt of table from: Looney and Gulledge 1985).

Number of size classes *k*	Level of significance α					Number of size classes *k*	Level of significance α				
	0.90	0.75	0.50	0.10	0.05		0.90	0.75	0.50	0.10	0.05
5	0.988	0.977	0.960	0.903	0.880	16	0.989	0.985	0.978	0.953	0.941
6	0.986	0.977	0.962	0.910	0.888	17	0.990	0.986	0.979	0.954	0.944
7	0.986	0.978	0.964	0.918	0.898	18	0.990	0.986	0.979	0.957	0.946
8	0.986	0.978	0.966	0.924	0.906	19	0.990	0.987	0.980	0.958	0.949
9	0.986	0.980	0.968	0.930	0.912	20	0.991	0.987	0.981	0.960	0.951
10	0.987	0.980	0.970	0.934	0.918	25	0.992	0.989	0.984	0.966	0.959
11	0.987	0.981	0.972	0.938	0.923	30	0.993	0.990	0.986	0.971	0.964
12	0.988	0.982	0.973	0.942	0.928	40	0.994	0.992	0.989	0.977	0.972
13	0.988	0.983	0.974	0.945	0.932	50	0.995	0.993	0.990	0.981	0.977
14	0.989	0.984	0.976	0.948	0.935	75	0.996	0.995	0.993	0.987	0.984
15	0.989	0.984	0.977	0.951	0.939	100	0.997	0.996	0.993	0.989	0.987

D'Agostino test for normality and lognormality
One of the standard tests for normality and lognormality that is applicable to sample sizes between 50 and 1,000 is the D'Agostino test. The D'Agostino test compares the value of the test statistic *Y* with a table value to accept or reject the null hypothesis that a distribution is normal. If data used in this test are log-transformed, the *Y* statistic can likewise be used to test for lognormality. Gilbert (1987) prefers this test over the Kolmogorov-Smirnov test because the latter is invalid if the parameters of the hypothesized distribution are estimated from the data set itself.

The D'Agostino test ranks the data from smallest to largest. Hence, the test can be used for pebble-count data. In the ranked list, the smallest particle size is listed as many times as the number of particles found in that size class, then the next larger size class is listed

as many times as the number of particles found in that size class, and so on. The D statistic is computed from

$$D = \frac{\sum\limits_{i=1}^{n}(i - 0.5(n+1))\,\phi_i}{n^2 \cdot s} \qquad (2.28)$$

and should be determined to the 5th decimal. s is the standard deviation and is computed from:

$$s = \sqrt{\frac{1}{n-1}\sum\limits_{i=1}^{n}(\phi_i - \phi_m)^2} \qquad (2.29)$$

where ϕ_m is the distribution mean, and i is the ranked order of the data, starting with 1 for the smallest datum, and reaching n for the largest datum. The test statistic Y is computed from:

$$Y = \frac{D - 0.28209479}{0.02998598/\sqrt{n}} \qquad (2.30)$$

The null hypothesis of a normal distribution is rejected at the significance level of $\alpha = 0.05$ if the test statistic Y is less than $Y_{\alpha/2}$, or greater than $Y_{1-\alpha/2}$. The quantiles for $\alpha/2 = 0.025$, and $1-\alpha/2 = 0.975$ are listed for various sample sizes in Table 2.7. The easiest way to obtain quantiles for sample sizes not listed is by interpolation between listed sample sizes. If higher accuracy is required, the quantiles for unlisted n can be predicted from a regression analysis of the quantiles for $\alpha/2$ and $1-\alpha/2$ versus n.

Table 2.7: Quantiles of D'Agostino's test for normality for $\alpha/2 = 0.025$, and $1-\alpha/2 = 0.975$ for $100 < n <500$ (abbreviated from Table A8 in Gilbert 1987, p. 262).

n	100	150	200	250	300	350	400	450	500
$\alpha/2$	-2.552	-2.452	-2.391	-2.348	-2.316	-2.291	-2.270	-2.253	-2.239
$1-\alpha/2$	1.303	1.423	1.496	1.545	1.528	1.610	1.633	1.652	1.668

2.1.5 Computation of particle distribution parameters

Particle-size distributions are commonly characterized by four distribution parameters:

- *mean*, which characterizes the central part of the distribution;
- *sorting* *(i.e. standard deviation)*, or width of the distribution, which is the range of particle sizes within which a preset percentage of all data are contained;
- *skewness*, which is a measure of deviation from symmetry of a distribution; and
- *kurtosis*, which is the flatness or peakedness of the distribution.

Particle distribution-parameters were designed during the 1930's to 1950's. Apart from serving as a means for general sediment classification, ratios of various particle distribution-parameters (e.g., mean versus sorting, or sorting versus skewness) can be used to distinguish between sediments of different origins, transport modes, and the duration or distance of transport.

The literature offers a variety of possibilities for computing distribution parameters. Distribution parameters can be computed using percentiles (graphic approaches), or the percentage frequency of a distribution (frequency approaches), and both methods can be applied to particle sizes in mm (geometric approaches), or to particle sizes in ϕ-units (arithmetic approaches) (Fig. 2.17). The particulars of the data sets (especially the accuracy of the distribution tails), the number of data sets to be analyzed, and the study objective play a role in the decision of which method should be used.
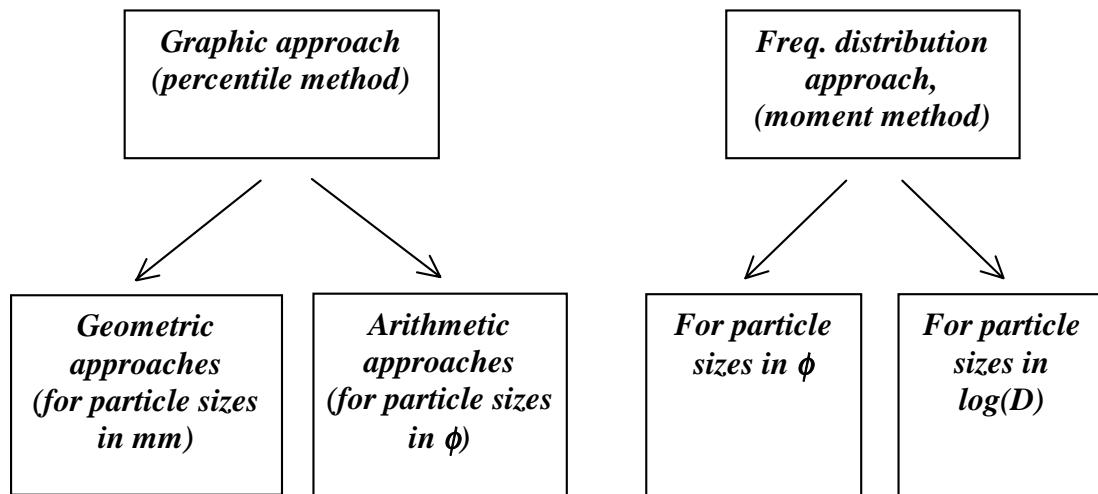
Fig. 2.17: Methods for computing particle-size distribution parameters and their applicability to particle size classes *D* in mm or ϕ-units

Some of the methods provide identical or very similar results when applied to the same data set, whereas results from other methods may be somewhat different or not even comparable. Thus, some methods can be used interchangeably, but others cannot.

56

An overview of the most common approaches to compute the four distribution parameters *mean, sorting, skewness,* and *kurtosis* is provided in Table 2.8. General differences between approaches are explained in the first part of this section. Possible methods used to compute distribution parameters are discussed in the remainder of this section. Finally, all distribution parameters are computed for the example particle-size distribution shown in Table 2.3 and Fig. 2.12, and results of these computations are compared in Table 2.14.

2.1.5.1 Graphic, or percentile methods (geometric and arithmetic)

Graphic methods compute distribution parameters from a few percentile values that are obtained from a cumulative particle-size frequency distribution. Traditionally, graphic methods required a plotted cumulative frequency distribution, preferably on probability paper, so that the percentiles used for the analysis could be easily read from the graph. This is still a viable, though tedious, procedure. For a computerized analysis, percentile values can be obtained from linear interpolation between the percentile values recorded for adjacent ϕ-size classes on the cumulative frequency distribution, or from linear interpolation between log-transformed mm sizes (Section 2.1.4.2). This interpolation requires some time-consuming cell-by-cell computation in spreadsheet programs, so that obtaining the percentile values continues to remain the most laborious part of computing distribution parameters by graphic methods. Once the necessary percentile values are interpolated, distribution parameters can be easily computed from a variety of equations. Equations for the same distribution parameter can employ a different range and number of percentiles, and use percentiles either in ϕ-units or in mm.

Percentiles in ϕ-units for arithmetic approaches and mm-units for geometric approaches
The four distribution parameters: mean, sorting, skewness, and kurtosis, have the most informative value when applied to distributions that are near-normal, or almost Gaussian distributed (see Section 2.1.4.3 for analysis of distribution types). Particle-size distributions in gravel-bed rivers tend to resemble normal distributions when computed in ϕ-units. The degree of normality reached is usually sufficient to compute distribution parameters, although normality may not be obtained in a strict statistical sense. Thus, arithmetic computations of particle-size distribution parameters (Folk and Ward 1957; Inman 1952) are always performed in ϕ-units. A geometric approach is required if computations are preferred in mm-units, because geometric approaches compensate for the absent log transformation of particle sizes. Thus, the first step in a particle-distribution analysis is to evaluate whether the sample distribution approaches a normal, or a lognormal distribution. If the distribution is normal in ϕ-units (or lognormal in mm), a graphic arithmetic approach in ϕ-units, the moment method in ϕ-units, or a geometric approach in mm should be used. If the distribution is normal in mm, which is less likely, mm should be used in a graphic arithmetic approach or the moment method (Fig. 2.17).

Table 2.8: Various methods for computing the distribution parameters mean, sorting, skewness, and kurtosis.

| Distribution parameter | Graphic methods | | | | | Moment Method |
| | Geometric approaches (Particle sizes in mm) | | Mixed approach | Arithmetic approaches (Particle sizes in ϕ-units) | | |
	n^{th} root computation	Log computation	Trask (1932)	Inman (1952)	Folk & Ward (1957)	
Mean (central value)	Root of percentile product $\sqrt{D_{16} \cdot D_{84}}$	Log of percentile product $\dfrac{\log(D_{16} \cdot D_{84})}{2}$	Arithmetic mean of 2 or more percentiles $\dfrac{D_{25} + D_{75}}{2}$	$\dfrac{\phi_{16} + \phi_{84}}{2} = \phi_m$	$\dfrac{\phi_{16}+\phi_{50}+\phi_{84}}{3}$	1st. Moment $\dfrac{\sum(\phi_{ci} \cdot m_i)}{n}$
Sorting (standard deviation)	Root of percentile ratio $\sqrt{\dfrac{D_{84}}{D_{16}}}$	Log of percentile ratio $\dfrac{\log(D_{84}/D_{16})}{2}$	Root of percentile ratio $\sqrt{\dfrac{D_{25}}{D_{75}}}$	Standard deviation $\dfrac{\phi_{84} - \phi_{16}}{2} = \sigma_\phi$	Weighted percentile difference $\dfrac{\phi_{84} - \phi_{16}}{4} + \dfrac{\phi_{95} - \phi_5}{6.6}$	2nd. Moment $\sqrt{\dfrac{\sum m_i(\phi_{ci} - \phi_m)^2}{n-1}}$
Skewness (symmetry)	Mean/Sorting (Fredle Index) $\sqrt{\dfrac{D_{16} \cdot D_{84}}{D_{75}/D_{25}}}$	Mean/Sorting $\dfrac{\log(D_{16} \cdot D_{84})}{\log(D_{75}/D_{25})}$	Mean/Mean $\dfrac{D_{25} \cdot D_{75}}{D_{50}^2}$	Mean1-Median/Sorting $\dfrac{\phi_m - \phi_{50}}{\sigma_\phi}$	Mean-Median/Sorting + Mean-Median/Sorting $\dfrac{\phi_{16}+\phi_{84}-2\phi_{50}}{2(\phi_{84} - \phi_{16})} + \dfrac{\phi_5+\phi_{95}-2\phi_{50}}{2(\phi_{95} - \phi_5)}$	3rd. Moment $\dfrac{\sum m_i(\phi_{ci} - \phi_m)^3}{n \cdot \sigma^3}$
Kurtosis (peakedness)	theoret.: Sorting/Sorting $\sqrt{\dfrac{D_{16}/D_{84}}{D_{75}/D_{25}}}$	theoret.: Sorting/Sorting $\dfrac{\log(D_{16}/D_{84})}{\log(D_{75}/D_{25})}$	Sorting/Sorting $\dfrac{D_{75} - D_{25}}{2(D_{90}-D_{10})}$	Mean-Sorting /Sorting $\dfrac{0.5(\phi_{95} - \phi_5) - \sigma_\phi}{\sigma_\phi}$	Sorting/Sorting $\dfrac{\phi_{95} - \phi_5}{2.44(\phi_{75} - \phi_{25})}$	4th. Moment $\dfrac{\sum m_i(\phi_{ci} - \phi_m)^4}{n \cdot \sigma^4}$

The difference between arithmetic and geometric approaches can best be explained for the parameter "mean". An arithmetic progression is a series of numbers in which the difference between each number and its predecessor is identical: for example, the series 2, 4, 6, 8, or the series 9, 7.5, 6, 4.5. The arithmetic mean is the sum of n terms divided by n. In a geometric progression, each term differs from its predecessor by the same factor (or multiplier) (Table 2.9), for example 2, 4, 8, 16 or -8, -2, -0.5, -0.125. The geometric mean is defined as the central term of an odd number of consecutive terms in a geometric progression. If the number of terms is even, or when the geometric progression is not known, the geometric mean is computed from the nth root of the product of n numbers (Table 2.9). An alternative to the nth root approach is the logarithmic approach, which

Table 2.9: Examples of geometric progressions with a central term, and computation of the geometric mean using the nth root, and the logarithmic approach.

Geometric progression	Ratio $t_3 : t_2 =$ $t_2 : t_1 =$ const.	Geometric mean		
		Central term	nth root approach	Logarithmic approach
4, 6, 9	1.5	6	$\sqrt[3]{4 \cdot 6 \cdot 9} = 6$	$\dfrac{\log (4 \cdot 6 \cdot 9)}{3} = 0.78 = \log 6$
$2, 1, \dfrac{1}{2}, \dfrac{1}{4}, \dfrac{1}{8}$	-0.5	$\dfrac{1}{2}$	$\sqrt[5]{2 \cdot 1 \cdot \dfrac{1}{2} \cdot \dfrac{1}{4} \cdot \dfrac{1}{8}} = 0.5$	$\dfrac{\log (2 \cdot 1 \cdot \dfrac{1}{2} \cdot \dfrac{1}{4} \cdot \dfrac{1}{8})}{5} = -0.30 = \log 0.5$
$3, 3^2, 3^3$	3	3^2	$\sqrt[3]{3 \cdot 3^2 \cdot 3^3} = 9$	$\dfrac{\log (3 \cdot 3^2 \cdot 3^3)}{3} = 0.95 = \log 9$

does not require computing the nth root. This is an advantage when a calculator does not feature the y^x command. The numerical result of the geometric mean from the logarithmic approach is identical to the log of the geometric mean computed by the nth root approach.

Graphic approaches to particle distribution-parameters compute the mean from two or three percentiles. If the arithmetic mean from percentiles in ϕ-units is transformed into mm-units, the result is identical to the geometric mean from the nth-root approach computed from the same percentiles in mm, and to the antilog of the mean from the geometric log approach.

Number and range of percentiles used
To compute the four distribution parameters, Inman (1952), and Folk and Ward (1957) used five different percentiles in ϕ-units: ϕ_{50} (the median), ϕ_{16} and ϕ_{84} (the percentiles at the points of curvature of a Gaussian distribution, approximately the data range of $\pm$ one standard deviation around the mean), and ϕ_5 and ϕ_{95} (two percentiles that characterize the tails of the distribution, the data range of approximately $\pm$ two standard deviations around

59

the median). In Gaussian distributions, the particle sizes of those five percentiles are almost evenly-spaced over the particle-size range. Geometric approaches are commonly based on four percentiles: D_{16} and D_{84} (the percentiles at the point of curvature), and D_{25} and D_{75} (the two quartiles). Trask's (1932) mixed approach uses only the three quartiles D_{25}, D_{50}, and D_{75}.

Statistical analyses are more powerful and informative when data from the entire particle-size range are included, but this holds true only if the accuracy of data is sufficiently high over the entire data range. Distribution tails are prone to sampling errors in samples from gravel-bed rivers. Small sample sizes in which the presence of a large particle accounts for 5 - 10% or more of the total sample weight cause errors at the coarse end. Operator bias against fines in pebble counts, or disregard for the spatial variability of fines within the sampling area, cause uncertainty at the fine end. If there is considerable doubt regarding the accuracy of the distribution tails, peripheral percentiles from the distribution tails should be excluded from the analysis. If the study focuses on the central tendency, the analysis should be limited to the central part of the distribution.

The accuracy of distribution parameters is increased when many percentiles are used for analysis. Up to 7 or 10 percentiles might be used, but eventually there is a trade off between the effort required for interpolating percentiles and the information gained by using a large number of percentiles. A set of 3 to 5 percentile values usually suffices when computing distribution parameters with the goal of describing and identifying a particle size-distribution. When the study objective is to detect minuscule differences between samples, more than 5 percentiles might have to be used. However, the most important factor for the ability of detecting small differences between samples is the necessity of obtaining a sufficiently large sample size (Section 5).

2.1.5.2 Moment, or frequency distribution method

The frequency distribution method, also called the moment method, uses the absolute or percentage frequency of each particle size-class to compute the four moments that are related to the four distribution parameters. Computations are usually performed in ϕ-units, because particle size-distributions tend to resemble a Gaussian distribution when computed in ϕ, but using log-transformed particle-size classes in mm for the analysis (i.e., $\log D$) would work as well.

The moment method requires that the percentage or absolute frequency for all particle-size classes is known, including the fine and the coarse tail, and that size classes are equidistant (e.g., 0.5 ϕ size classes). An unsieved remainder, such as the contents of the pan, or the particle-size category "smaller than 2 mm" cannot be included in the analysis unless this sediment is further differentiated into discrete sieve classes. This measure truncates a sample at the fine end. Similarly, a sample may have to be truncated at the upper end if the percent frequency contributed by one or two particles in the largest size class is unduly high. Truncation, however, alters the shape of the distribution and thus its percentiles

and all summary statistics computed from it. Truncated samples can only be compared among each other if all samples have been truncated at the same upper and lower size classes.

The advantage of the moment method is that the computations of the distribution parameters can be completely computerized once the data are entered. This is a convenient attribute when dealing with a large number of data sets.

Graphic approaches versus moment method
Graphic approaches are mathematically easy to compute once the percentiles have been determined. However, determining the percentiles for a larger number of samples is a rather tedious and time consuming effort when applying graphic methods to a large number of samples. Graphic methods have the advantage of being both standardized and flexible. The Folk and Ward (1957) approach in ϕ-units offers a rating scheme that can be used to classify samples, for example as "poorly" or "well" sorted, or "moderately" or "extremely skewed". Flexibility, by contrast, results from the user's choice of either focusing on central percentiles or extending the analysis to peripheral ones, depending on the accuracy of the distribution tails or the study objective. Graphic approaches can further be modified with respect to the number of percentiles used, and even by altering the computation itself. However, modifications might provide numerical values that differ from the ones obtained by "standard" approaches. If this is the case, classifications of the degree of sorting or skewness, such as those introduced by Folk and Ward (1957), may not be applicable.

The moment method is most suitable for complete and reliable particle-size frequency distributions because, apart from truncation, the user can determine only the width of particle size-classes (e.g., 0.25, 0.5, or 1 ϕ-units). Folk (1966) showed that the moment method overpredicts values of standard deviation if the sediment is only sieved in a few large sieve classes, and the weight midpoint is not equal to the center of class sieve size D_c. To avoid this problem, moment methods should only be applied to sediment sieved in sufficiently small increments. Particle-size classes of 0.5 ϕ should be appropriate for gravel-bed streams with particles ranging between sand and cobbles.

The selection of sieve classes usually needs to be made before sampling, because sieving in smaller size classes requires a larger sample size. Disadvantages of the moment method are the lack of standardized numerical values that distinguish between "poorly" and "moderately" sorted particle size-distributions, or between the degrees of skewness. The moment method is mathematically less straightforward than graphic methods, particularly for the two higher moments representing the parameters skewness and kurtosis. The power expressions of the moment equations need to be solved before they can be applied to grouped data, and the solutions become lengthy for the third and the fourth moment. However, once the solved equations are entered into spreadsheets, computations can be applied to an unlimited number of data sets. The computational rigidity, and the suitability for complete computer processing make the moment method most suitable for analyzing large numbers of samples, that have accurate tails or that can all be truncated at the same upper and lower size classes.

2.1.5.3 Central tendency (mode, median, and mean)

The central tendency of a particle-size distribution can be characterized by its mode, its median, and its mean.

Mode
The mode is the center of the size class that contains most of the sediment, either in terms of weight frequency or number frequency. The mode can be computed in terms of mm sizes or in ϕ-units. The particle-size distribution shown in Table 2.3 and Fig. 2.12 has its mode in the center of the size class 45.3 to 64 mm, or -5.5 to -6.0 ϕ. An analysis of modality determines the number of modes in a distribution. Distributions can be unimodal (one mode), bimodal (two modes), or polymodal (several modes). An irregularity of a frequency distribution in which two non-contiguous size classes have higher weight frequencies than their two neighbors, such as the size classes 45.3 and 22.6 mm in Table 2.3 and Fig. 2.12, does not qualify for bimodality. Bimodality and its computation is explained in Section 2.1.5.9.

Median
The median is the center of the cumulative frequency distribution. The median can be computed in terms of mm sizes as D_{50} or in terms of ϕ-units as ϕ_{50} and is probably the most frequently used parameter in the description of gravel-bed rivers. The distribution in Table 2.3 has a D_{50} of 32 mm, and a ϕ_{50} of -5.0.

Mean
The mean can be considered as the mathematical center of a data set. Means can be computed by a variety of approaches.

Mode, median and mean are equal in symmetrical (unskewed), normally distributed data sets, but not in skewed distributions which, however, are typical of fluvial gravel sediment.

Graphic arithmetic means
The arithmetic mean is the nth fraction of a sum of n numbers. The graphic arithmetic mean is usually computed from two or three percentiles in ϕ-units that have equal distances from the median. It is assumed that particle sizes approximate a normal or Gaussian distribution when expressed in ϕ-units (Section 2.1.2.2). Computations in ϕ-units are usually carried out to two decimals.

Inman (1952) computes the mean from the 16th and the 84th percentile in ϕ-units, both of which are equidistant to the median in a normal distribution.

$$\phi_{m,I} = \frac{\phi_{16} + \phi_{84}}{2} \qquad (2.31)$$

Trask (1932) used the two quartile values.

$$\phi_{m,T} = \frac{\phi_{25} + \phi_{75}}{2} \qquad (2.32)$$

Cumulative distribution curves from unrepresentatively small samples are often jagged and only little accuracy can be placed upon a particular percentile. It is anticipated that these errors tend to cancel each other out if the graphic mean is computed from several percentiles. Thus, Folk and Ward (1957) added the ϕ_{50} as a third datum to the computation.

$$\phi_{m,F\&W} = \frac{\phi_{16} + \phi_{50} + \phi_{84}}{3} \qquad (2.33)$$

Briggs (1977, cited after Gordon et al. 1992) extended the computation evenly over the entire data range and used nine percentile values (see also Folk 1966).

$$\phi_{m,B} = \frac{\phi_{10} + \phi_{20} + \phi_{30} + ... + \phi_{90}}{9} \qquad (2.34)$$

At some point, there is a trade-off between increased accuracy due to a large number of percentiles used for the computations and the computational effort of determining percentiles. The moment method is usually more practical if the entire data range is to be included in the analysis.

Computations of $\phi_{m,I}$, $\phi_{m,F\&W}$, and $\phi_{m,B}$ are identical for distributions that are symmetrical and truly normal in terms of ϕ-units. In particle-size distributions skewed towards a tail of fine particles, typical of gravel-bed rivers, the particle size of $\phi_{m,B}$ is larger than the particle size of $\phi_{m,F\&W}$ which is larger than the particle size of $\phi_{m,I}$.

Graphic geometric mean, square root approach
The geometric mean is the nth root of the product of n numbers. For particle-size distributions, the geometric mean is commonly computed from the square root of two percentiles in mm (Kondolf and Wolman 1993; Yang 1996).

$$D_{gm,sq} = \sqrt{D_{84} \cdot D_{16}} \qquad\qquad (2.35)$$

Graphic geometric mean, cube root approach
Alternatively, the cube root of three percentiles can be taken (Kondolf and Wolman 1993)

$$D_{gm,cu} = (D_{84} \cdot D_{50} \cdot D_{16})^{1/3} \qquad\qquad (2.36)$$

More percentiles could be used if necessary for the study objective. When applied to the same data set, the graphic geometric mean computed in mm from the square or cube root approach is equivalent to the arithmetic mean computed in ϕ-units, transformed into mm (Eq. 2.5).

Graphic geometric mean, log approach
The graphic geometric mean can also be computed from the mathematically more simple log approach. This is an advantage should a calculator not feature the y^x command.

$$D_{gm,log} = 10 \verb|^| \left(\frac{\log (D_{16} \cdot D_{84})}{2} \right) \qquad\qquad (2.37)$$

This geometric mean is equivalent to the geometric mean computed with the square root approach in Eq. 2.35.

Geometric mean from a frequency distribution (power approach)
A geometric mean can also be computed from a particle-size frequency-distribution instead of percentiles. This approach ensures that the mean represents the entire particle-size distribution and does not rely only on a few percentiles. Another advantage is that this computation can be fully computerized and does not require the time consuming task of determining percentiles. Platts et al. (1983) suggest the following equation:

$$D_{gm,pw} = (D_{c1}{}^{m\%_1} \cdot D_{c2}{}^{m\%_2} \cdot \; ... \; \cdot D_{ck}{}^{m\%_k})^{1/100} \qquad\qquad (2.38)$$

where D_{c1} to D_{ck} are the centers of the particle-size classes 1 to k, k is the number of size classes, and $m_{\%i}$ is the percentage particle weight for the ith size class. The computations can likewise be performed for number frequencies, in which case $m_{\%i}$ is substituted by $n_{\%i}$. $D_{gm,pw}$ yields the same result as the mm-transformed mean obtained from the 1st moment method based on ϕ-units.

The first moment (arithmetic mean from a frequency distribution)
Moment methods use all particle size-classes present and compute the arithmetic mean $\phi_{m,frq}$ of a frequency distributions from

$$\phi_{m,frq} = \frac{1}{m_{tot}} \sum_{i=1}^{n}(\phi_{ci} \cdot m_i) \tag{2.39}$$

where ϕ_{ci} is the center of the ith size class in ϕ-units (Section 2.1.5.2), m_i is the weight of particles retained on the ith size class sieve, and m_{tot} is the total weight of particles per sample. For computation using number frequencies, m_i is substituted by n_i, the number of particles per size class, and m_{tot} by n, the total number of particles per sample. For percentage frequency distributions, the equation becomes

$$\phi_{m,frq} = \frac{1}{100} \sum_{i=1}^{k}(\phi_{ci} \cdot m_{\%i}) \tag{2.40}$$

where $m_{\%i}$ is the percentage frequency by weight for particles retained on the ith size class, and k is the number of particle size-classes in the sample. For computations based on frequency by number, $m_{\%i}$ is substituted by $n_{\%i}$.

Mean in mm from a log frequency distribution (log frequency approach)
In analogy to the arithmetic mean computed from the first moment, the mean particle size in mm D_m can also be computed from the antilog of log-transformed particle size classes in mm (log D) (Gordon et al. 1992)

$$D_{m,logfrq} = 10^{\left(\frac{1}{100} \sum_{i=1}^{k}\{\log(D_{ci}) \cdot m_{\%i}\}\right)} \tag{2.41}$$

where D_{ci} is the center of class of the size classes 1 to k, and $m_{\%i}$ is the percentage by weight for the ith size class. Alternatively, $n_{\%i}$, the percent frequency by number can be used instead of $m_{\%i}$. Results of this computation are equal to the power approach in Eq. 2.38 and equal to the arithmetic mean computed by the 1st moment in equation 2.40.

2.1.5.4 Standard deviation and sorting

The standard deviation (σ) expresses the spread or dispersion within normally distributed data sets. Plus and minus one standard deviation ($\sigma = \pm 1$) comprises the central part of

the cumulative frequency distribution that contains 68.26% of all data. Thus, one standard deviation encompasses all data within the interval of the 16th percentile (p_{16}) and the 50th percentile (p_{50}) because

$$p_{16\%} = 50\% - \frac{68.26\%}{2} = 50\% - 34.13\% = 15.86\% \approx 16\% \tag{2.42}$$

plus all the data between the 50th and the 84th percentile (p_{84}) because

$$p_{84\%} = 50\% + \frac{68.26\%}{2} = 50\% + 34.13\% = 84.13\% \approx 84\% \tag{2.43}$$

Thus, the interval between the 84th and 16th percentile (p_{84} and p_{16}) indicates the range of the mode $\mu \pm 1$ standard deviation $((\mu - 1\sigma) + (\mu + 1\sigma))$. A distribution has a standard deviation of $\sigma = \pm 1$ if

$$\sigma = p_{50} - p_{15.86} = 1 \quad \text{and} \quad \sigma = p_{84.13} - p_{50} = 1 \tag{2.44}$$

In symmetrical distributions, Eq. 2.44 is equal to

$$\sigma = \frac{p_{84.13} - p_{15.86}}{2} = 1 \tag{2.44a}$$

Plus and minus two standard deviations ($\pm 2\sigma$) encompass 95.44% of all data, i.e., the data between the 97.72th and 2.28th percentile. A distribution has a standard deviation of $\sigma = \pm 2$ if

$$2\sigma = \frac{p_{97.72\%} - p_{2.28\%}}{2} = 2 \tag{2.45}$$

The computation of standard deviation can become somewhat complicated for grouped data (see computation of the second moment, Eqs. 2.56 to 2.58). Therefore, sedimentologists analyze the spread or dispersion of a distribution from a sorting coefficient that is are computed from a few percentiles of the distribution. The terms sorting coefficient and standard deviation are synonymous for normal distributions, and

their numerical value is identical if the distribution is truly normal. The numerical values of sorting coefficients computed for particle-size distributions in ϕ units have been standardized to compare the spread or dispersion between distributions.

The sorting of a particle-size distribution can be computed in several ways. Some approaches yield identical values, some obtain identity after a transformation, while others are non-comparable. This makes it necessary to analyze the relation between different sorting coefficients.

Graphic arithmetic sorting coefficients
Particle-size distributions of fluvial sediment tend to roughly approximate normal distributions when particle sizes are expressed in ϕ-sizes. In accordance to Eq. 2.44a, Inman's (1952) sorting coefficient s_I uses almost the same percentile difference, but s_I is always positive since it is the *absolute* difference, whereas the standard deviation is defined as the interval of $\pm s$ around the mean.

$$s_I = \left| \frac{\phi_{84} - \phi_{16}}{2} \right| \tag{2.46}$$

As Inman's sorting coefficient uses two percentiles only, particle-size distributions that are quite different can have the same sorting coefficient if only those two percentiles are identical. Folk and Ward (1957) therefore include a broader range of the cumulative size-distribution curve into the sorting analysis and compute sorting as

$$s_{F\&W} = \frac{\phi_{84} - \phi_{16}}{4} + \frac{\phi_{95} - \phi_5}{6.6} \tag{2.47}$$

Folk and Ward (1957) classify the degree of sorting of fluvial sediment into 7 categories (Table 2.10). A chart for visual estimation of sorting is provided in Fig. 2.18.

The two sorting coefficients s_I and $s_{F\&W}$ have identical results when applied to symmetrical normal distributions, although equality may not be present if the distribution is not strictly normal or somewhat skewed. However, fluvial gravel deposits that approach normal distributions in ϕ-units and are only slightly asymmetrical, and which are "poorly" sorted in terms of Folk and Ward (1957), have an Inman (1952) sorting coefficient around 1.5 as well.

Table 2.10: Classification of the degree of sorting (from Folk and Ward 1957)

Sorting Coefficient			Characterization
	>	4	extremely poor
2	-	4	very poor
1	-	2	poor
0.71	-	1	moderate
0.50	-	0.71	moderately well
0.35	-	0.5	well
	<	0.35	very well
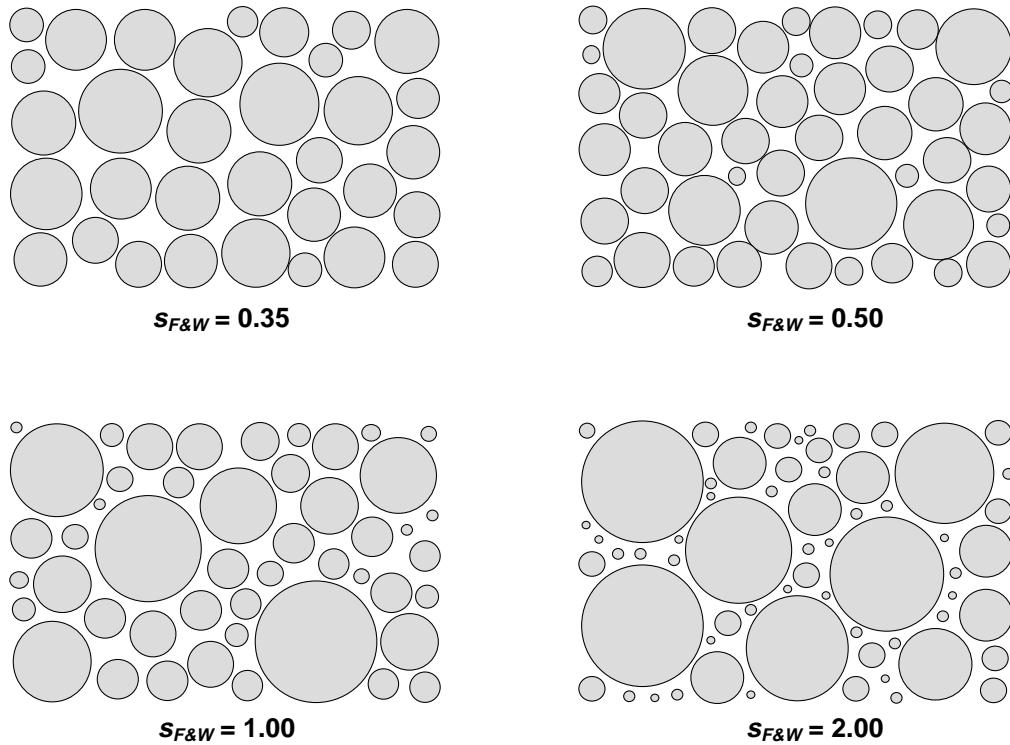
Fig. 2.18: A chart for visual estimation of sediment sorting for the same D_{50} (Redrawn from Pettijohn et al. (1972), by permission of Springer Verlag).

ϕ-based sorting coefficients for fluvial gravel typically range between about 0.5 and 2. Fig. 2.19 shows three example particle-size distributions with a common D_{50} of 32 mm, but with three different sorting coefficients of $s = 0.5$, 1.0, and 1.5. Particle sizes in uncoupled gravel-bed streams might obtain a sorting coefficient of about 0.5 after a long

fluvial transport. Mountain gravel-bed streams with grain sizes ranging from sand to boulders more typically have sorting coefficients in the range of 1.5 to 2.
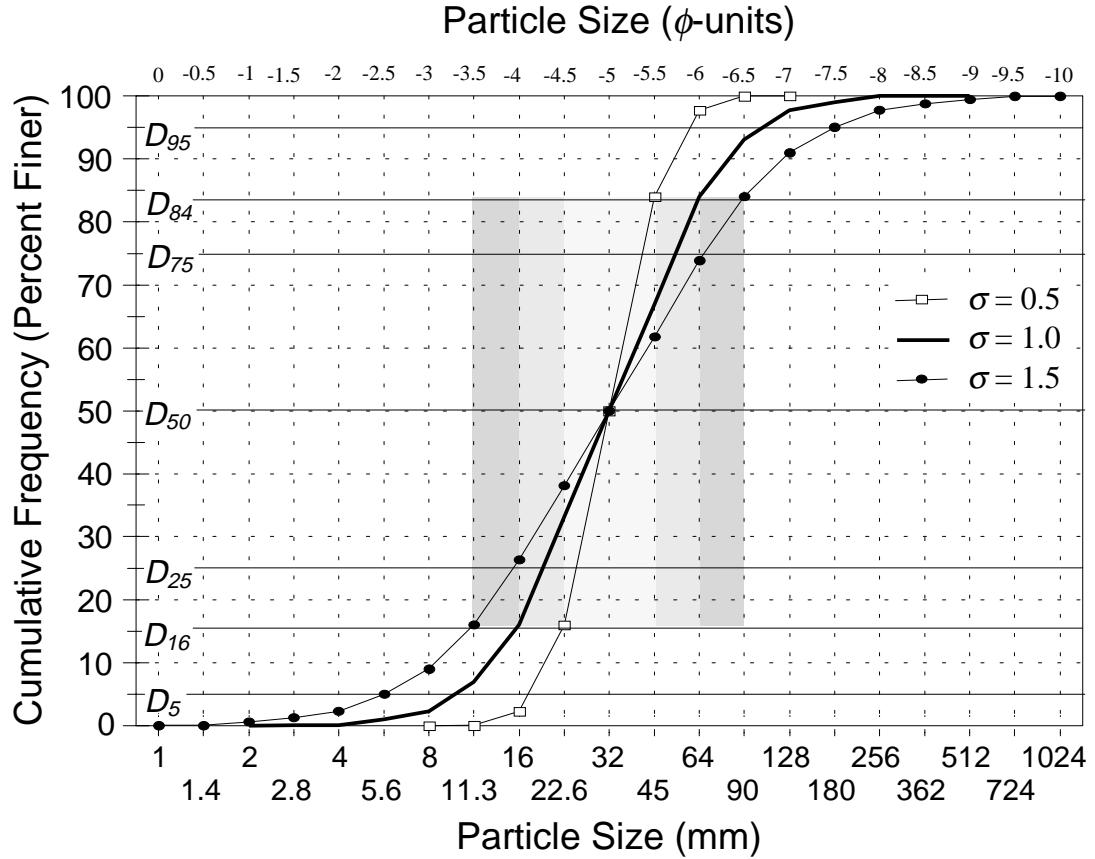
Fig. 2.19: Three particle-size distributions with a common D_{50} of 32 mm, but standard deviations of $\sigma = 0.5$, 1.0, and 1.5. For the curve with $\sigma = 0.5$, the range of one standard deviation between D_{16} and D_{84} is indicated by the lightest gray shade, for the curves with $\sigma = 1$, and $\sigma = 1.5$, the ranges of one standard deviation are indicated by the medium, and the darkest gray shade, respectively.

Graphic geometric sorting coefficients, log approach

Analogous to the standard deviation of particle sizes in ϕ-units in a normal distribution where $2s = \phi_{84} - \phi_{16}$, and $s = (\phi_{84} - \phi_{16})/2$, the standard deviation of a lognormal distribution for particle sizes in mm can be expressed as (Simons and Sentürk 1992)

$$\log s = \frac{\log D_{84} - \log D_{16}}{2} = \frac{\log\left(\dfrac{D_{84}}{D_{16}}\right)}{2} \tag{2.48}$$

The geometric sorting coefficient $s_{g,log}$ can be computed for percentiles in mm by taking the antilog of Eq. 2.48 which yields the same numerical results as the square root expression in Eq. 2.53.

$$s_{g,log1} = 10^{\wedge}\left(\frac{\log(D_{84}) - \log(D_{16})}{2}\right) = 10^{\wedge}\left(\frac{\log\left(\frac{D_{84}}{D_{16}}\right)}{2}\right)$$ (2.49)

Since the term in parenthesis in the first equation is the log of the arithmetic Inman sorting coefficient $s_I = (\phi_{84} - \phi_{16})/2$, results computed by $s_{g,log1}$ and s_I are convertible. By analogy to Eqs. 2.4 and 2.3,

$$s_{g,log,1} = 2^{sI}$$ (2.50)

and

$$s_I = \frac{\log(s_{g,log1})}{\log(2)}$$ (2.51)

The log approach for a geometric sorting coefficient can include the D_{50} value, so that Eq. 2.49 can be rewritten as:

$$s_{g,log2} = 10^{\wedge}\left(\log\left(\frac{\left(\frac{D_{84}}{D_{50}} + \frac{D_{50}}{D_{16}}\right)}{2}\right)\right)$$ (2.52)

Eq. 2.49 and Eq. 2.52 yield identical results if distributions are symmetrical. When applied to the distribution in Table 2.3, Eq. 2.49 provides a numerical value of 3.84 which is similar but not identical to the numerical value of 3.88 provided by Eq. 2.52 for the same data set. Eq. 2.52 can be simplified by eliminating the log and the antilog. This measure yields the gradation coefficient.

Gradation coefficient
The gradation coefficient is a term used in engineering. It computes the spread of a distribution from percentiles in mm (Simons and Sentürk 1992; Julien 1995; Yang 1996)

70

$$s_{grad} = \frac{\left(\dfrac{D_{84}}{D_{50}} + \dfrac{D_{50}}{D_{16}}\right)}{2} \tag{2.53}$$

Eq. 2.53 may be seen as a simplified notation of the log approach in Eq. 2.52, yielding the same result. Note the conceptual difference between the terms "sorting" and "gradation" – sedimentologists refer to a sediment that spreads over a wide size range as poorly sorted, while engineers refer to a poorly sorted sediment as well graded, i.e., it has a wide range of particle sizes that is sufficient for a given application.

Graphic geometric sorting coefficients, square root approach
Instead of an antilog, the logarithmic expression $\log s = (\log D_{84} - \log D_{16})/2$ in Eq. 2.48 can also be solved by a square root equation (Simons and Sentürk 1992; Julien 1995; and Yang 1996)

$$s_{g,sq} = \sqrt{\frac{D_{84}}{D_{16}}} \tag{2.54}$$

Eq. 2.54 and 2.48 yield identical results. An equation of similar form but with different percentiles was proposed by Trask (1932)

$$s_{g,T} = \sqrt{\frac{D_{75}}{D_{25}}} \tag{2.55}$$

Results of Eqs. 2.54 and 2.55 are different because they are based on different percentiles.

Graphic geometric sorting coefficients computed from percentiles in mm are dimensionless.

The second moment (arithmetic sorting from a frequency distribution)
The general form of the equation for the 2nd moment, i.e., the distribution variance, for grouped (or binned) data is

$$s_{frq}{}^{2} = \frac{1}{n\text{-}1} \sum_{i=1}^{k} n_i \, (\phi_{ci} - \phi_m)^2 \tag{2.56}$$

71

where ϕ_{ci} is the center of class in ϕ-units of ith size class, n_i is the number of particles retained for the ith size class, k is the number of size classes in the sample, n is the total number of particles, and ϕ_m is the arithmetic mean of the distribution in ϕ-units. Eq. 2.56 can likewise be applied to the weight of particles for the ith size class, in which case n_i is substituted by the weight of particles in the ith size class m_i. If Eq. 2.56 is applied to percent frequencies, n_i or m_i are substituted by $n_{\%i}$ and $m_{\%i}$, respectively, and m_{tot} or n are set to 100%.

$$s_{frq}{}^2 = \frac{1}{100\text{-}1} \sum_{i=1}^{k} n_{\%i} \, (\phi_{ci} - \phi_m)^2 \tag{2.57}$$

For the actual computation of the sorting parameter, the quadratic expressions in Eq. 2.56 or 2.57 need to be solved and rearranged, and the square root needs to be taken because standard deviation is defined as the square root of variance ($s \equiv \sqrt{s^2}$). Eq. 2.58 is the solution of Eq. 2.56. The solution is similar for Eq. 2.57 for which n_i is substituted by $n_{\%i}$, and $n = 100$.

$$s_{frq} = \sqrt{\frac{\sum_{i=1}^{k} (n_i \cdot \phi_{ci}{}^2) - \left(\frac{\left(\sum_{i=1}^{k} n_i \cdot \phi_{ci} \right)^2}{n} \right)}{n-1}} = \sqrt{\frac{\sum_{i=1}^{k} (n_i \cdot \phi_{ci}{}^2) - n \cdot \phi_m{}^2}{n-1}} \tag{2.58}$$

Conversion between standard deviation of the log-transformed and the original data
If Eqs. 2.56 to 2.58 were applied to particle sizes in mm (exchange all symbols ϕ for D in Eq. 2.58 and compute as above), the resulting numerical value s_{logfrq} has no resemblance to the geometric graphic sorting computed for percentiles in mm (Eqs. 2.49 and 2.52 – 2.54). However, it is possible to compute the graphic arithmetic standard deviation for particle sizes in ϕ-units s_ϕ from the s_{logfrq} (Eqs. 2.56 to 2.58) using the following equation (Church et al. 1987):

$$s_\phi = c \left[\ln \left(\left(\frac{s_{logfrq}}{D_{gm}} \right)^2 + 1 \right) \right]^{0.5} \tag{2.59}$$

D_{gm} is the geometric distribution mean, and $c = 1.4427$ when log-transformations are based on ϕ-units (e.g., equations by Inman), or $c = 0.4343$ for transformations based on the $\log_{10}$ of particle sizes, and $c = 1$ for the ln of particle sizes. Using the example distribution in Table 2.3 and Fig. 2.12, the logarithmic standard deviation s_{logfrq} computed for mm sizes using Eqs. 2.56 to 5.58 is 58.13 mm, the distribution mean D_{gm} (e.g., from

the square root approach in Eq. 2.35) is 27.2 mm. Eq. 2.59 computes a standard deviation of $s_{,\phi} = 1.89$ which is similar to the Inman sorting coefficient of $s_{,I} = 1.94$ (Eq. 2.31), but lower than the standard deviation computed from the second moment of $s_{frq} = 2.02$ (Eq. 2.58). Equity of results requires a true normal/lognormal distribution.

The graphic arithmetic sorting coefficients computed for particle sizes in ϕ-units (s_I or $s_{F\&W}$) yields the same numerical value as the standard deviation s_{freq} computed using equation 2.56 to 2.58 if both distributions are truly normal, and both results are in units of ϕ. Graphic arithmetic sorting coefficients and the standard deviation computed using Eqs. 2,56 to 2.58 produce similar numerical values if the particle-size distribution is not truly normal.

2.1.5.5 Skewness

Normal distributions are symmetric around the mean and not skewed towards either side of the distribution. Distributions with negative skewness are skewed towards the low end tail of the distributions, whereas distributions with positive skewness are skewed towards a high end tail (Fig. 2.20). The degree of skewness of a distribution can be seen as a degree of deviation from normality.
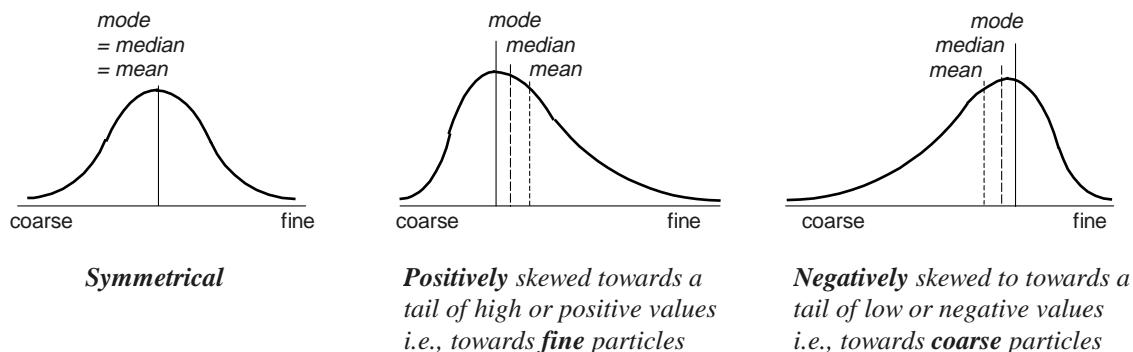
Fig. 2.20: Shape of symmetrical, positively and negatively skewed frequency distributions

When applied to particle-size distributions in ϕ-units, in which the coarsest particles sizes have the smallest numerical values (e.g., $-7\phi = 128$ mm, $-1\phi = 2$ mm, $+2\phi = 0.25$ mm), the term skewness is reversed: positive skewness is towards a tail of fine particles (high ϕ-values, and negative skewness is towards a tail of coarse particles (low ϕ-values).

Bed-material size distributions in ϕ-units in mountain gravel-bed rivers are often skewed towards a tail of finer gravel and sand (positively skewed), and thus deviate from symmetrical normal distributions. In positively skewed distributions, particle frequency of the largest size classes comprise the bulk of the sample, while finer particles cover a wide

range of sizes, but the frequency per size class is low. Positive skewness of a sample can also be the result of unrepresentative sampling in which a few large clasts comprise 30 to 50% of the total sample weight. When analyzing a particle-size distribution for skewness, samples need to be representative such that the weight of the largest size class does not constitute more than a small percentage of total weight. Church et al. (1987) suggested that the maximum allowable weight of the largest size class was 0.1% of the total weight for $D_{max} \leq 32$ mm, 1% for $D_{max} \leq 64$ mm, and 5% for $D_{max} \leq 128$ mm (Section 5.4.1.1).

Particle-size distributions in ϕ-units that are mostly comprised of sand and fine gravel with a few large gravel particles are skewed towards a coarse tail. Such distributions are negatively skewed.

Skewness may be computed from various modifications of the ratio between distribution mean and sorting. Computations may focus on the central part of the distribution, or include the distribution tails to various degrees. The user should select the computational method that suits the data situation and provides the clearest answer to the study objective. If, for example, little confidence can be placed into the tails of a distribution, they should not be included in the analysis because they might distort the result. However, omitting the tails excludes information that under ideal circumstances should have been included.

Graphic arithmetic skewness
Graphic arithmetic skewness is computed from several percentiles in ϕ-units. The percentiles need to refer to the percent *coarser* cumulative frequency distribution if positive skewness is to yield positive skewness values and negative skewness negative values. However, the percent *finer* is the more commonly used form of a cumulative frequency distribution for bed-material samples. Thus, if graphic arithmetic skewness is computed from the percent *finer* distribution, skewness values need to be multiplied by -1 to obtain the correct sign.

The computed value for skewness is sensitive to the range of data used for its computation. Inman (1952) computes skewness as the difference between mean and median divided by sorting.

$$sk_{a,I1} = \frac{\phi_m - \phi_{50}}{\sigma_\phi} = \frac{\dfrac{\phi_{16} + \phi_{84}}{2} - \phi_{50}}{\dfrac{\phi_{84} - \phi_{16}}{2}} = \frac{\phi_{16} + \phi_{84} - 2\phi_{50}}{\phi_{84} - \phi_{16}} \qquad (2.60)$$

In order to account for skewness in the distribution tails, Inman (1952) suggested a second computation in which the data range includes the 95th and 5th percentiles.

74

$$sk_{a,I2} = \frac{\phi_5 + \phi_{95} - (2 \cdot \phi_{50})}{2 \cdot (\phi_{84} - \phi_{16})}$$

(2.60a)

Folk and Ward (1957) combined both of Inman's equations and slightly modified the second one.

$$sk_{a,F+W} = \frac{\phi_{16} + \phi_{84} - (2 \cdot \phi_{50})}{2 \cdot (\phi_{84} - \phi_{16})} + \frac{\phi_5 + \phi_{95} - (2 \cdot \phi_{50})}{2 \cdot (\phi_{95} - \phi_5)}$$

(2.61)

Warren (1974) simplified the Folk and Ward equation for skewness into a form that yields a numerical identical result, but is easier to compute.

$$sk_{a,W} = \frac{\phi_{84} - \phi_{50}}{\phi_{84} - \phi_{16}} - \frac{\phi_{50} - \phi_5}{\phi_{95} - \phi_5}$$

(2.61a)

The numerical values of skewness computed with Eqs. 2.60 or 2.60a are not identical to those from Eq. 2.61 and 2.61a, but all three equations yield 0 for symmetrical distributions, and -1 and +1 for very negatively and very positively skewed distributions. The Folk and Ward (1957) and the Warren (1974) skewness coefficients can be verbally classified into the following categories (Table 2.11).

Table 2.11: Classification of skewness values (from: Folk and Ward 1957)

Skewness value	Description in terms of:	
	ϕ-units	Relative particle size
-0.3 to -1	very negatively skewed	very skewed towards the fine side
-0.1 to -0.3	negatively skewed	skewed towards the fine side
-0.1 to 0.1	nearly symmetrical	nearly symmetrical
0.1 to 0.3	positively skewed	skewed towards the coarse side
0.3 to 1	very positively skewed	very skewed towards the coarse side

Gordon et al. (1992) suggest a computation with a slightly smaller data range, which may be useful when the tails of the distribution are unreliable. Results from Eq. 2.62 and Eqs. 2.61 and 2.61a are not identical.

$$sk_{a,Gor} = \frac{\phi_{84} - \phi_{50}}{\phi_{84} - \phi_{16}} - \frac{\phi_{50} - \phi_{10}}{\phi_{90} - \phi_{10}} \tag{2.62}$$

The quartile skewness coefficient $sk_{a,quart}$ uses only the central 50 percent of the data and completely neglects the distribution tails.

$$sk_{a,quart} = \frac{(\phi_{75} - \phi_{50}) - (\phi_{50} - \phi_{25})}{\phi_{75} - \phi_{25}} \tag{2.63}$$

Trask (1932) limits his equation to the central 50 percent as well, but uses mm units.

$$sk_{a,T} = \frac{D_{25} \cdot D_{75}}{D_{50}^{2}} \tag{2.64}$$

Geometric skewness from the square root approach (Fredle Index)

As with arithmetic skewness (Eqs. 2.60 – 2.63), geometric skewness is the ratio of the geometric mean to geometric sorting. Recall that the geometric mean and geometric sorting can be computed in a variety of ways. A simple expression for geometric skewness is

$$sk_{g,F1} = \left(\frac{D_{84} \cdot D_{16}}{\frac{D_{75}}{D_{25}}} \right)^{0.5} = \text{Fredle index} \tag{2.65}$$

which is also an expression for the Fredle index that is used by fishery biologists to relate permeability and porosity of spawning gravel (Lotspeich and Everest 1981).

Geometric skewness from frequency distributions and percentiles

Platts et al. (1983) compute the Fredle index from:

$$sk_{g,F2} = \frac{(D_{c1}^{m\%_1} \cdot D_{c2}^{m\%_2} ... D_{ck}^{m\%_k})^{1/100}}{\left(\frac{D_{75}}{D_{25}} \right)} \tag{2.66}$$

The numerator of Eq. 2.66 is identical to the geometric mean computed from frequency distributions (power approach, Eq. 2.38). D_{c1} to D_{ck} are the midpoint diameters of particles retained on the kth sieve class, and m_1 to m_k are the percentage weight of particles retained on the kth sieve class. Rice (1995) uses the square root of the denominator, which is the Trask (1932) sorting coefficient (Eq. 2.55).

$$sk_{g,F3} = \frac{(D_{c1}{}^{m\%_1} \cdot \ D_{c2}{}^{m\%_2} ... D_{ck}{}^{m\%k})^{1/100}}{\sqrt{\dfrac{D_{75}}{D_{25}}}} \tag{2.67}$$

Equations 2.65 and 2.67 yield almost identical results. The Fredle index can only be compared between samples if all size distributions are truncated at a common large particle size, such as at 64 mm (Rice 1995), because the value of this index is affected by the truncation point.

A graphic logarithmic approach to compute skewness is not available. But in analogy to graphic logarithmic mean and sorting, a graphic logarithmic skewness could theoretically be computed from the ratio of mean and sorting

$$sk_{g,log} = \frac{\log (D_{16} \cdot \ D_{84})}{\log (D_{75}/D_{25})} \tag{2.68}$$

The third moment (arithmetic skewness from frequency distributions)
The general form of the equation for the 3rd moment for grouped (binned) data is

$$Sk_{frq} = \frac{\displaystyle\sum_{i=1}^{k} m_i (\phi_{ci} - \phi_m)^3}{m_{tot} \cdot \ \sigma^3} \tag{2.69}$$

where ϕ_{ci} is the center of the ith class, ϕ_m is the distribution mean, k is the number of classes, m_i is the particle weight in the ith class, m_{tot} is the total weight of particles, and σ is the distribution sorting as computed from the square root of the 2nd moment (see Section 2.1.5.4). Eq. 2.69 needs to be solved before it can be applied to grouped data. Gordon et al. (1992) provide the following solution

$$sk_{frq} = \frac{m_{tot}}{(m_{tot}-1)\cdot\ (m_{tot}-2)} \cdot \frac{\left(\sum_{i=1}^{k} \phi_{ci}^{3}\cdot\ m_i\right) - 3\phi_m\left(\sum_{i=1}^{k} \phi_{ci}^{2}\cdot\ m_i\right) + 2\ m_{tot}\cdot\ \phi_m^{3}}{s^3} \qquad (2.70)$$

Eqs. 2.69 and 2.70 can be applied to number-frequencies of particles as well. In this case, m_i is substituted by n_i, the number of particles per size class, and m_{tot} by n, the total number of particles per sample. Eqs. 2.69 and 2.70 can also be applied to percent frequencies. In this case, m_i and n_i are substituted by $m_{\%i}$, and $m_{\%i}$, the percentage particle weight and number for the ith size class, and m_{tot} and n are set to 100.

Skewness values computed using the moment method produce positive values for positively skewed distributions, and negative values for negative distributions. However, skewness values from the moment method are not bound to the +1 to -1 interval as is the graphic arithmetic skewness, but may reach values of ±3 or ±4 or more.

2.1.5.6 Kurtosis

Kurtosis denotes the peakedness or flatness of a distribution in comparison to a normal distribution. This measure is only infrequently used to characterize particle-size distributions in gravel-bed rivers.

Graphic arithmetic kurtosis
For particle-size distributions in ϕ-units, Folk and Ward (1957) propose to compute kurtosis using the tails and the quartiles of the distribution.

$$ku_{a,F\&W} = \frac{\phi_{95} - \phi_5}{2.44\cdot\ (\phi_{75} - \phi_{25})} \qquad (2.71)$$

Kurtosis as computed by the Folk and Ward approach can be verbally classified into five categories (Table 2.12)

Table 2.12: Classification of kurtosis values (from Folk and Ward 1957)

Value	Classification	Explanation
< 0.67	very platykurtic	very flat frequency distribution
0.67 - 0.90	platykurtic	flat
0.90 - 1.11	mesokurtic	not especially peaked, normal
1.11 - 1.50	leptokurtic	highly peaked
> 1.50	very leptokurtic	very highly peaked

The Inman (1952) equation is also based on particle sizes in ϕ-units and focuses on the tails of the distribution

$$ku_{a,I} = \frac{0.5\,(\phi_{95} - \phi_5) - \dfrac{\phi_{84} - \phi_{16}}{2}}{\dfrac{\phi_{84} - \phi_{16}}{2}} \tag{2.72}$$

When original untransformed particle sizes in mm are used, kurtosis can be computed from the Trask (1932) equation

$$ku_{a,Tr} = \frac{D_{75} - D_{25}}{2\,(D_{90} - D_{10})} \tag{2.73}$$

Graphic geometric kurtosis
Graphic approaches to compute kurtosis are not available. If kurtosis is regarded as the ratio of two sorting coefficients, kurtosis, in analogy to the square root approach, could hypothetically be computed from

$$ku_{g,sq} = \sqrt{\frac{D_{16}/D_{84}}{D_{75}/D_{25}}} \tag{2.74}$$

Another theoretical computation of kurtosis is analogous to the logarithmic approach

$$ku_{g,log} = \frac{\log\,(D_{16}/D_{84})}{\log\,(D_{75}/D_{25})} \tag{2.75}$$

The fourth moment (arithmetic kurtosis) from frequency distributions)
Kurtosis can also be computed as the fourth moment ku_{frq}. The general form of the equation is

$$ku_{frq} = \frac{\displaystyle\sum_{i=1}^{k} m_i\,(\phi_{ci} - \phi_m)^4}{m_{tot} \cdot \sigma^4} \tag{2.76}$$

79

where ϕ_{ci} is the center of the ith class, ϕ_m is the distribution mean, k is the number of classes, m_i is the absolute frequency of particle weights or numbers in the ith class, m_{tot} is the total weight of particles, and σ is the distribution sorting as computed from the square root of the 2nd moment (see Section 2.1.5.4). Eq. 2.76 can likewise be used for number frequencies ($m_i \rightarrow n_i$; $m_{tot} \rightarrow n$), or for percentage frequencies ($m_i \rightarrow m_{\%i}$ or $n_{\%i}$; $m_{tot} \rightarrow$ 100). Eq. 2.76 becomes rather extensive when solving the term $m_i (\phi_{ci} - \phi_m)^4$ and will not be shown here since kurtosis is infrequently used to characterize a particle-size distribution.

2.1.5.7 Comparison between methods

The four distribution parameters (mean, sorting, skewness and kurtosis) were computed for the example particle-size distribution in Table 2.3 using several methods. The distribution is poorly sorted and skewed towards large particles. The same methods and equations as shown in Table 2.8 were applied. The results of those computations are listed in Table 2.14 for a comparison of methods.

Mean
Arithmetic and geometric mean are both in units of length and mutually convertible. The arithmetic mean of particle sizes in ϕ-units, converted back into units of mm (Eq. 2.5 or 2.6), equals the geometric mean of particle sizes in mm, if the computations are based on the same percentiles (Table 2.13). Similarly, geometric mean, computed in mm and transformed to ϕ-units using Eq. 2.3 or 2.4 equals the arithmetic mean computed for ϕ-units.

All of the means are smaller than the D_{50} or ϕ_{50} because the particle-size distribution is skewed towards fine particles. Trask's mean is considerably larger than the distribution D_{50} in skewed distributions because skewed distributions have a large mm-value of the D_{75}.

Sorting
Arithmetic sorting coefficients and the standard deviation computed from the moment approach produce identical values for true normal and symmetrical distributions (Table 2.14). Arithmetic sorting coefficients computed from ϕ-unit for the distribution in Table 2.3 differ somewhat between methods because the distribution is not truly normal, but all values are generally within the same range. Hence, the Inman sorting $s_I = 1.94$ (Eq. 2.46) and the Folk and Ward sorting $s_{F\&W} = 1.70$ (Eq. 2.47) are not identical. The difference between s_I and the 2nd moment $s_{frq} = 2.02$ (Eq. 2.58) may be attributed to truncation of the distribution at the fine end, because the unsieved remainder in the size class smaller than 2 mm was excluded in the moment method, but is included in the computation of percentiles from the cumulative percentage frequency (i.e., the percent finer).

Table 2.13: Equality between various geometric and arithmetic means when computed by different approaches for the same distribution and expressed in the same units. Numbers in parenthesis indicate equation numbers in Section 2.

Geometric mean (computed in mm)	=	Arithmetic mean (comp. in ϕ), expressed in mm
Geom. mean (computed in mm), expressed in ϕ	=	Arithmetic mean (computed in ϕ)

Square root appr. (35) $\quad \sqrt{D_{16} \cdot D_{84}} \quad$ = $\quad$ Inman appr. (31) $\quad \dfrac{\phi_{16} + \phi_{84}}{2}$

Log appr. (37) $\quad 10^{\left(\frac{\log(D_{16} \cdot D_{84})}{2}\right)} \quad$ = $\quad$ Inman appr. (31) $\quad \dfrac{\phi_{16} + \phi_{84}}{2}$

Cube root appr. (36) $\quad (D_{16} \cdot D_{50} \cdot D_{84})^{1.3} \quad$ = $\quad$ Folk & Ward appr. (33) $\quad \dfrac{\phi_{16} + \phi_{50} + \phi_{84}}{3}$

Power appr. (38) $\quad (D_{c1}^{\,m\%1} \cdot D_{c2}^{\,m\%2} \cdot \ ... \cdot D_{ck}^{\,m\%k})^{1/100} = \quad$ 1st moment (40) $\quad \dfrac{1}{100} \sum_{i=1}^{k} (\phi_{ci} \cdot m_{\%i})$

Log freq. appr. (41) $\quad 10^{\left(\frac{1}{100}\sum_{i=1}^{k}\{\log(D_{ci}) \cdot m_{\%i}\}\right)} \quad$ = $\quad$ 1st moment (40) $\quad \dfrac{1}{100} \sum_{i=1}^{k} (\phi_{ci} \cdot m_{\%i})$

Table 2.14: Results of distribution parameters computed with several methods for the example particle size-distribution in Table 2.3 (Small numbers in *italics* refer to equation numbers in Section 2).

($D_5 = 1.8$, $\quad D_{16} = 7.1$, $\quad D_{25} = 12.7$, $\quad D_{50} = 32.0$, $\quad D_{75} = 74.7$, $\quad D_{84} = 104.3$, $\quad D_{95} = 195.8$ mm;
$\phi_5 = -0.89$, $\quad \phi_{16} = -2.82$, $\quad \phi_{25} = -3.67$, $\quad \phi_{50} = -5.00$, $\quad \phi_{75} = -6.22$, $\quad \phi_{84} = -6.70$, $\quad \phi_{95} = -7.61$).

	Freq.distr.appr.	Graphic (or percentile) approaches							Freq.distr.appr.
	Geometric approaches (for mm)						Arithmetic approaches (in ϕ)		
	power appr.	grad. coeff.	square root	log appr.	cube root	Trask (1932)	Inman (1952)	Folk & Ward (1957)	Moment Method*
Mean (ϕ)	-	-	-	-	-	-	-4.76	-4.84	-4.74
(mm)	26.8	-	27.2	27.2	28.7	43.7	27.2	28.7	26.8
Eq.	*38*	*-*	*35*	*37*	*36*	*32*	*31*	*33*	*40*
Sorting (ϕ)	-	-	-	-	-	-	1.94	1.70	2.02
(mm)	-	-	-	-	-	-	3.84	3.25	4.06
(-)	-	3.88	3.84	3.84	-	2.42	-	-	-
Eq.		*53*	*54*	*49, 52*	*-*	*55*	*46*	*47*	*58*
Skewness (-)	11.1	-	11.2	3.73	-	19.0	0.12	0.17	0.72
Eq.	*66*	*-*	*65*	*68*	*-*	*64*	*60*	*6 1*	*70*
Kurtosis (-)	-	-	1.6	1.5	-	0.2	0.7	1.1	-
Eq.	*-*	*-*	*74*	*75*	*-*	*73*	*72*	*71*	*76*

* Computations for the moment method excluded sediment passing the 2 mm sieve from the analysis.

Geometric sorting coefficients computed from percentiles in mm are dimensionless and only a measure of the logarithmic standard deviation which has units of mm. The square root approach (Eq. 2.54) and the log approach (Eq. 2.49) yield identical results $s_{g,sq} = s_{g,log} = 3.84$, which in a true lognormal distribution would be identical to the gradation coefficient $s_{grad} = 3.88$ (Eq. 2.53) as well. Some of the geometric and arithmetic sorting coefficients are transformable.

The geometric sorting coefficient of the untransformed data in mm $s_{log,1}$ and Inman's arithmetic sorting coefficient s_I computed for ϕ-units are convertible using Eqs. 2.51 and 2.52. Similarly, the standard deviation in ϕ-units can be estimated from the standard deviation computed from particle sizes in mm according to the moment method (Eqs. 2.56 – 2.58) by applying Eq. 2.59. The Trask sorting parameter s_T is not comparable with sorting computed by the other methods because it is based on different percentiles.

The various computations of skewness and kurtosis do not compare well because their computations are too dissimilar.

2.1.5.8 Percent fines

Stream monitoring and fisheries studies are often concerned with the amount of fine sediment (sand and fine gravel) in the streambed because large amounts of fine sediment impair the spawning success of salmonid fish. Depending on the fish species concerned, or on the monitoring objective, fine sediment might comprise medium sand < 0.85 mm, sand < 2 mm, or various sizes of fine gravel $< 3.36, 4.4, 6.4,$ or 9.5 mm (Reiser and Bradley 1993; Rice 1995). The amount of fine sediment is usually computed as the cumulative percent frequency finer than a specified particle size and referred to as the "percent fines". The percent fines is a more sensitive indicator of the amount of fines than the D_5 or D_{10}, because the size of small percentiles is affected by the coarse part of the distribution.

For a comparison of the percent fines over space or time, Church et al. (1987) recommend that the percent fines be computed for size distributions truncated at a certain large particle size. This is to ensure that the percent fines is not affected by the presence of a few large particles. If, for example, a large cobble was added to one of two otherwise identical gravel samples, and that cobble comprised 20% of the total sample mass, then the percent fines would be smaller in the sample with the cobble than in the sample without the cobble. The cut-off particle size for truncation should be some large gravel size present in all samples, e.g., 45 or 64 mm.

The percentage surface fines computed for a given deposit does not only depend on whether the sample was truncated or not, but also strongly depends on the sampling method. Picking particles off the surface (an areal surface sample) produces a lower percentage surface fines than removing a thin layer of particles from the surface (an armor layer sample). This aspect is further discussed under bimodality in Section 2.1.5.9 because a large percent fines in a gravel bed leads to a bimodal particle-size distribution. See also Sections 4.1.2 and 4.1.3 for the effect of different sampling methods on the resulting

particle-size distribution. The percentage fines in a sample also varies between different methods for identifying the particle to be picked up from the streambed, and is likely to vary between operators (Section 4.1.1.3).

2.1.5.9 Bimodality

A bimodal particle-size distribution has two modes, i.e., two distinct peaks in the frequency distribution, one in the finer and one in the coarser fraction. If the percent sand and fine gravel becomes high enough, the distribution becomes bimodal, developing a mode (peak) in the sand range in addition to the other mode (peak) in the gravel range. Bimodality can indicate the presence of two distinct particle-size populations, supplied from a different source, with perhaps different petrology and abrasion resistance, and each population may have had a different transport distance. The recognition and characterization of the degree of bimodality is important for studies of sedimentation and fluvial geomorphology because incipient motion conditions and transport behavior are different in unimodal and bimodal sediment mixtures (Wilcock 1993). Bimodality is also of concern for matters of stream ecology and fish spawning habitat, especially if one of the distribution modes is in the size range of sand to pea-gravel.

Bimodality parameters
Wilcock (1993) proposed a parameter *B* to characterize the degree of bimodality. The parameter is based on the distance between the two modes, and on the amount of sediment contained in the modes. The distance between the modes is expressed in the equation as the ratio of the particle size in mm of the coarse mode D_{cm} and the fine mode D_{fm}. In analogy to the definition of geometric standard deviation, the square root is taken from this ratio. To this ratio is added the proportion of sediment contained in the coarse modes P_{cm} and in the fine mode P_{fm}. These proportions are obtained by summing the decimal frequency of four (*k*) contiguous size classes of 1/4 ϕ-units that contain the mode.

$$P_{cm} = \sum_{i=1}^{k} m_{\%cmi} \quad \text{and} \quad P_{fm} = \sum_{i=1}^{k} m_{fmi} \tag{2.77}$$

For sieving in 1/2 ϕ-units, *k* becomes 2, comprising the size class of the mode and the largest neighboring size class. For polymodal distributions, Eq. 2.77 is applied to all modes. If all sediment is contained in one of the two modes, $P_{cm} + P_{fm} = 1$. This value decreases towards 0 as the degree of bimodality reduces. Bimodality may be computed from (Wilcock 1993):

$$B = \left(\frac{D_{cm}}{D_{fm}} \right)^{0.5} \cdot (P_{cm} + P_{fm}) \tag{2.78}$$

Wilcock (1993) found a threshold value of $B = 1.7$, and that gravel is entrained as unimodal sediment if the bed-material bimodality value is low ($B<1.7$). By contrast, bedload is entrained as bimodal sediment if the bed-material is bimodal ($B>1.7$). The particle-size distribution in Table 2.3 has a coarse mode in the size class of 45.3 mm. Eq. 2.78 could be applied to test if the increased frequency for the size class of 22.6 mm qualifies for bimodality. The square root of the ratio of the particle-size class of the coarse mode (45.3 mm) and the presumed fine mode (22.6 mm) = $2^{0.5}$ = 1.41. The decimal frequency of the coarse mode and its largest neighboring size class (64 mm), and the decimal frequency of the presumed fine mode and its largest neighboring size class (16 mm) are summed, yielding $0.111 + 0.109 + 0.106 + 0.094 = 0.42$. The product of the two bracketed terms in Eq. 2.78 is 0.6, which is smaller than the threshold value of 1.7. Thus, the particle-size distribution in Table 2.3 is not bimodal.

Sambrook Smith et al. (1997) proposed a slightly different bimodality index (B^*). This index accounts for the relative size of the two modes and produces a numerical value that reflects the magnitude of the difference in the particle size of the fine and the coarse mode. The bimodality index is applicable to particle-size distributions in ϕ units.

$$B^* = \left|\phi_{m2} - \phi_{m1}\right| \left(\frac{P_{2m}}{P_{1m}}\right) \tag{2.79}$$

ϕ_{1m} and ϕ_{2m} are the ϕ-sizes of the primary and the secondary mode, respectively, and P_{1m} and P_{2m} are the proportions of sediment contained in the primary and secondary mode. The above index is always positive. Bimodality starts at $B^* > 1.5$ - 2.0. Exchanging the absolute signs in Eq. 2.79 for brackets renders B^* negative for a primary mode in the fine sediment. Applied to the particle-size distribution on Table 2.3, the primary and secondary modes are –5.5 and –4.5 ϕ, and contain 11.1 and 10.6% of the sediment, respectively. Thus, Eq. 2.79 yields |-5.5 - -4.5| · (11.1/10.6) = 1.0 · 1.05 = 1.05 and indicates that the distribution is not bimodal.

Surface bimodality and percent fines: effect of different sampling methods
Bimodality and the percent fines (Section 2.1.5.8) are related, although not by a monotonic function, and both the degree of bimodality and the percent fines are altered depending on how the sediment on the stream surface is sampled. Sambrook Smith et al. (1997) developed a numerical model to show this change. As sand is supplied to a gravel surface, sand first fills the voids between the gravel particles, until, as more sand is added, even the big particles become buried. The entire amount of sand in the experiment adds up to 100 %. For various percentages of sand added, the surface sediment is repeatedly sampled using two different methods: (1) picking individual particles off the surface (areal surface samples), and (2) removing a layer of surface sediment (armor layer sample). Both the percent surface sand and the degree of bimodality were computed for given

84

percentages of sand added to the streambed, and both parameters varied depending on the sampling method used.

When particles were picked off the surface, the percent sand computed from those areal samples S_a quickly rose to 80% as the voids between the large clasts started to be filled (20% sand added). The percent sand computed from the volumetric armor layer samples S_v increased slowly, reaching not even 40% when the entire surface was covered with sand (at $S_a = 100$) (Fig. 2.21).
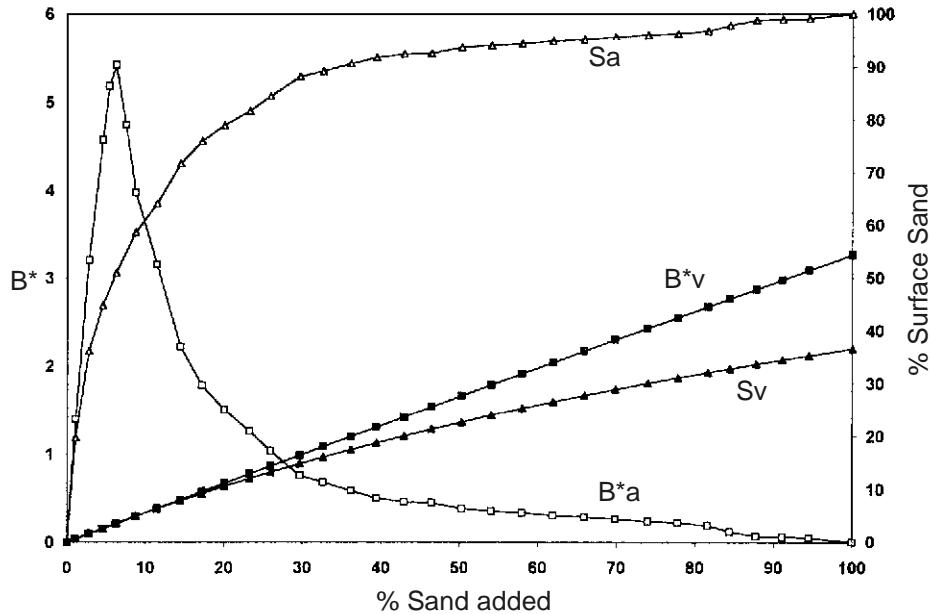
Fig. 2.21: Percent surface sand and degree of bimodality computed for two different sampling methods for increasing amounts of sand. S_a and B^*_a are the percent surface sand and degree of bimodality computed for areal surface samples, S_v and B^*_v are the percent surface sand and the degree of bimodality computed for an armor layer sample (Reprinted from Sambrook Smith et al. (1997), by permission of the American Geophysical Union).

The degree of bimodality differed even more between the two sampling methods. For the areal samples, bimodality B^*_a, increased sharply and was most pronounced when about 50% of the surface was covered by sand ($S_a \approx 50\%$). For larger amounts of sand, the degree of bimodality again decreased. When using armor layer samples, bimodality B^*_v increased slowly as progressively more sand was added to the bed.

2.2 Shape analysis

Particle forms are characterized by two factors: shape and angularity. Shape refers to the ratio of the three axes lengths, whereas angularity refers to whether a particle has angular edges as opposed to a rounded surface.

Many parameters for characterizing particle form were developed in the 1930s to 1960s because it was realized that particle form affects the area exposed to forces of flow, drag forces, lift forces, and therefore particle entrainment, transport, and deposition. Thus, two particles of the same weight or the same *b*-axis size but with different shapes can respond quite differently to water flow. It is therefore important to consider whether a particular study requires knowledge of the longest, the intermediate, or the shortest axis, or of all axes.

2.2.1 Compact, platy, bladed, and elongated particle shapes

Particles are classified into four basic shapes according to the ratios of the three particle axes, where *a* is the longest axis, *b* is the intermediate axis, and *c* is the shortest axis. The length of the particle axes can be measured manually using a ruler, calipers, or a pebble box (Sections 2.1.3.7 – 2.1.3.8). An approximation of particle axes lengths can also be computed from the axes of an ellipse that best fits the planimetrically determined outline of a particle on a photograph (see photosieving, Section 4.1.3.3). The ellipse-approximation eliminates the effects of angularity on particle shape, and thus improves the determination of particle shape for angular particles (Diepenbroek and De Jong 1994).

The particle shape of a disc is characterized by its small *c*-axis. The degree of disc-shape is quantified by the axis ratio of *c/b* (Krumbein 1941). A sphere-like particle, in turn, has almost identical *a*, *b*, and *c* axes. A bladed particle is thin and long, i.e., it has small ratios of *c/b* and *b/a*, whereas a rod-like particle is long, which is quantified by a small *b/a* ratio (Fig. 2.22). Fig. 2.23 depicts these particle shapes using blocks for simplicity.
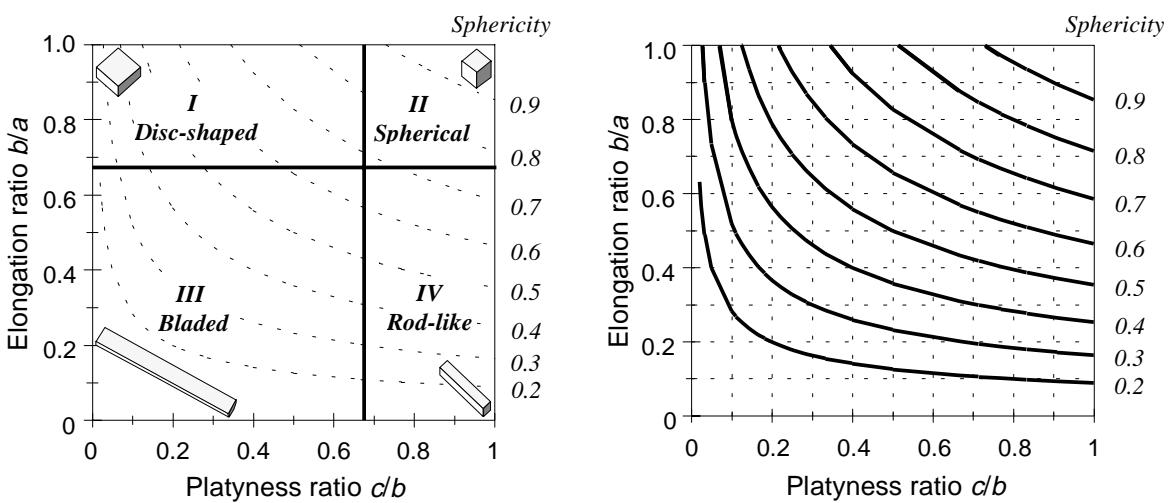
Fig. 2.22: (A) Relation between axes ratios and particle shape (Zingg's classification) (Redrawn from Krumbein (1941), by permission of the Society for Sedimentary Geology). (B) Relation between sphericity and particle shape. Lines of equal sphericity shown as function of the axes ratios *b/a* and *c/b*. (Redrawn from Krumbein (1941), by permission of the Society for Sedimentary Geology).

Sneed and Folk (1958) classify particle shape in terms of platyness, bladedness, elongatedness, and compactness (Fig. 2.23). The form factor F distinguishes between platy (i.e., disc shaped), bladed (i.e., ellipsoid) and elongated (i.e., rod shaped) particles and is computed from

$$F = \frac{a - b}{a - c}$$

(2.80)

$F < 0.33$ defines platy particles, $0.33 < F < 0.67$ defines bladed particles, and $F > 0.67$ defines elongated particles. The degree of platyness, bladedness, and elongatedness, i.e., the degree of deviation from compactness S, is defined by the ratio of

$$S = \frac{c}{a}$$

(2.81)
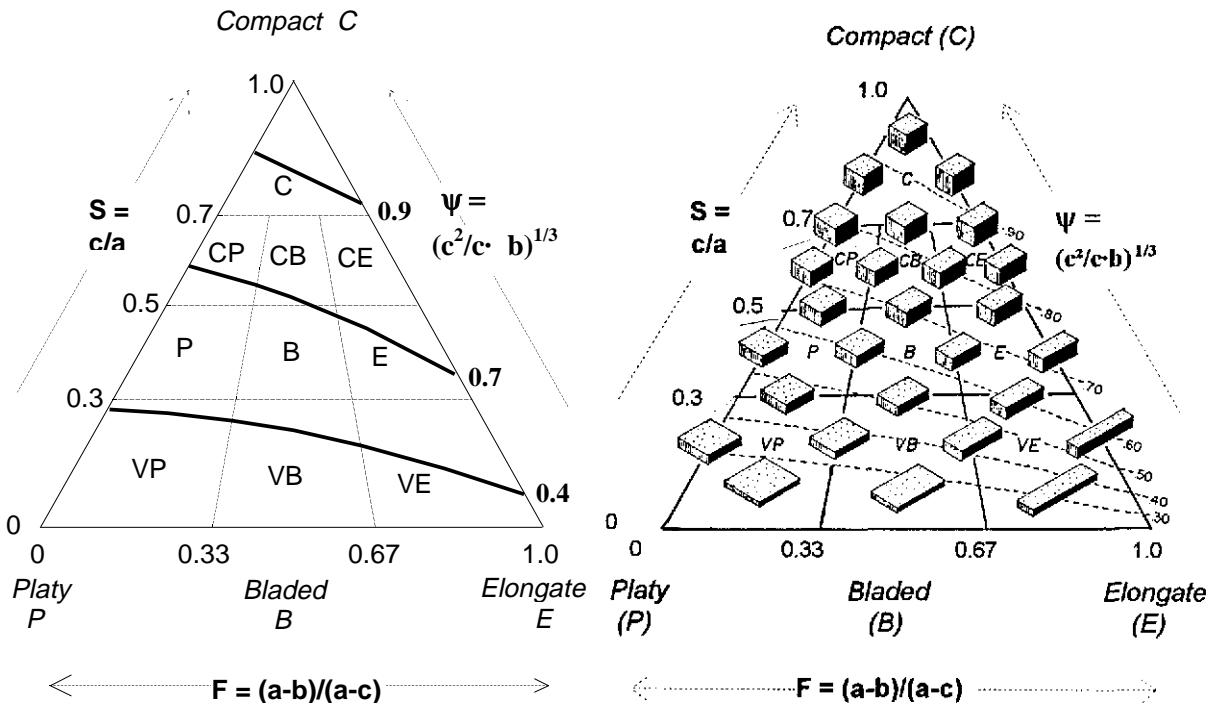
Fig. 2.23: (A) Sphericity-form diagram showing relation between particle shape and sphericity (Redrawn from Sneed and Folk (1958), by permission of the University of Chicago Press). (B) Form triangle with illustration of particle shapes using blocks of the appropriate axes ratios; all blocks have the same volume (Reprinted from Sneed and Folk (1958), by permission of the University of Chicago Press).

Particles are compact (*C*) with a shape close to a sphere if the *S* factor > 0.7. Particles classify as **c**ompact *platy*, **b**laded, or *elongated* if 0.5 < *S* < 0.7, as *platy*, **b**laded, or *elongated* for 0.3 < *S* < 0.5, and as **v**ery *platy*, **b**laded, or *elongated* for *S* < 0.3. The four classes for compact, platy, bladed, and elongated, plus the degrees of deviation from sphericity (e.g., compact bladed or very bladed) yield a total of 10 shape categories. The numerical values of the *F* and *S* factors are plotted in a triangular diagram from which the descriptive term of particle shape can be read.

2.2.2 Sphericity

Particle sphericity refers to how well a particle of a given shape relates to the transport properties of a sphere, whereas the expression roundness refers to the degree to which the edges of a particle are rounded (Section 2.2.3). Sphericity can be used as an indication of fluvial transport distance (Section 2.2.2.1), as well as a measure of particle suspensibility and transportability, i.e., the ability of a particle to remain in transport once entrained (Section 2.2.2.2). Since both concepts involve different principles, i.e., abrasion versus suspensibility, it is important to use different definitions of sphericity in each case.

2.2.2.1 Indication of fluvial transport distance

As particles are transported over long distances, abrasion wears off not only the particle edges (see roundness, Section 2.2.3), but may tend to equalize the three axes lengths as well, thus making a particle more spherical. Wadell (1932) defined this kind of sphericity as the third cube of the ratio of a measure for particle volume to the volume of the sphere circumscribing it. This expression was simplified by Krumbein (1941) and Pye and Pye (1943) who suggested computing sphericity ψ as

$$\psi = \left(\frac{b \cdot c}{a^2} \right)^{1/3} \tag{2.82}$$

Krumbein's sphericity reaches the value of 1 for perfect spheres and decreases towards 0 for extremely platy or elongated particles. Particles of different shapes can have the same sphericity value. However, platyness and elongatedness do not increase at even rates as the degree of sphericity decreases. For example, a particle with an elongation ratio of b/a = 0.6, and a platyness ratio of c/b = 0.2 has a sphericity value of ψ = 0.42, but a particle with an elongation ratio of b/a = 0.2, and platyness ratio of c/b = 0.6, has a sphericity value of ψ = 0.32 (Fig. 2.22). This sphericity index acknowledges that as sphericity increases with transport distance, the degree of elongatedness wears off more quickly or pronouncedly during fluvial transport than the degree of platyness.

Particles of different structural properties from different geological parent material have different susceptibilities to becoming sphere-like. Granite tends to break into cubic blocks

and reaches a high degree of sphericity quickly with increasing transport distance, whereas the "layered" structure of schist produces disc-shaped particles that do not necessarily become highly spherical even after long transport distances. Similarly, large basalt particles tend to chip pieces off during transport, thus producing small elongated instead of spherical particles.

Not all researchers agree on the degree to which fluvial or coastal transport affects particle sphericity. Bartolomä (1992) concluded that sphericity and shape are predominantly controlled by the structural properties of the source rock, and barely affected by transport, and that consequently sphericity and roundness (Section 2.2.3) are independent properties.

2.2.2.2 Indication of particle transportability

Two definitions of sphericity are commonly used to refer to particle transportability: the Corey (1949) shape factor C, and the Sneed and Folk (1958) effective settling sphericity ψ_r. Both definitions are similar and transformable, and both definitions reach the value of 1 for perfect spheres and decrease towards 0 with increasing departure from sphericity.

Corey shape factor
The Corey (1949) shape factor is used as a parameter to determine the particle settling velocity which for particles of equal weight is affected by particle shape. The shape factor is computed from (Yang 1996, p.4):

$$C = \frac{c}{(a \cdot b)^{0.5}} \tag{2.83}$$

Ellipsoidal or compact bladed gravel particles with long fluvial transport distances have values around 0.7, whereas bladed particle shapes in mountain streams have values around 0.5.

Sneed and Folk effective settling sphericity
Sneed and Folk (1958) define the effective settling sphericity as

$$\psi_r = \left(\frac{c^2}{a \cdot b} \right)^{1/3} \tag{2.84}$$

and provide a diagram to show how effective settling sphericity is related to particle shape: the form factor F that distinguishes between platy, bladed, and elongated particles (Eq. 2.80) and the degree of compactness S (Eq. 2.81) (Fig. 2.23).

Lines of equal settling sphericity go diagonally across the diagram, and show that for the same degree of flatness (axis ratio of c/a) platy particles offer more resistance to settling than elongated particles. Thus, the same value of $\psi_r = 0.7$ is obtained for compact platy as well as elongated particles (Fig. 2.23). This definition of settling sphericity indicates the tendency of platy particles to settle relatively slowly. Thus, platy particles easily remain suspended in flow, and once entrained can be transported over long distances.

If lines of equal Corey shape factors were included in the Sneed and Folk diagram (Fig. 2.23), they would plot approximately parallel but below to the lines of equal settling sphericity. Lines of equal values of the Krumbein (1941) sphericity would also plot diagonally across the Sneed and Folk diagram, but point into the opposite direction of the Sneed and Folk sphericity. Compact elongated and platy particles would plot on the same line indicating a similar transport distance. The Krumbein sphericity, referring to transport distance, and the Sneed and Folk sphericity, referring to transportability, intersect and have the same numerical values for particles roughly along the dividing line between bladed and elongated particles with F values around 0.67.

2.2.3 Roundness or angularity: analytical and visual approaches

Roundness describes how well the "edges" of a particle are rounded. Roundness and sphericity are not conceptually related and are largely independent, however, nearly spherical fluvial particles seldom show any sharp edges, whereas particles that are ellipsoidal, bladed, or elongated are much more likely to show sharp edges.

Angular particles tend to wedge into each other and do not roll well. Thus, angularity reduces particle mobility and probability of entrainment. Roundness increases as the edges wear due to abrasion. Thus, high angularity also indicates that a particle has not been transported over a long distance. A number of different roundness indices has been developed and are summarized by Swan (1974).

Wadell (1932) developed a complicated procedure of measuring and computing particle roundness P that computes the mean size of the radii r that can be fitted into the number of corners n that a particle has and divides this number by the radius of the maximum inscribed circle R so that

$$P = \frac{\Sigma r_n}{n \cdot R} \qquad (2.85)$$

On the basis of Wadell's results, Krumbein (1941) developed a chart for the visual estimate of particle roundness which has values between 0.1 (for very angular) and 0.9 (for very smooth particles) (Fig. 2.24). Mean roundness P_m for a deposit is computed by a weighting approach that multiplies the roundness index P by the number of particles n that
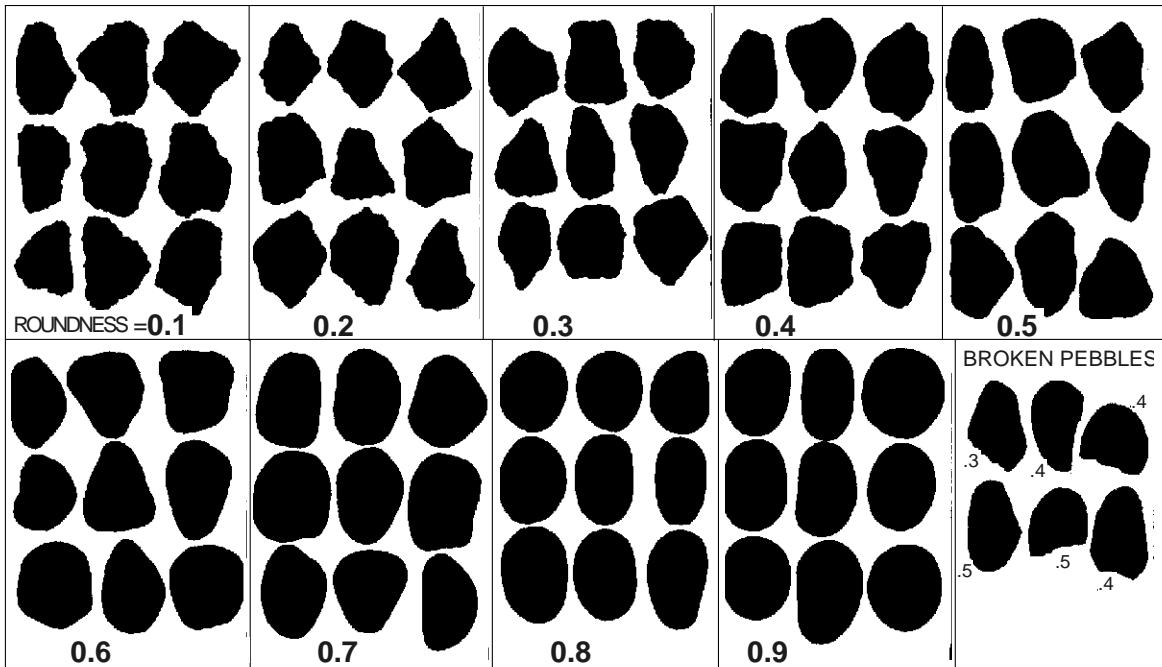
Fig. 2.24: Images for visual analysis of roundness for pebbles 16 - 32 mm. The analysis should be carried out for each particle-size class individually. The chart should be enlarged so that shown particle *b*-axes are of the same length as the particles to be analyzed. (Slightly modified from Krumbein (1941), by permission of the Society for Sedimentary Geology).

have that roundness, sums the *Pn* products and divides by the total number of particles in the sample Σ*n*.

$$ P_m = \frac{\Sigma P \cdot n}{\Sigma n} \qquad (2.86) $$

Further discussion of conceptual and practical issues regarding particle roundness are provided by Diepenbroek et al. (1992).

2.2.4 Shape/roundness matrix: visual field classification

Some field studies might want to classify particles not only by one, but by two parameters combined, such as particle shape and angularity, in order to differentiate between deposits of different sedimentary origins or depositional processes. Crofts (1974) designed a chart for visual field evaluation of particle shape and angularity (Fig. 2.25). For 50 random particles collected from a 1-m^2 area, the first step of the visual analysis distinguishes between spherical and flat particles. Particles are assigned to one of the 6 shape categories ranging from very spherical to very flat (neglecting the degree of elongatedness). Then

sphericity   –   flatness
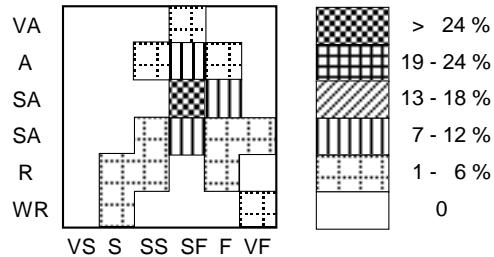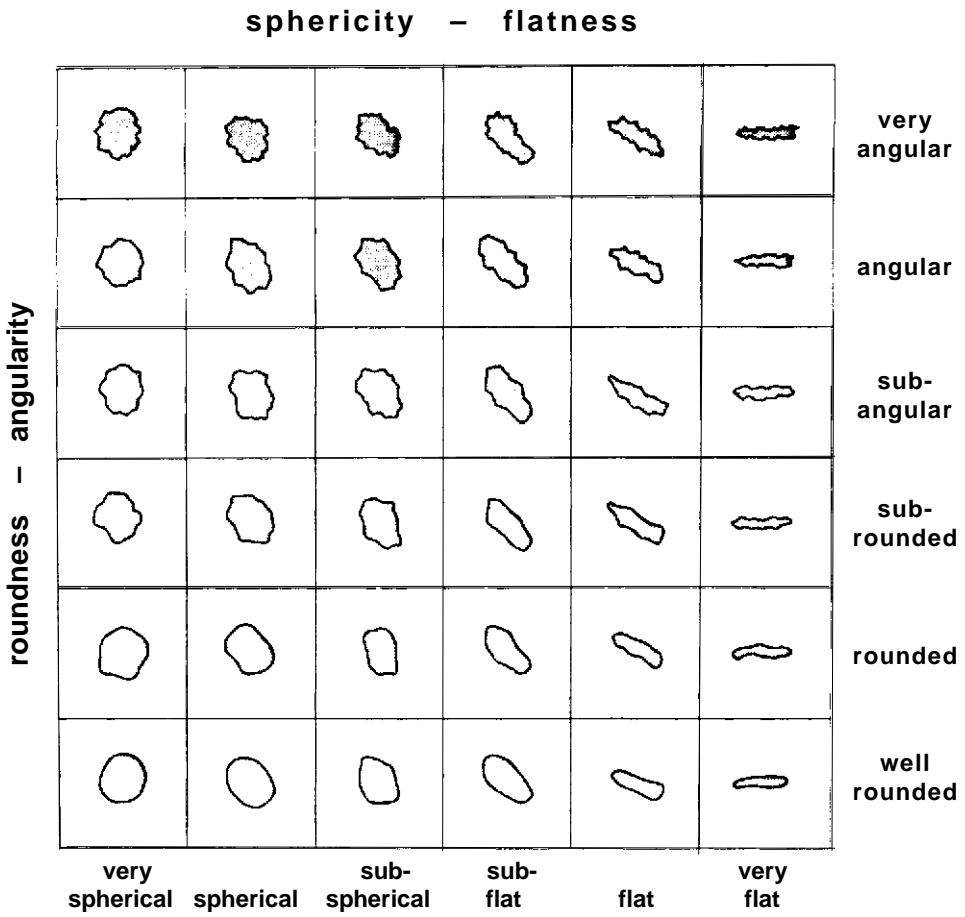
Fig. 2.25: Visual 6-by-6 matrix distinguishing between the degrees of sphericity-to-flatness and roundness-to-angularity (top), and example of plotted results (bottom). (Reprinted from Crofts (1974), by permission of the Society for Sedimentary Geology.)

each particle is sorted into one of the 6 degrees of angularity. The number of particles within each of the potential 36 shape-angularity categories is recorded and may be plotted as a bivariate scattergram. For such a plot, the number of particles per category is grouped into 4 - 6 evenly spaced intervals, and each consecutive interval is assigned an increasing degree of shading or hatching. The visual analysis of 50 particles from one field location takes less than 30 minutes including the time for field plotting the results.

The same approach as outlined above can be applied to any two-particle parameters if their variability can be described in certain visually distinguishable increments. For best results, the visual classification matrix should be larger than 4 by 4, but not exceed 9 by 9 fields. Each study needs to find the optimum matrix size, as well as the optimum sample size, compromising between accuracy and time expenditure.

Visual field classification can also be used to distinguish between three particle parameters. An example in which particle-size mixtures are visually classified into three major and 12 minor size categories, and results are plotted in ternary diagrams, is provided by Buffington and Montgomery (1999a) (Section 4.1.3.5).

2.2.5 Pivot angles and their computation

One of the most important applications of particle-shape parameters in sediment transport studies of gravel-bed rivers is the determination of the pivot angle, also called the angle of repose or intergranular friction angle. The pivot angle is the angle Φ that a top particle of the diameter D has to overcome when rolling over a bottom particle with the diameter K that is partially under and partially in front of it (Fig. 2.26). Thus, pivot angles control the force required for particle motion, and are an integral part of force-balancing equations.
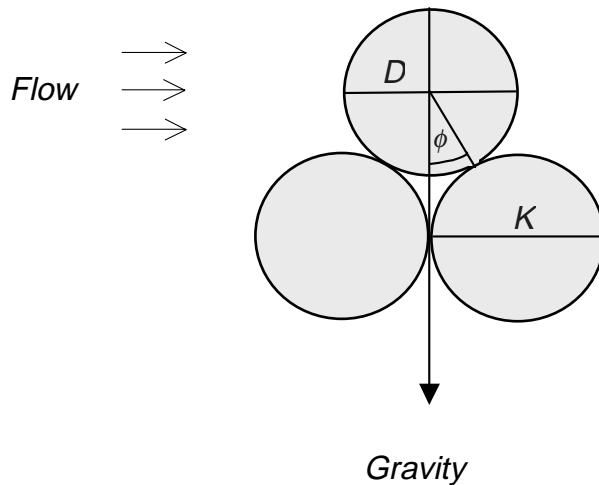
Fig. 2.26: Definition of pivot angle Φ, and particle diameters D (top particle), and K (bottom particle).

Pivot angles are difficult to measure in the field (Johnston et al. 1998). Measurements are therefore either performed on pieces of reconstructed streambed in a lab (Kirchner et al. 1990) or the pivot angle is estimated from various particle parameters such as:

- particle roundness,
- particle shape,
- packing (base of two, three, or four bottom particles *K*), and
- relative particle size *D/K*.

Angularity or roundness

Pivot angles increase with angularity (Fig. 2.27), a reason why riprap is often angular. In order to rotate an even-sized triangle (all inside angles = 60°) situated on a flat plain over one of its angles, a pivot angle of 60° needs to be overcome. The pivot angle for a square with four angles of 45° is 45. Pivot angles *Φ* for even-sided polygons can be expressed as (Julien 1995):

$$\Phi = \frac{180°}{n} \tag{2.87}$$

where *n* is the number of angles within the polygon. For a sphere, the number of inside angles is indefinitely large, thus $\Phi = 180°/\infty = 0°$, which means that there is no pivot angle for a sphere on a flat surface. Pivot angles on a streambed may exceed those in Fig. 2.27 because surface particles may be nestled in shallow depressions on top of three or four bottom particles.

$$\Phi = \frac{180°}{3} = 60° \qquad \Phi = \frac{180°}{4} = 45° \qquad \Phi = \frac{180°}{5} = 36° \qquad \Phi = \frac{180°}{6} = 30° \qquad \Phi = \frac{180°}{\infty} = 0°$$
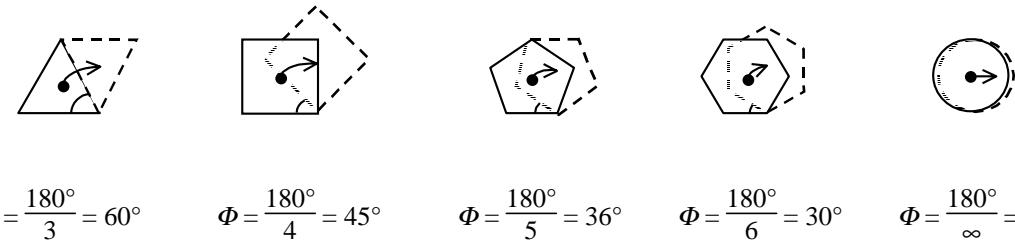
Fig. 2.27: Effect of angularity on pivot angles on a flat surface (Redrawn from Julien (1995), by permission of Cambridge University Press).

Particle packing

Pivot angles vary with packing patterns of the bottom particles. A spherical top particle *D* can be nestled on a base of two, three, or four spherical bottom particles *K* (Fig. 2.28). Pivot angles described in Fig. 2.28 vary with three parameters: (1) the size ratio *D/K*, (2) whether the top particle *D* rolls over the top (grain-top rotation) or over the saddle between two spheres *K* (saddle-top rotation) and (3) the number of bottom particles *K* comprising the base for the top particle *D* (Li and Komar 1986; Julien 1995).

3 cylinders
$\Phi = 30°$

4 spheres
$\Phi = 19.5°$

5 spheres
$\Phi = 35.3°$
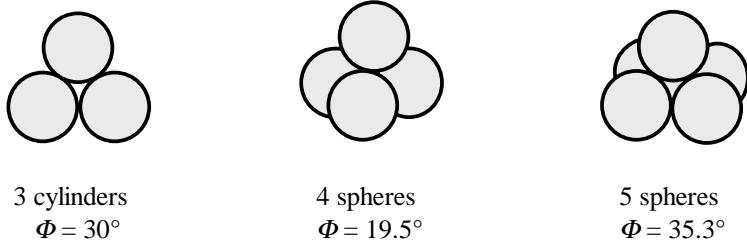
Fig. 2.28: Pivot angles for unsized particles ($D/K = 1$) with different packing: top particles lying on top of two (left), three (center), and four particles (right). (Redrawn from Julien (1995), by permission of Cambridge University Press).

Particle shape
Spherical particles have smaller pivot angles than particles with ellipsoidal, elongated, or platy particle shapes. Pivot angles for spheres are approximately 10° lower than those for ellipsoids which are about 10° lower than those for angular particles (Li and Komar 1986).

Relative size
Miller and Byrne (1966) express the effect of relative particle size D/K on the pivot angle Φ by a negative power function.

$$\Phi = a \left(\frac{D}{K}\right)^{-b}$$

(2.88)

Pivot angles for small surface particles D nestled on top of large bottom particles K with $D/K \approx 0.3$ are 40-50° larger than the pivot angles for large surface particles on top of small bottom particles with $D/K \approx 3$ (Fig. 2.29). This effect of relative size is seen for all particle shapes.

Pivot angles in channel beds
Kirchner et al. (1990) measured pivot angles on water-worked flume surfaces and concluded that pivot angles obtained from experiments with well sorted and well rounded particles in regular packing are too low, and vary too much with relative size. Kirchner et al. (1990) therefore suggest the following *a*-coefficient and *b*-exponent for Eq. (2.86) (Fig. 2.30):

$$\Phi_{50} = 55.2 \left(\frac{D}{K_{50}}\right)^{-0.31}$$

(2.89)
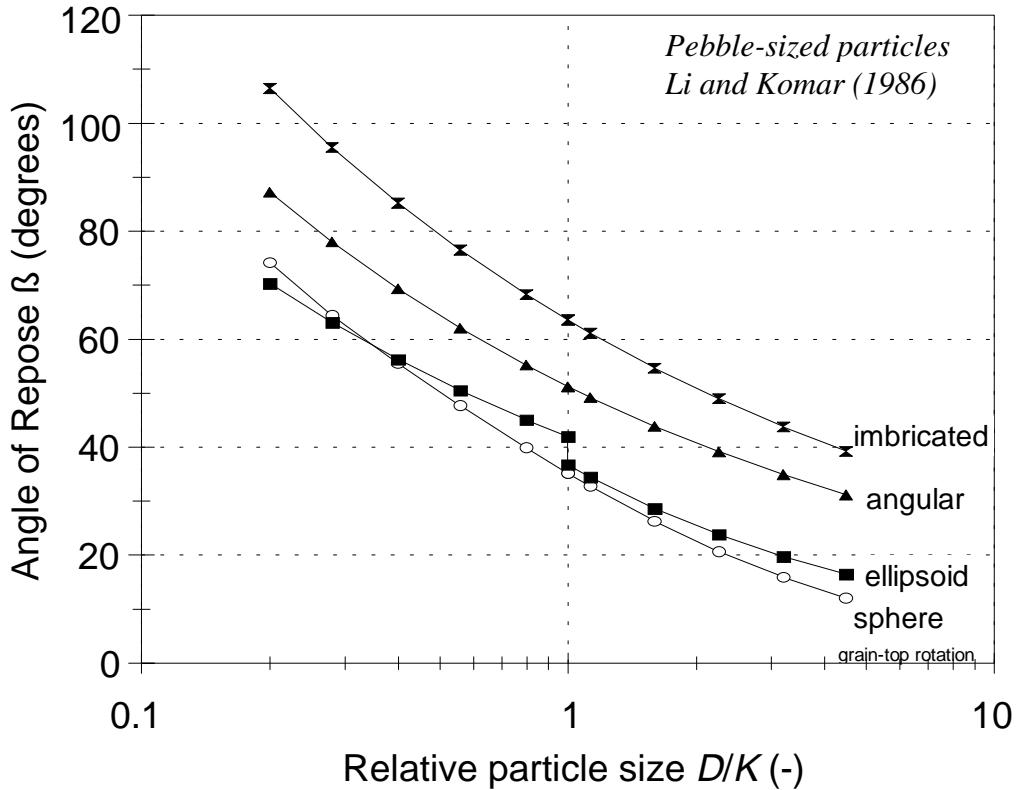
Fig. 2.29: Pivot angles for spherical, ellipsoidal, and angular particle shapes as well as for imbricated deposits as functions of relative particle size, i.e., the ratio of entrained particle size D to bottom particle size K (plotted with data from Li and Komar 1986).

where Φ_{50} is the median pivot angle, and K_{50} is the median size of the bottom bed-material particles. Gravel-bed rivers with particles of various dimensions, various relative sizes, shapes, rotation modes, and packing have a wide range of small and large pivot angles (Buffington et al. 1992). Each riverbed is characterized by a unique probability distribution of pivot angles, and the parameters of the distribution (median, skewness, and kurtosis) are a function of various particle parameters.

Buffington et al. (1992) include a term for bed-material sorting σ in their equation and provide the coefficient x (Eq. 2.90). Adjusting x facilitates computing the probability distribution of pivot angles. $\tan\Phi$, to which critical shear stress τ_c is proportional, can vary widely on a given streambed, indicating the differential erodibility of surface particles.

$$\Phi_x = a_x \left(\frac{D}{K_{50}}\right)^{-b_x} \cdot \sigma^{-c_x} \tag{2.90}$$

96
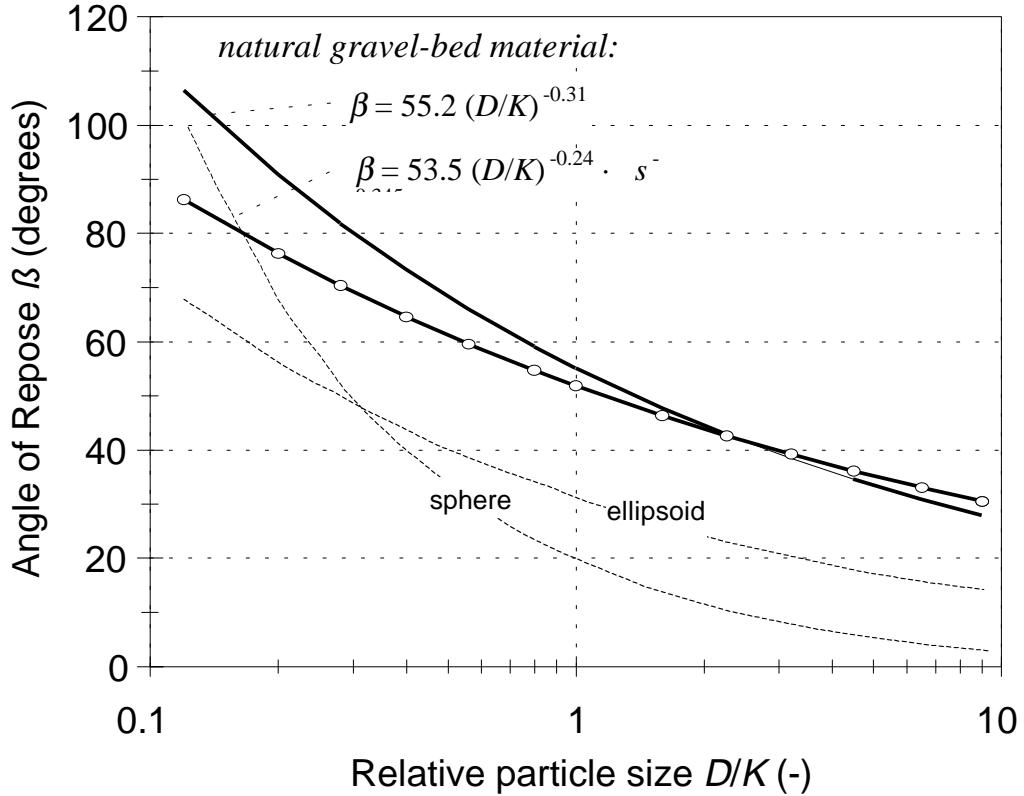
Fig. 2.30: Pivot angles for particles on channel surfaces computed from Eq. 2.89 by Kirchner et al. (1990) (thick line); Median pivot angles computed from Eq. 2.90 by Buffington et al. (1992) (thick line with bullets). For comparison: pivot angles for saddle-top rotation of well sorted spheres and ellipsoids in regular packing, based on results by Li and Komar (1986) (thin hatched lines).

2.2.6 Sample size for shape analysis

The number of particles used to establish the dominant bed-material particle shape depends on the variability of the particle shapes found at a site. There also might be several populations of particle shapes corresponding to differences in hardness of the source rock and differences in travel distance. Particles originating from soft rocks, or those traveled farthest are more rounded and more ellipsoidal than hard rocks or bedload supplied to the mainstem stream by a small tributary just upstream. Particles from local rockfall or debris flows are usually angular and deviate from a spherical or ellipsoidal particle shape.

Because the situation can be quite different from stream to stream, pilot studies are recommended. The first step is to visually identify particle-shape populations. Then collect 25 particles from each population, measure the 3 axes, compute the *S* and *F* form factors (Eqs. 2.80 and 2.81) and plot them in a sphericity-form diagram (Fig. 2.23). If the data for 25 particles do not plot closely together, more particles may need to be analyzed or the criteria for identifying particle shapes need to be changed. Another option is to

apply Student's *t*-statistics to measured particle-shape parameters and to determine the sample size necessary for an acceptable accuracy and a given particle-shape variability (see Section 5 on sample size).

2.3 Particle density, specific weight, specific gravity, and submerged specific weight

Many equations for sediment transport or the initiation of particle motion require particle density or the specific particle weight as input. Particle density is particle weight (or mass) (*m*) divided by its volume *V*. Conventionally, particle density is abbreviated by the Greek letter "rho" with the subscript *s* for sediment (ρ_s) to distinguish it from the fluid density (in this case water) which is noted by ρ_f.

$$\rho_s = \frac{m}{V} \tag{2.91}$$

The units of particle density are g/cm^3, or kg/m^3. Particle mass is measured by weight and particle volume is either measured or estimated from particle shape. To measure particle volume, take a large measuring beaker for large particles, or a graded cylinder for small rocks, fill it about half full with water and record the volume of water. Place the particle into the water (particle must be completely submerged) and record the water volume corresponding to the elevated water level. The difference between the two water volumes in the beaker is the particle volume. When particles are small, or when one wants to know the average density of particles in a mixture, several particles can be analyzed together. To reduce measurement errors, the entire analysis should be repeated several times with new particles.

The density of quartz and feldspar particles is 2.65 g/cm^3 or 2,650 kg/m^3. This value can often be used as a first approximation of particle density because many particles contain a high percentage of quartz and feldspar. Rock density is less than the one for quartz when rocks have pores filled with water or air. Sandstone rocks, for example, have a density of about 2.2 g/cm^3. Solid, dark volcanic rocks or those with high metal content have a density of more than 3 g/cm^3. Density is to some extent dependent on particle size. Cobble and gravel-sized pieces of vesicular basalt or pumice might have densities between 2 and 1 g/cm^3. This value can increase to about 3 g/cm^3 when vesicular volcanic rock is ground into sand size and the vesicular structure is lost. Table 2.15 presents particle densities for common geological materials.

Table 2.15: Particle densities (g/cm^3) of various materials[*]

Material	Density
humus, pumice	<1.5
sandstone	2.1 - 2.2
limestone, quartz, granite, porphyry	2.7
feldspars (the "white" in granite)	2.5 - 2.8
dolomite, anhydrite	2.9
micas (the flaky, shiny parts of granite)	2.7 - 3.3
apatite	3.1 - 3.3
peridotite, gabbro	>3.2
basalt, diabas	3.3
iron	7.2

[*]*for comparison: water density at 4°C = 1.00 g/cm^3*

Specific particle weight

Specific particle weight γ_s is the product of particle density ρ_s and acceleration due to gravity g. For most applications in gravel-bed rivers g can be assumed to take a value of 981 cm/s^2, or 9.81 m/s^2.

$$\gamma_s = \rho_s \cdot g = 2.65 \cdot 981 \frac{g \cdot cm}{cm^3 \cdot s^2} = 2{,}600 \frac{g}{cm^2 \cdot s^2} \tag{2.92}$$

Specific gravity of sediment and water

Specific gravity is the dimensionless ratio of specific weights or densities. For quartz particles with a density of 2.65 g/cm^3 and water with a density of 1 g/cm^3, the specific gravity is

$$G_s = \frac{\gamma_s}{\gamma_w} = \frac{\rho_s}{\rho_w} = \frac{2.65}{1} = 2.65 \tag{2.93}$$

The density of pure water at 4°C (ρ_{pw}) is 1 g/cm^3. River water with suspended sediment concentration and a temperature above 4°C may have a density (ρ_{rw}) higher than 1, perhaps 1.005. The specific gravity of river water G_{rw} is computed from

$$G_{rw} = \frac{\gamma_{rw}}{\gamma_{pw}} = \frac{\rho_{rw}}{\rho_{pw}} = \frac{1.005}{1} = 1.005 \tag{2.94}$$

Submerged specific weight

The submerged specific weight ρ'_s of a quartz particle is the difference between the particle density and the fluid density. For clear water, the submerged specific particle weight is

$$\rho'_s = \rho_s - \rho_f = 2.65 - 1 = 1.65 \text{ g/cm}^3. \tag{2.95}$$

For heavily sediment-laden water with a sediment concentration of 100 g/l, fluid density increases to 1.23 g/cm^3. Thus, the submerged specific particle weight is reduced to 1.42 g/cm^3. This reduction in the specific weight of particles in heavily sediment-laden flow leads to an increase in particle mobility and may even cause boulders to "swim".

2.4 Bulk density, porosity, and void ratio

Knowledge of sediment bulk density is needed to evaluate the pore space available for aquatic habitat (Milhous 2001). Bulk density ρ_b is defined as the ratio of the weight of a bulk material m_b that is contained in a specific bulk volume V_b.

$$\rho_b = \frac{m_b}{V_b} \tag{2.96}$$

In situ gravel sediment, inundated sediment

Bulk density of riverbed material should be measured on undisturbed samples in their original packing because the bulk density changes when the natural packing is disturbed by shoveling the sediment. Piston cores also disturb the original packing and are not suitable for measurements of bulk density in gravel deposits.

Milhous (pers. comm. 2000) suggested that bulk density of inundated sediment in gravel-bed rivers may be measured in situ from large freeze cores (Section 4.2.4.8) taken from the substrate below the water surface, so that the sample is completely saturated with water (i.e., all pores filled with water, none with air). The cores are weighed frozen and fully waterlogged (m_w), as well as after the ice has melted and the sediment has dried (m_s). To compute the bulk density of the sediment in the core, the dry sediment mass is divided by the total core volume which is the volume of the sediment particles V_s plus the volume of the water in the pores V_w.

$$\rho_b = \frac{m_s}{V_w + V_s} \tag{2.97}$$

The volume of the sediment particles is calculated from

$$V_s = \frac{m_s}{\rho_{rw} \cdot G_s} \qquad (2.98)$$

where ρ_{rw} is the density of the river water, and G_s is the specific gravity of the sediment (Section 2.3). The volume of the water contained in the sample is computed from

$$V_w = \frac{m_w}{\rho_{rw} \cdot G_{rw}} \qquad (2.99)$$

where G_{rw} is the specific gravity of the river water (Section 2.3).

In situ gravel sediment, dry surface
Milhous (2001) suggested the following technique for measuring the bulk density of subsurface sediment in a dry part of the streambed:

Step 1: Measure the volume of water that displaces the surface sediment or the armor layer
Remove all surface particles from a dry streambed area for a measurement of the subsurface sediment bulk density. Alternatively, remove the armor layer (Sections 4.1.3.1, 4.1.3.2, 4.2.1.2) before measuring the subarmor bulk density. Place a square frame, 0.6 – 0.9 m in length, and 2.5 – 5 cm high onto the area cleared of armor sediment (Fig. 2.31). Place some sediment along the inside of the frame just next to the frame to create a smooth transition between sediment and frame. Smooth out the corners as well. Do not sample or disturb this sediment. Cover the exposed subsurface sediment surface with a plastic sheet, and fit it snugly into all corners within the inside of the frame. Fill the plastic-lined depression with water (river water is fine) and measure the water volume needed until overflow using a large laboratory cylinder. Alternatively, weigh the amount of water needed to fill the plastic sheet and compute the volume using a fluid density of 1,000 kg/m^3 for clear, cold water. Discard the water and remove the plastic sheet (Fig. 2.32 top). Be careful not to disturb the frame or the exposed sediment surface.

Step 2: Measure the volume of water that displaces the subsurface or subarmor sediment
Take a subsurface bed-material sample with a volume of about 20 liters from inside the area within the frame (See Section 4.2.2 for vertical extent of a subsurface bulk sample). This sample is later dried, weighed, and sieved. When extracting the sample, the operator should try to create a hole with a smooth bottom. The operator should be

Fig. 2.31: Frame for measuring in situ subsurface sediment bulk density (Photo courtesy of R. Milhous).

careful not to disturb the exposed subsurface sediment surface or the position of the frame while taking the subsurface sample. After the subsurface sample is taken, carefully line the hole with plastic sheeting and extend the sheet over the exposed sediment surface within the frame, and the frame itself. Make sure that the plastic sheet fits snugly into the hole and leaves no cavities. Air-filled cavities are especially prone to develop in the bottom of the hole. Make sure the plastic sheet is everywhere in contact with the bottom of the hole. Refill the plastic sheet with water and measure the volume needed until overflow onto the gravel surface (Fig. 2.32 bottom).

The volume displacing the subsurface sample V_{sub} is the difference between the volume of the second V_2 and the first measurement V_1.

$$V_{sub} = V_2 - V_1 \tag{2.100}$$

The bulk density of the bed material ρ_{sub} is the ratio of dry weight of the subsurface sediment removed from the hole m_{sub} to the volume of the subsurface sample V_{sub}.

$$\rho_{sub} = \frac{m_{sub}}{V_{sub}} \qquad\qquad\qquad\qquad (2.101)$$

Bulk density measured this way in several gravel-bed rivers ranged between 1.7 and 2.6 g/cm^3, with a mean of 2.1 g/cm^3.

Step 1:
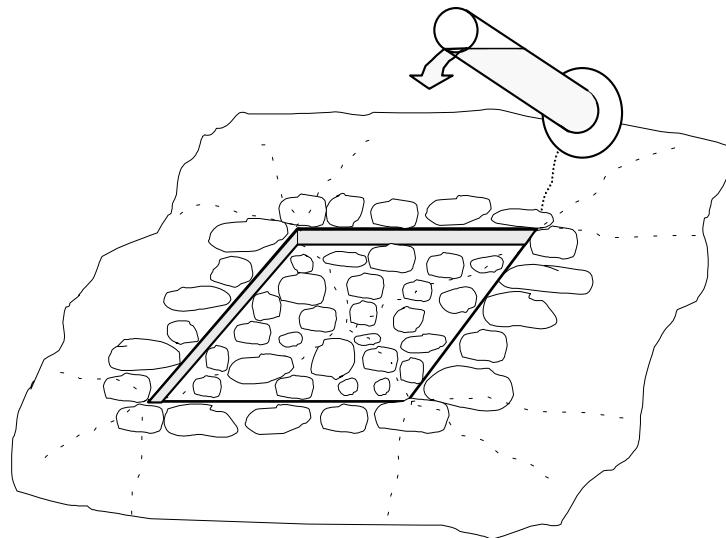
Step 2:
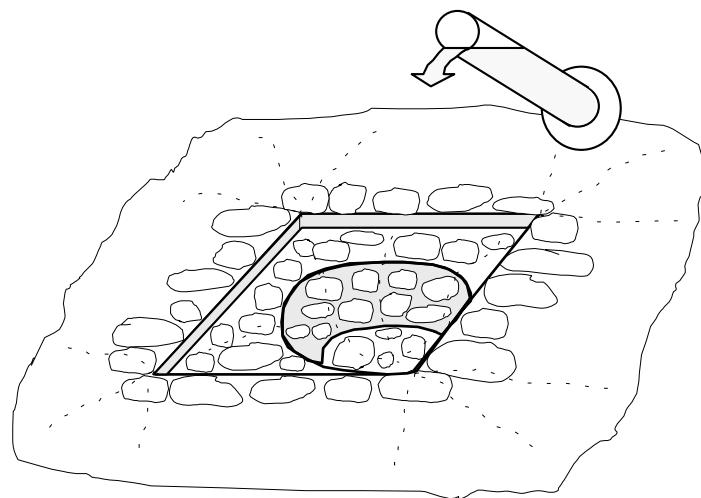
Fig. 2.32: In situ measurements of the subsurface sediment bulk density.

Repeating density measurements to determine a mean value is advisable, because differences in material packing as well as operator errors are likely to produce a range of results. Note also that a 20-liter sample volume yields a sample mass of approximately 10

kg and that several subsamples may be required to obtain the total sample mass necessary for a preset accuracy of the particle-size analysis.

If the sediment porosity p is known, bulk density may also be computed from

$$\rho_b = \rho_s \cdot \ (1 - p) \tag{2.102}$$

Effect of particle packing on bulk density

Particle packing can significantly affect bulk density. The weight of quartz sand filling a 10 liter pail (1,000 cm^3; ca. 2.5 gallons) is not 2.65 g/cm^3 times 1,000 cm^3 = 26.5 kg, but considerably less (approximately 20 kg). The exact weight depends on how closely the quartz grains are packed. Particle packing can range between open and dense. The packing is open or cubic when each unisized sphere has a neighbor exactly on top and beneath, on the north, east, south, and west side. The resulting bulk density for this packing is 1.39 g/cm^3. In the densest packing (rhombohedral), six spheres are clustered around the center sphere, and have a top sphere in the "pocket" or depressions between the bottom spheres. In this case, the bulk density is 1.96. Assemblages of natural particles are seldom unisized, however. Thus, small particles fit between the voids left by larger particles, and the packing becomes denser the wider the particle-size distribution. Packing also becomes more dense as the deposit becomes more compacted due to pressure or shock waves (e.g., more rice grains can be filled into a jar if one gently hits the bottom of the jar). Bulk densities for various sediments are presented in Table 2.16.

Table 2.16: Bulk density and porosity for various sediments with a particle density of 2.65 g/cm^3.

Description	Bulk density (g/cm^3)	Porosity (-)
Unisized spheres in open (cubical) packing *(theoretical)*	1.39	0.48
Unisized spheres in closest packing *(theoretical)*	1.96	0.26
Clay	1.59 – 1.06	0.40 – 0.60
Silt	1.72 – 1.33	0.35 – 0.50
Fine sand (Smith and Wheatcraft 1993)	2.12 – 1.46	0.20 – 0.45
Coarse sand	2.25 – 1.72	0.15 – 0.35
Surface soil of wet clay	1.12	0.58
Surface soil of loam texture	1.28	0.52
Subsoil of sandy texture (Marshall and Holmes 1988)	1.61	0.39
Sandy loam compacted by heavy traffic	1.90	0.28
Sandstone	2.12	0.20
sand-gravel mixture (Carling and Reader 1982, *freeze cores)*	2.30	0.13
range in several gravel-bed rivers	2.60 - 1.70	0.02 – 0.36
mean of several gravel-bed rivers (Milhous, 2001, *volume difference)*	2.10	0.21

Porosity

Porosity is defined as the ratio of the space taken up by voids to the total volume of sediment. Porosity is a dimensionless number less than 1, and may be expressed as a percentage. Porosity p can be computed in two ways. One possibility is:

$$p = \frac{V_v}{V_t} = \frac{V_t - V_s}{V_t} = \frac{V_t - \left(\frac{m_s}{\rho_s}\right)}{V_t} \qquad (2.103)$$

where V_v is the volume of the void or pore spaces, V_t is the total volume of sediment, and V_s is the volume of the sediment without pores. The dry mass of the sediment is m_s and particle density is ρ_s. Alternatively, porosity may be computed from:

$$p = \left(1 - \frac{\rho_b}{\rho_s}\right) \qquad (2.104)$$

Eqs. 2.102 and 2.104 show that bulk density of a sediment deposit is inversely related to porosity, and one term can be used to compute the other. Porosity is a measure important for aquatic habitat studies, as well as for assessing the potential amount of fines in a streambed. However, little is known about the spatial and temporal variability of porosity and bulk density in gravel-beds because in-situ measurements of bulk density are time consuming and therefore rare.

Void ratio

The void ratio e is a parameter similar to sediment porosity, and is computed from the ratio of the volume of voids to the volume of sediment particles:

$$e = \frac{V_v}{V_s} = \frac{V_t - V_s}{V_s} = \frac{V_t - \left(\frac{m_s}{\rho_s}\right)}{\frac{m_s}{\rho_s}} \qquad (2.105)$$

Similar to porosity, void ratio also yields values smaller than 1, but the values are somewhat larger.

<u>Example 2.1:</u>

A subsurface sample taken with the water displacement method described in Section 2.4 has a total volume of $V_t = 0.020$ m^3 or 20 liter, and a dry mass of m_b = 42 kg. The parent material is mainly quartz with a particle density of ρ_s = 2,650 kg/m^3.

Bulk density $\rho_b = m_b/V_t$ = 42 kg/0.02 m^3 = 2,100 kg/m^3.

Sed. volume $V_s = m_b/\rho_s$ = 42 kg/2650 m^3 = 0.01585 m^3.

Void volume $V_v = V_t - V_s$ = 0.020 m^3 - 0.01585 m^3 = 0.00415 m^3.

Porosity (1) $p = V_v/V_t$ = 0.00415 m^3/0.020 m^3 = 0.208 or 20.8%

Porosity (2) $p = 1-(\rho_b/\rho_s)$ = 1-(2,100(kg/m^3)/2,650(kg/m^3))   = 1-0.792 = 0.208

Void ratio $e = V_v/V_s$ = 0.00415 m^3/0.01585 m^3 = 0.2619